Justus-Liebig-Universität Gießen **Klinik Für Neurologie**

Evaluation of the Fibroblast Growth Factor Receptor 2 (FGFR2) in Experimental Autoimmune Encephalomyelitis (EAE) and its Possible Role in Multiple Sclerosis (MS)

DISSERTATION

Submitted to the

Faculty of Medicine

In partial fulfillment of the requirements for the

PhD-Degree

of the Faculties of Veterinary Medicine and Medicine
of the Justus-Liebig University Giessen, Germany

By

Salar Kamali, M.Sc.
Orumieh, Iran

Giessen, 2016
Germany

Multiple Sclerosis Research Group
Department of Neurology
Justus Liebig University Giessen
Prof. Dr. Manfred Kaps

First Supervisor:

PD Dr. med. Martin Berghoff
Faculty of Medicine
Multiple sclerosis research group
Neurology Clinic
Justus-Liebig-University Giessen, Germany

Co-supervisor:

Prof. Dr. Wolfgang Clauss
Faculty of Biology
Institute for Animal Physiology
Justus-Liebig-University Giessen, Germany

Committee members:

Prof. Dr. Klaus-Dieter Schlüter
Department of Physiology
Faculty of Medicine
Justus-Liebig-University

Prof. Dr. R. Lakes-Harlan
Institute of Animal Physiology
Department of Integrative Sensory Physiology
Justus-Liebig-University

Prof. Dr. Bernhard Rosengarten
Faculty of Medicine
Department of Neurology
Justus-Liebig-University Giessen

Doctoral Defense: 06.04.2016

Dedicated to my dear father, the greatest inspiration of my life, my loving family and friends

and

The Mother Nature

توانا بود هر که دانا بود ز دانش دل پیر برنا بود

فردوسی

Thy source of might is knowledge, education makes old hearts grow young again

Ferdowsi

DECLARATION

I hereby declare that the present thesis is my original work and that it has not been previously presented in this or any other university for any degree. I have appropriately acknowledged and referenced all text passages that are derived literally from or are based on the content of published or unpublished work of others, and all information that relates to verbal communications. I have abided by the principles of good scientific conduct laid down in the charter of the Justus Liebig University of Giessen in carrying out the investigations described in the dissertation.

Salar Kamali

Giessen, Germany

INDEX

ABBREVIATIONS

BDNF	Brain-derived neurotrophic factor
BSA	Bovine serum albumin
BBB	Blood brain barrier
CNS	Central nervous system
CSF	Cerebrospinal fluid
DNA	Deoxyribonucleic acid
EAE	Experimental autoimmune encephalomyelitis
ECL	Enhanced chemiluminescence
ERK	extracellular signal-regulated kinases
FGF	Fibroblast growth factor
FGFR	Fibroblast growth factor receptor
$Fgfr2^{ind-/-}$	Oligodendrocyte specific inducible Fgfr2 knockout
GA	Glatiramer acetate
GAPDH	Glyceraldehyde 3-phosphate dehydrogenase
h	hour
H and E	Hematoxylin and Eosin
KO	Knockout
LFB/PAS	Luxol fast blue/periodic acid Schiff
MBP	Myelin Basic protein
MOG	Myelin oligodendrocyte glycoprotein
MS	Multiple sclerosis
OL	Oligodendrocyte
OPC	Oligodendrocyte progenitor cells
p.i	Post immunization
PBS	Phosphate buffered saline
PCR	Polymerase chain reaction
PFA	Paraformaldehyde
PLP	Proteolipid protein
RT	Room temperature
PCR	Polymerase chain reaction
SDS	Sodium dodecyl sulfate
TBS	Tris buffered saline
TBST	Tris buffered saline with Tween20
TrkB	Neurotrophic tyrosine kinase, receptor, type 2
WT	Wildtypte

List of Figures

List of Tables

ABSTRACT

A salient feature in the course of multiple sclerosis (MS) is myelin and axonal damage followed by oligodendrocyte degeneration. The current MS therapies are mainly focused on restricting inflammation by moderating the immune response, whereas the oligodendroglial preservation and regeneration have been poorly understood. It is long known that fibroblast growth factors (FGFs) and their receptors (FGFRs) play profound roles in neurons and oligodendrocyte proliferation, migration and differentiation as well as central nervous system (CNS) development. Yet, this study is the first to investigate the role of oligodendroglial FGFR2 in the pathology of experimental autoimmune encephalomyelitis (EAE) utilizing a conditional oligodendrocyte knockout mice. Concerning the various physiological and pathological roles attributed to FGFR2 signaling, we hypothesized that EAE immunization will affect Fgfr2 knockout mice more severely. Surprisingly, we observed a milder EAE disease course as well as a reduced inflammation, lymphocyte and macrophage infiltration, demyelination and axonal damage in oligodendroglial Fgfr2 knockout mice. Protein analysis showed a shift in FGFR2 downstream signaling, leading to lower ERK phosphorylation and increased AKT phosphorylation in oligodendroglial Fgfr2 knockout mice. Moreover, we report that TrkB (the receptor for brain derived neurotrophic factor) was up-regulated in oligodendroglial Fgfr2 knockout mice which is known to induce neuroprotective and neuro-regenerative effects. These findings suggest a novel and not previously described role for oligodendroglial Fgfr2 in the course of EAE.

1 INTRODUCTION

1.1 Multiple sclerosis

Multiple sclerosis (MS) is the most common autoimmune inflammatory disorder affecting central nervous system (CNS) (Kieseier et al., 2005). The initial description of MS dates back to 14th century but it was Jean-Martin Charcot in 1868 (a French neurologist) who first described MS as a separate neurological condition (Compston, 1988, Kumar et al., 2010). A century following Charcot's discovery, the progress on understanding and treating MS has been very slow and only during the recent decades a meaningful forward momentum has been generated. Multiple sclerosis is a complex chronic inflammatory disease characterized by demyelination, oligodendrocyte and axonal injury (Hoglund and Maghazachi, 2014). The prevalence of MS is not uniform around the world, nor across the genders (female: male sex ratio ~ 3:1) (von Budingen et al., 2015). MS occurs more commonly in people living in the northern hemisphere (Caucasian root) and Europe is considered to be a high prevalence region for MS (defined by Kurtzke as a prevalence ≥ 30/100,000) (Kingwell et al., 2013). According to the Multiple Sclerosis International Federation (MSIF) until June 2013, worldwide up to 2.3 million people were affected by MS.

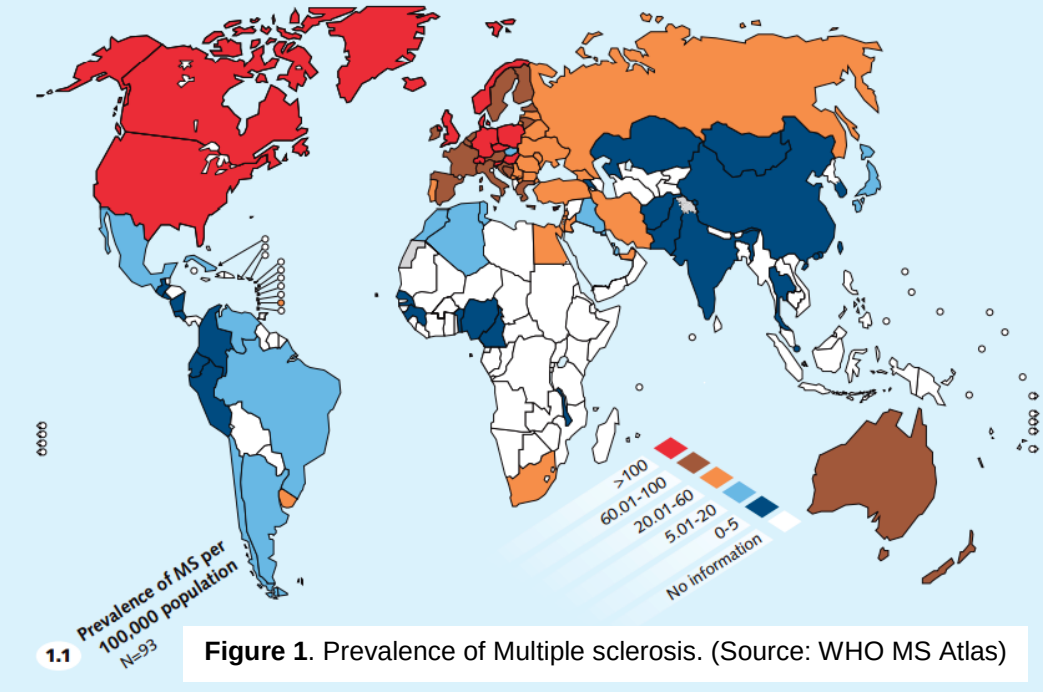

Figure 1. Prevalence of Multiple sclerosis. (Source: WHO MS Atlas)

1.1.1 Etiology

Multiple sclerosis is a complex autoimmune disorder with its exact underlying pathology remained unclear. There are enough evidence associating MS pathogenesis to both genetic susceptibility and environmental factors (Figure 2).

Genetic: In a pure genetically controlled disorder, the occurrence rate of the condition is 100% within the identical twins. In MS this ratio drops to 25 percent and even lower (3%) in siblings or children of patients with MS (Hoglund and Maghazachi, 2014). In recent years using genome wide association studies (GWAS) over 50 genes with MS risk factors were identified, most of which are associated with the immune system, including interleukin (IL)-2 and IL-7 (Gourraud et al., 2012).

Environment: The exact environmental factors behind MS are not precisely discovered however, several environmental exposures are known to increase the risk of MS development. Epidemiology studies suggest involvement of viruses, particularly Epstein-Barr virus (EBV), measles, and HTLV-1 in the pathogenesis of MS. (Gustavsen et al., 2014). Low levels of sun exposure (vitamin D status), especially in early childhood, are also known to increase risk of MS (Aivo et al., 2015). Scientific investigations draw links between MS development and its progress with other lifestyle elements such as; smoking, obesity, vitamin A levels, exercise, alcohol consumption and so on (Fragoso, 2014).

1.1.2 Symptoms and life quality of patients

MS has highly variable clinical symptoms and progression patterns among patients while each individual's symptoms could also change over time. These symptoms depend not only on the location of MS lesions but also on the slowed conduction properties displayed by affected axons (Newland et al., 2014). Different MS related symptoms include fatigue, pain, sleep disturbance, depression, anxiety, irritability, cognitive impairment, spasticity, ataxia, and poor balance as well as MS generated symptom clusters (symptoms that are related to each other and occur together) such as functional walking capacity, and perceived health and illness intrusiveness (Figure 3) (Shahrbanian et al., 2015).

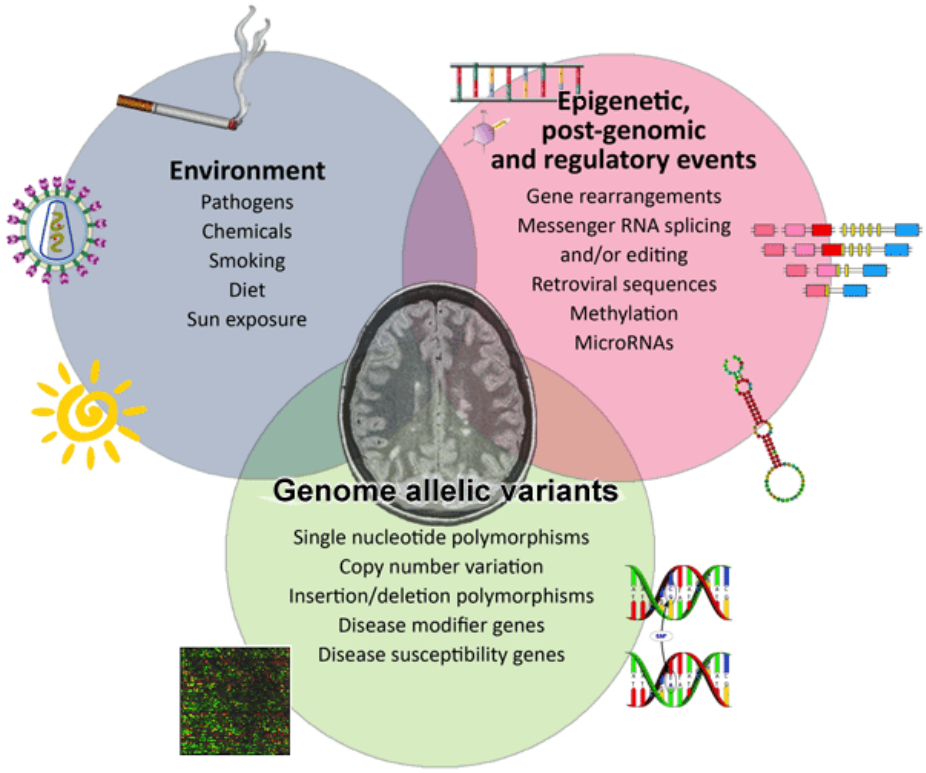

Figure 2. Different elements attributed in MS development (*Image by J.Oksenberg/UCSF*)

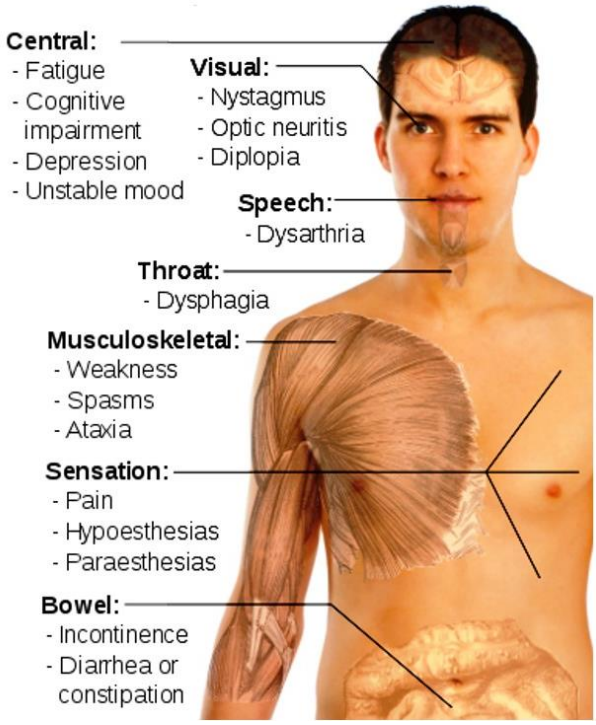

Figure 3. The major symptoms of MS are shown in the image (*Image by J.Oksenberg/UCSF*)

The timing, pattern, and co-occurrence of symptoms may influence symptom recognition and adversely affect quality of life. Some symptoms interact to make each other worse, for example, pain and depression, social withdrawal due to fear of incontinence, sedentary lifestyle and in general a deteriorated quality of life might appear (Newland et al., 2014). Structural equation modelling (SEM) enables researchers to examine diagnostic overlap for MS and depression and the complex relationships between patients' physical and mental health states (Gunzler et al., 2015). Multiple Sclerosis can also have a considerable influence on the individual's sense of self. Physical changes and functional limitations may lead to a sense of loss of identity or role strain, especially when the individual can no longer perform previously valued activities (Pagnini et al., 2014). People with MS struggle to continue working and a higher percentage of people with MS are unemployed compared to the rest of population. A Danish study found that the probability of remaining without an early pension 20 years after entry to the study was at 22% for people with MS while at 86% for non-MS controls (Sweetland et al., 2012).

1.1.3 Diagnosis

The initial MS diagnostic criteria were based on clinical features. The oldest of such criteria was Schumacher criteria which called for 2 separate clinical relapses in time and space while further specified signs and symptoms were missing Later Poser criteria added laboratory and paraclinical parameters for diagnosis with presence of oligoclonal bands in the CSF (Poser et al., 1983). With the advance of new neurological techniques such as magnetic resonance imaging (MRI) the need for clinical evidence is replaced with radiological and chemical markers (McDonald et al., 2001, Hurwitz, 2009). Currently the revised McDonald criteria is the most commonly used method in diagnosis of MS. McDonald criteria focus on clinical, radiography, and laboratory of the lesions at different times and different areas (Karussis, 2014).

Table 1. The 2010 revised McDonald Criteria for Diagnosis of MS (Polman et al., 2011)

Clinical Presentation	Additional Data Needed for MS Diagnosis
≥ 2 attacks; objective clinical evidence of ≥ 2 lesions or objective clinical evidence of 1 lesion with reasonable historical evidence of a prior attack	None
≥ 2 attacks; objective clinical evidence of 1 lesion	Dissemination in space, demonstrated by: ≥ 1 T2 lesion in at least 2 of 4 MS-typical regions of the CNS (periventricular, juxtacortical, infratentorial, or spinal cord); or Await a further clinical attack implicating a different CNS site.
1 attack; objective clinical evidence of ≥ 2 lesions	Dissemination in time, demonstrated by: Simultaneous presence of asymptomatic gadolinium-enhancing and nonenhancing lesions at any time; or A new T2 and/or gadolinium-enhancing lesion(s) on follow-up MRI, irrespective of its timing with reference to a baseline scan; or Await a second clinical attack.
1 attack; objective clinical evidence of 1 lesion (clinically isolated syndrome)	Dissemination in space and time, demonstrated by: For DIS: ≥ 1 T2 lesion in at least 2 of 4 MS-typical regions of the CNS (periventricular, juxtacortical, infratentorial, or spinal cord); or Await a second clinical attack implicating a different CNS site; and For DIT: Simultaneous presence of asymptomatic gadolinium-enhancing and nonenhancing lesions at any time; or A new T2 and/or gadolinium-enhancing lesion(s) on follow-up MRI, irrespective of its timing with reference to a baseline scan; or Await a second clinical attack.
Insidious neurological progression suggestive of MS (PPMS)	1 year of disease progression (retrospectively or prospectively determined) plus 2 of 3 of the following criteria: 1. Evidence for DIS in the brain based on ≥ 1 T2 lesions in the MS-characteristic (periventricular, juxtacortical, or infratentorial) regions 2. Evidence for DIS in the spinal cord based on ≥ 2 T2 lesions in the cord 3. Positive CSF (isoelectric focusing evidence of oligoclonal bands and/or elevated IgG index)

1.1.4 Subtypes

The vast variability of the clinical course of MS raised a need for a common language to describe the clinical courses and pathology of multiple sclerosis. This was addressed by the National MS Society in 1996, in defining four distinct clinical subtypes of MS:

- **Relapsing remitting MS (RRMS)** is characterized by clearly defined disease relapses with full recovery. Periods between disease relapses are characterized by a lack of disease progression.

- **Secondary progressive MS (SPMS)** is characterized by an initial relapsing-remitting disease course followed by progression with or without occasional relapses, minor remissions and plateaus.

- **Primary progressive MS (PPMS**) is defined as disease progression from onset with occasional plateaus and temporary minor improvements. The essential element in PPMS is a gradual, nearly continuously worsening with minor fluctuations, but no distinct relapses.

- **Progressive-relapsing MS (PRMS)** is defined as progressive disease from onset, with clear acute relapses, with or without recovery, with periods between relapses characterized by continuing progression.

Clinically isolated syndrome (CIS) was not included in the initial MS clinical description. CIS is now recognized as the first clinical presentation of a disease that shows characteristics of inflammatory demyelination that could be MS, but has yet to fulfil criteria of dissemination in time (Lublin et al., 2014).

1.1.5 Pathology

MS is considered primarily an inflammatory immune-mediated disease of the CNS in which auto-aggressive T-cells cross the blood–brain barrier (BBB) inflicting demyelination and axonal loss eventually leading to progressive disability (Ortiz et al., 2014). The MS inflammatory process is triggered by T-cells autoimmune reaction, targeting myelin antigens, possibly initiated through molecular mimicry mechanisms (cross-reactive

antigens expressed by viruses or other microorganisms, and myelin components) (Karussis, 2014). It is also proposed that due to malfunction in immunoregulatory mechanisms (such as those involving Th2, Th3, and CD8+ T-cells), myelin-specific T-cells which maybe naturally present, expand to critical pathogenic numbers (Venken et al., 2010). T-cell activation leads to myelin and oligodendrocyte phagocytosis by macrophages. Humoral immunity follows up by secretion of anti-myelin antibodies from B cells and subsequent fixation of complement and opsonization of the myelin sheath and the oligodendrocytes by macrophages (Bruck, 2005). Cytokines (IFN-γ and TNF) and chemokines released from these immune cells can be detected in MS lesions which can arise anywhere in the CNS (Cheng and Chen, 2014). However, the lesions are more likely to occur in optic nerve, spinal cord, brain stem, and periventricular areas. Furthermore, brain tissue immediately adjacent to the subarachnoid space, i.e. subpial gray matter, is especially vulnerable to demyelination (Stadelmann et al., 2011). The loss of myelin greatly enhances the propensity of axons for transport disturbance. Non-specific immune mediators, e.g. nitric oxide (NO), reactive oxygen species (ROS), and proteases lead to damage of naked and also myelinated axons as indicated by experimental studies. Neuronal antigens have been identified as targets of the immune reaction. Specific immune reactions against neurofilament, beta-synuclein, contactin-2/TAG-1, and neurofascin lead to CNS inflammation (Boretius et al., 2012). Such substances include free radicals, which can cause oxidative stress, and glutamic acid, which can cause excitotoxicity. Initial nonfatal damage to oligodendrocytes may initiate activation of an apoptotic cascade, perhaps by activation of death ligands or receptors such as Fas, FasL or Trail, that will result in delayed oligodendrocyte death. These apoptotic proteins can be activated by tumour necrosis factor, released from pro-inflammatory T cells in multiple sclerosis lesions, and have been demonstrated to promote oligodendrocyte cell death *in vitro*. Finally myelin sheath injury may render oligodendrocytes vulnerable to environmental toxins or viruses (Bruck, 2005).

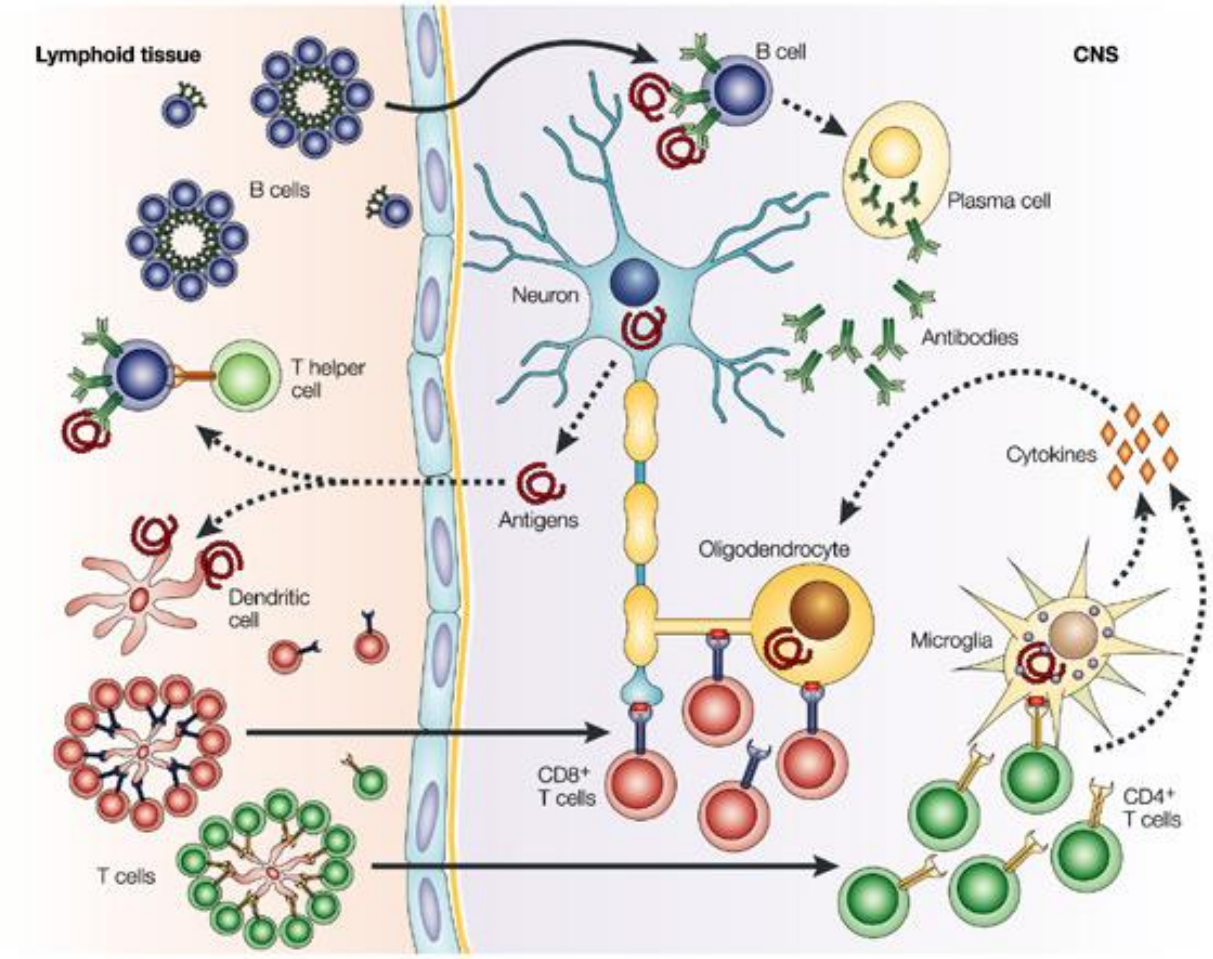

Figure 4. **Immune responses in multiple sclerosis.** Hypothetical view of immune responses in acute multiple sclerosis lesions. Independent of the causative event, two steps are required to induce an immune response in the central nervous system (CNS): a pro-inflammatory milieu in the CNS, leading to up-regulation of major histocompatibility complex (MHC) molecules, costimulatory receptors and inflammatory cytokines and an antigen-driven acquired immune response. T- and B-cell responses are primed in the peripheral lymphoid tissue by antigens that are released from the CNS or by cross-reactive foreign antigens. Dendritic cells that present neural antigens are strong stimulators of T-cell responses. After clonal expansion, T and B cells infiltrate the CNS. Clonally expanded B cells re-encounter their specific antigen, mature to plasma cells and release large amounts of immunoglobulin-γ (IgG) antibodies. These antibodies bind soluble or membrane-bound antigen on expressing cells. Clonally expanded CD8+ T cells also invade the brain and could encounter their specific peptide ligand, presented by glial or neuronal cells on MHC class I molecules. The recognition of specific MHC–peptide complexes on these cells prompts direct damage to expressing cells. CD4+ T cells migrate into the CNS and encounter antigens that are presented by microglial cells on MHC class II molecules. Reactivation of these cells leads to heightened production of inflammatory cytokines. These cytokines attract other immune cells, such as macrophages, which contribute to inflammation through the release of injurious immune mediators and direct phagocytic attack on the myelin sheath (Hemmer et al., 2002).

1.1.6 Treatment

To date, no concrete remedy has been established for MS treatment although, various immunomodulatory agents reducing disease effects are available. Immunomodulatory therapies in MS are directed against the presumed autoimmune pathogenic mechanism of the disease (Hemmer et al., 2002). The first disease modifying treatment (DMT) approved by the Food and Drug Administration (FDA) was interferon beta-1b (IFNb-1b) in 1993 (Paty and Li, 1993). Since then structurally diverse MS drugs have been developed which are classified based on their specificity of their modulatory mechanism into: immunomodulators and immunosuppressants (Mulakayala et al., 2013).

Immunomodulators like interferon beta (INFβ-1a, INFβ-1b) and glatiramer acetate (GA) moderate the malfunctioning of the lymphocytes by regulating their activation. They reduce the number of clinical relapses in the relapsing-remitting phase of the disease, and the formation of new lesions assessed by magnetic resonance imaging (MRI) (Pawate and Bagnato, 2015).

Immunosuppressants reduce the number of circulating lymphocytes along with the healthy immune cells of the body, which may lead to considerable side effects. Each of these compounds has a unique mechanism of action and typically administered orally or intravenously. The most common orally administrated compounds include: cladribine, fumaric acid, teriflunomide, laquinimod. The example for intravenous compounds are cyclophosphamide (Kieseier et al., 2005, Mulakayala et al., 2013).

With the development of monoclonal antibodies such as alemtuzumab, natalizumab, ocrelizumab, rituximab (all administered intravenously), daclizumab (subcutaneous admistration), and small molecules like fingolimod (taken orally), specific immunomodulation has become an important therapeutic option for MS treatment (Mulakayala et al., 2013).

1.2 Animal models of MS and EAE

1.2.1 Overview

MS is a complex human disease and a single animal model cannot address the spectrum of MS heterogeneity in clinical and radiological presentation (Pachner, 2011). Over the last decades different animal models have been used to study the pathogenic mechanisms of MS which could serve as a testing tool to study disease development and in order to establish novel therapeutic approaches (Procaccini et al., 2015). Animal models are precious resources in investigating CNS tissue which is the main target of multiple sclerosis. This could fill the gap of direct access to human tissues, biopsies, or autopsy samples which are rarely performed. The established animal models for MS are i) the experimental autoimmune/allergic encephalomyelitis (EAE); ii) Theiler's murine encephalomyelitis virus (TMEV) induced models and iii) toxin-induced models of demyelination, such as the cuprizone and the lyso-phosphatidylcholine (lyso- lecithin) (Table 2) (Procaccini et al., 2015, Gold, 2006).

1.2.2 EAE

EAE is the oldest and most frequently used experimental model to study immune regulation of MS (Webb, 2014). This model is studied in many different species, including primates and rodents and is a CD4+ Th1 cell mediated autoimmune disease in CNS (Linker and Lee, 2009, Skundric, 2005). EAE model is heterogeneous and influenced by the selected antigen, species and the genetic background (Pachner, 2011). The specific mechanisms that lead to the onset of the disease, spontaneous recovery and relapse are not completely understood. It seems that upon EAE immunization pro-inflammatory cytokines released within the CNS by infiltrating immune cells, or locally produced in response to CNS inflammation, may contribute to increase vascular permeability, inflammatory cell extravasation, antigen presentation, glial activation and the destruction of oligodendrocytes and myelin (Giatti et al., 2013). No single EAE model can fully reproduce the spectrum of MS and instead different genetic backgrounds need to be immunized with different antigens in order to provide the immunological and histopathological aspects of the MS (Kuerten et al., 2008).

1.2.3 EAE subtypes

EAE is induced through two major subtypes: 1) active immunization with myelin peptides 2) passively or adoptively transferred EAE (Fig. 5) (Skundric, 2005). In active EAE, susceptible strains of mice are immunized with an appropriate myelin antigen or peptide emulsified in a mineral oil-based adjuvant (Freund's adjuvant) with an additional heat-inactivated mycobacteria (complete Freund's adjuvant, CFA) (Linker and Lee, 2009). Some models (especially in mice) also require the intraperitoneal injection of pertussis toxin on the day of immunization and 48 hrs later which play a role in the breakdown of the blood-brain-barrier and also deplete regulatory T cells, thus enhance autoimmune reactions (Racke, 2001). In all cases, the relevant immunogen is derived from self-CNS proteins such as myelin basic protein (MBP), proteolipid protein (PLP) or myelin oligodendrocyte glycoprotein (MOG) (Linker and Lee, 2009, Gold, 2006).

EAE could also be induced through the passive or adoptive transfer by injecting mice with activated, myelin-specific T cells (Racke, 2001). Classic models of adoptive transfer involve the immunization of donor mice with PLP-derived peptides, isolation of peripheral lymphoid cells after 7/10 days of culture, *in vitro* re-stimulation with myelin peptide and subsequent transfer into naïve recipients. These models were useful to demonstrate the central role of $CD4^+$ T cells in the pathogenesis of EAE. The limitations of this method is that the T cells directed against a specific antigenic epitope and the encephalitogenic capacity of transferred T cells not necessarily reflects the *in vivo* condition in donor animals. The decreased capability of knockout T cells to transfer the disease could, for example, reflect defective antigen presentation in the donor animals, rather than alteration in T cell functions from lesions. This aspect, combined with the pleiotropic nature of immune gene expression, makes it difficult to use the adoptive transfer model to define the contributions of individual genes to encephalitogenic T cell function (Procaccini et al., 2015).

Table 2. Characteristics of different mouse models of MS (Procaccini et al., 2015)

Model of MS	Mechanism	Application	Involved cells	Translational value
Relapsing–remitting EAE in SJL/J mice	Immunization of SJL/J mice with $PLP_{139-151}$	Study of neuroinflmmation and immune system activation	CD8, CD4, Th17, monocytes, macrophages, B cells, Treg cells	Relapsing–remitting MS, study of the relapse rate, testing therapeutical agents
Chronic EAE in C57BL/6J mice	Immunization of C57BL/6J mice with MOG_{35-55}	Study of neuroinflmmation and immune system activation	CD8, CD4, Th17, monocytes, macrophages, B cells, Treg cells	Primary progressive MS, secondary progressive MS, testing therapeutical agents
EAE in transgenic mice	T cell clone (2D2) expressing Vα and Vβ chains reacting specifically to MOG_{35-55}, or B cell heavy chain knock-in mouse strain (IgH MOG)	Study of neuroinflmmation and immune system activation	CD8, CD4, Th17, monocytes, macrophages, B cells, Treg cells	*In vitro* study of immune cell activation and function
Theiler's murine encephalomyelitis virus (TMEV)	Infection with picornavirus, such as Theiler's murine encephalomyelitis virus (TMEV)	Study of axonal damage and inflammatory-induced demyelination	Macrophage/microglia, oligodendrocyte, astrocytes and CD4, CD8	Primary progressive MS, study of brain, brainstem and spinal cord lesions, study of new therapeutic approaches targeting adhesion molecules, axonal degeneration
Cuprizone-induced MS	Feeding C57BL/6 mice with 0.2% cuprizone for 6 weeks	Study of the de- and re-myelination processes	Oligodendrocytes, astrocytes, microglia	Therapeutical trials designed to repress demyelination or accelerate remyelination
Lysolecithin-induced MS	Lysolecithin injection in SJL/J mice	Study of the de- and re-myelination processes	Oligodendrocytes, astrocytes, microglia	Therapeutical trials designed to repress demyelination or accelerate remyelination

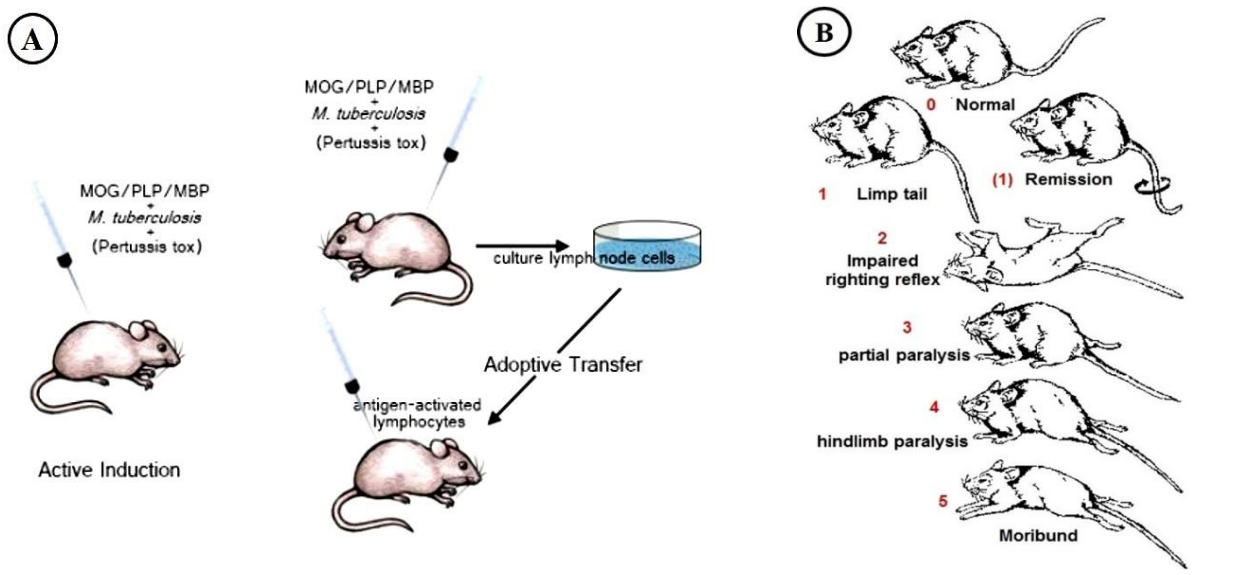

Figure 5. A) Methods of EAE induction. **Active** induction involves injecting animals with myelin proteins such as MOG, PLP, or MBP along with *Mycobacterium tuberculosis* and pertussis toxin, both of which act as immunostimulants. In **adoptive transfer**, the lymph nodes of immunized animal (with myelin antigens) are removed and antigen-primed lymphocytes are extracted and cultured *in vitro*. These activated immune cells are then injected into another animal to induce the disease (MS Discovery Forum). **B)** 5-points scale of EAE clinical score in mice (Hooks Laboratory, EAE protocol).

1.2.4 MOG induced EAE

In the C57BL/6 mouse strain, the H-2b MHC haplotype governs the ability to induce encephalitogenicity and to develop demyelinating autoantibodies in response to mouse or rat MOG. Transfer of these demyelinating anti-MOG antibodies also enhances demyelination and exacerbates disease severity in mouse models of EAE. Over the last 15 years, the avenue of genetically engineered mice has greatly promoted the investigation of EAE pathomechanisms, particularly after backcrossing strains on the C57BL/6 background. MOG-EAE in the C57BL/6 mouse is one of the most widely used models in neuroimmunological research (Linker and Lee, 2009).

EAE inducing antigen has specific activation pattern and produce particular symptoms and intensity. In SJL mice $PLP_{139-151}$ EAE induction leads to relapsing-remitting disease while MOG_{1-20} or MOG_{92-106} develop either acute or chronic sustained EAE (Skundric, 2005). In mice MOG_{35-55} peptide can induce EAE in C57BL/6 mice or Biozzi ABH mice resulting in a relapsing-remitting or chronic disease course (Linker and Lee, 2009). While several peptides could induce T cell responses, only MOG_{35-55} is able to induce CNS autoimmunity upon immunization (Rangachari and Kuchroo, 2013). MOG_{35-55}-induced EAE is generally characterized by CD4+ T cells, macrophages and granulocytes detection within the lesions throughout the disease (Kuerten et al., 2008). MOG_{35-55}-driven EAE analysis also provide information on CD8+ T cell function in CNS autoimmunity. CD8+ T cells have a role in MS pathology since it is shown that CD8+ T cells outnumber CD4+ T cells in MS lesions by as much as 10 to 1 (Rangachari and Kuchroo, 2013).

The clinical course of EAE, depending on the strain and the antigen used, will manifest in the form of weakness in 10 to 15 days after immunization (Racke, 2001). The weakness in EAE is usually associated with flaccidity, that is, decreased muscle tone. Most EAE investigators use a relatively subjective visual assessment grading scale of zero to five for grading weakness rather than objective neurobehavioral analyses (Pachner, 2011). This scaling is characterized by an ascending paralysis beginning at the tail, followed by hindlimb and forelimb paralysis (Fig 5B) (Procaccini et al., 2015).

1.3 Glial cells and MS

1.3.1 Glia

The nervous system is formed by two major cell types, neurons and glial cells (Araque and Navarrete, 2010). Glial cells also referred as neuroglia or glia, are non-neuronal cells in the CNS. They represent the most abundant cell population in the central nervous system and for years they have been thought to provide just structural and trophic support to neurons (Jessen and Mirsky, 1980). Glial cells are essential for the organization and function of the nervous system. In addition to their “traditional” roles in providing nourishment and support for neurons, glial cells regulate synaptic transmission, maintain the blood-brain barrier, mediate communication between the nervous and immune systems and monitor the nutritional state of organisms. Highlighting their critical role during embryogenesis and in postnatal life, several developmental, degenerative, and inflammatory disorders of the nervous system have been associated with deficits in glial cell function (Boesmans et al., 2015).

There are three types of glial cells in the mature central nervous system: astrocytes, oligodendrocytes, and microglia (Figure 6) (Nagelhus et al., 2013). Astrocytes, the most numerous cell type in brain, fill most of the space between neurons and blood vessels. Recent studies show that astrocytes have strong impact on neuronal function, neuronal development, and brain ageing. Astrocytes regulate extracellular ion concentration, water homeostasis and the acid-base balance in the brain. They also actively modulate synaptic transmission by releasing neuroactive compounds (Araque and Navarrete, 2010, Nagelhus et al., 2013). Oligodendrocytes, which are also restricted to the central nervous system, lay down a laminated, lipid-rich wrapping called myelin around axons. Myelin has important effects on the speed of the transmission of electrical signals. In the peripheral nervous system, the cells that elaborate myelin are called Schwann cells (Neuroscience / edited by Dale Purves: Third Edition). Microglia are hematopoietic in origin, have phagocytic capability, and are found in the CNS. They perform functions related to the immune response in a wide variety of neuroinflammatory processes. Their high functional plasticity is demonstrated by the fact that they are activated by a number of different diseases that affect the CNS. Activated microglia express different types of cell surface

molecules, including Fc receptors, scavenger receptors, cytokine and chemokine receptors, CD11b, CD11c, CD14, and major histocompatibility complex (MHC) molecules (Lopategui Cabezas et al., 2014).

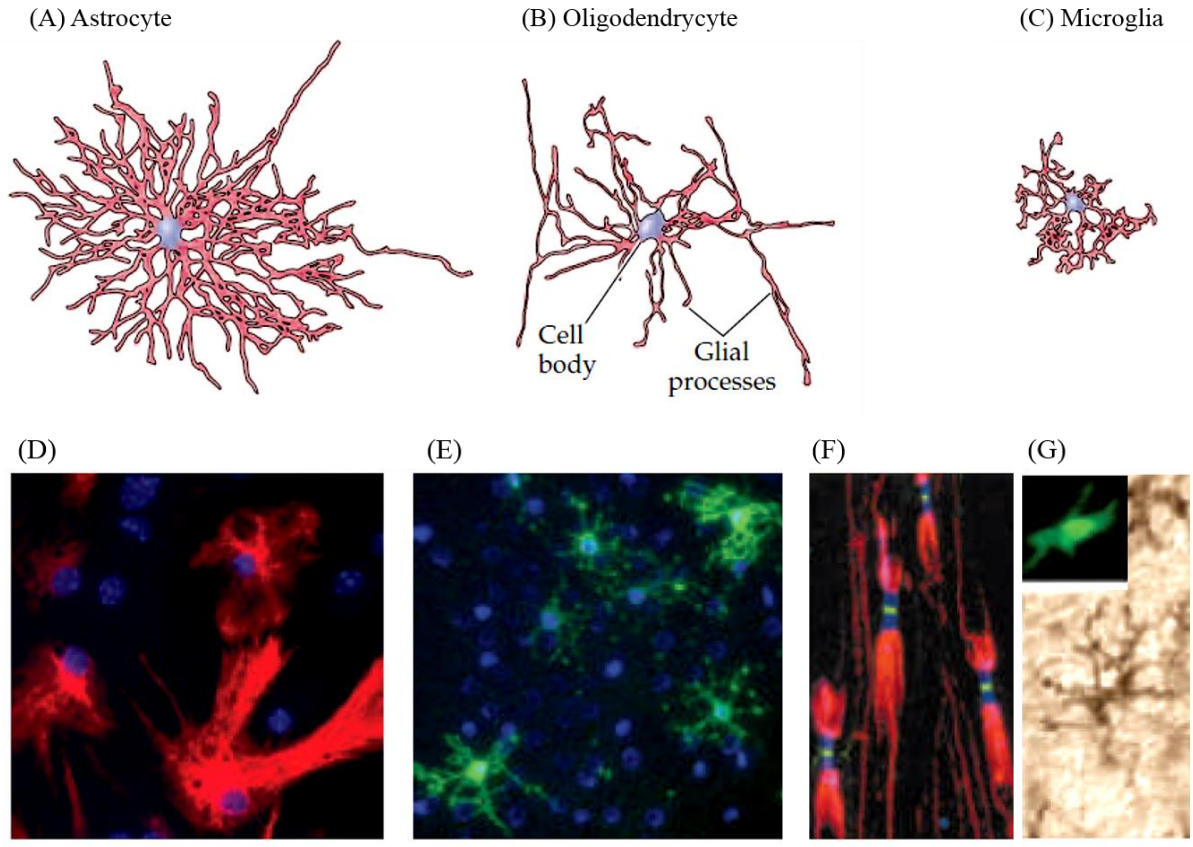

Figure 6. Varieties of neuroglial cells. **(A)** Tracings of an astrocyte, **(B)** an oligodendrocyte, **(C)** a microglial cell. **(D)** Astrocytes in tissue culture, labelled (red) with an antibody against an astrocyte-specific protein. **(E)** Oligodendroglial cells in tissue culture labelled with an antibody against an oligodendroglial-specific protein. **(F)** Peripheral axon are ensheathed by myelin (labelled red) except at a distinct region called the node of Ranvier. The green label indicates ion channels concentrated in the node; the blue label indicates a molecularly distinct region called the paranode. **(G)** Microglial cells from the spinal cord, labelled with a cell type-specific antibody. Inset: Higher-magnification image of a single microglial cell labelled with a macrophage-selective marker (Neuroscience / edited by Dale Purves: Third Edition).

1.3.2 Glial related neurological disorders

Glial cells are associated to numerous neurological disorders such as Creutzfeldt-Jakob disease, HIV-associated dementia, cerebral infarct, ALS, and epilepsy (Steinhauser and Seifert, 2012, Lopategui Cabezas et al., 2014). Inflammatory response of glial cells could exacerbate pathogenesis of neurodegenerative and autoimmune diseases such as Alzheimer's disease, Parkinson's disease and Multiple sclerosis. In these diseases, inflammation occurs in order to clean up the lesion and to limit disease progression. However, prolonged and sustained inflammatory reactions could cause cytotoxic effects and increase the severity of the disease. Immunoreactive glial cells release proinflammatory cytokines, chemokines and deleterious free radicals in neurodegenerative diseases (Kempuraj et al., 2013).

1.3.3 Oligodendroglia and myelin

A series of highly complex coordinated processes regulate the development of healthy and functional nervous system during fetal life (From et al., 2014). Myelinogenesis, the establishment of the myelin sheath, is critical for optimization of conduction velocity, as well as maturation, survival, and regenerative capacity of the axons (Paz Soldan and Pirko, 2012). Myelin is a lipoprotein ensheathment of the axons with about 1 μm thickness (Patel and Balabanov, 2012). The composition of myelin is ~70% lipid and 30% protein, which is in contrast to other membranes typically made of 30–50% lipid. Various classes of lipids are present in oligodendrocytes and myelin membranes, including cholesterol, phospholipids, and glycosphingolipids (Jackman et al., 2009). Major myelin proteins include ~50% proteolipid protein (PLP), a group of myelin basic protein (MBP) isoforms (~30% of the total), and minor proteins such as MOG, CNPase, MAG (Mallucci et al., 2015). Myelinated axons conduct action potentials by a saltatory mode between nodes of Ranvier to increase both the speed and energy efficiency of nerve conduction (Mitew et al., 2014). In rodents and humans, myelinogenesis occurs predominantly postnatally (within the first 3 weeks and 2 years, respectively), by regulated steps that ensure myelination at the appropriate time and location (From et al., 2014).

Oligodendrocytes are the myelin producing cells in the CNS (Bankston et al., 2013). The generation of myelin during development involves a finely-tuned pathway of oligodendrocyte precursor cell (OPC) specification, proliferation and migration followed by differentiation and the subsequent myelination of appropriate axons (Mitew et al., 2014). OPCs originate in sequential waves from particular germinal regions in specific areas of the developing CNS (Mitew et al., 2014). Once generated, they migrate towards their destinations where they differentiate into mature oligodendrocytes (Bradl and Lassmann, 2010). Two different populations of oligodendrocyte precursor cells have been identified during development (i) one type of OPC is characterized by the expression of plp/dm-20 and these do not depend on PDGF-AA growth factor; (ii) the second and largest population of oligodendrocyte precursor cells does depend on this growth factor and express PDGFRα (Clemente et al., 2013). The oligodendrocytes differentiation involves signalling processes between the Notch1 receptor, its ligand Jagged 1 located on the axonal surface, and c-secretase (Bradl and Lassmann, 2010). Only maturing oligodendrocytes initiate and maintain myelin formation within a brief period of time during differentiation. Therefore, a tremendous amount of proteins and other biomolecules should be synthesized, sorted, and trafficked in short period of time (Bryant et al., 2009). For instance, MBP is targeted by transport of its mRNA which is assembled into granules in the soma of oligodendrocytes, transported along processes, and then localized to the myelin membrane (Bradl and Lassmann, 2010). In adult CNS, 5% of all cells are OPCs that retain the capacity to proliferate, migrate, and differentiate into oligodendrocytes. These endogenous oligodendrocyte precursor cells react to damage in demyelinating diseases, like MS, representing a key element in spontaneous remyelination (Crawford et al., 2014).

1.3.4 Oligodendroglia in MS and EAE

Oligodendroglial diseases invariably produce some degree of demyelination, which is thought to underlie their clinical signs and symptoms. The most directly associated disorder with oligodendroglial injury is multiple sclerosis (Morrison et al., 2013). MS oligodendrocyte injuries could be studied under 2 categories of specific and non-specific injuries (Patel and Balabanov, 2012).

Specific mechanisms of oligodendrocyte injury are modulated by T and B cells. CD8+ lymphocytes, the MHC class I restricted T cells, are involved in antigen-specific cytotoxicity and are the most common lymphocyte subset identified in acute MS lesions. CD8+ cytotoxicity is mediated through cell surface FasL, IFN-γ, TNF-α, lymphotoxin, granzyme B, and perforin. In inflammation, oligodendrocytes upregulate the expression of MHC class I molecule, as well as Fas, IFN-γ and TNF-α receptors rendering them direct targets of CD8+ cells (Patel and Balabanov, 2012, Mars et al., 2011). Activated helper T cells (TH) 1 produce proinflammatory, cytotoxic factors of TNF-α, IFN-γ, which promote oligodendrocyte death and demyelination (Cudrici et al., 2006). The γδ T cells (not MHC restricted lymphocytes) are also present in the acute lesions and destroy oligodendrocytes by expressing stress proteins such as heat-shock proteins and alpha-crystallin (Harirchian et al., 2012). B-cells can exert effector functions as antigen-presenting cells, by cytokine and antibody production. Memory B-cells serve as highly efficient antigen-specific APCs and myelin-reactive memory B-cells can be found in the peripheral blood of MS patients (von Budingen et al., 2015).

Non-specific injury occurs as a complication of the inflammatory process. Monocytes, microglia, and astrocytes present in the lesions express receptors (MHC class II, Toll-like, and Fc receptors) and secrete a variety of molecular signals required for propagation of the inflammatory process. They also produce factors with cytotoxic activity, which contribute to the expansion of tissue injury, including proteolytic and lipolytic enzymes, reactive oxygen and nitrogen species (O_2 −, H_2O_2, OH−, NO, ONOO−), and excitotoxins (Patel and Balabanov, 2012). The most vulnerable cells of the CNS to such factors are oligodendrocytes and this is due to ceramide, a component of the myelin sphingolipids which can activate pro-apoptotic signalling in response to oxidative injury (Schenck et al.,

2007). The other facts making oligodendrocytes prone to oxidative stress are their high metabolic rate (necessary for myelin maintenance) and large amounts of protein output (making it susceptible to endoplasmic reticulum stress) (Patel and Balabanov, 2012).

In MS, successful remyelination in the injured CNS is dependent on the survival and differentiation of oligodendrocyte progenitor cells rather than regeneration by mature, myelinating oligodendrocytes (Moore et al., 2015). Nevertheless, remyelination efficiency is generally low and repair gradually fails as the disease progresses over time, ultimately leading to significant clinical disability. This failure of remyelination was shown to be mainly due to a blockade of oligodendroglial differentiation and maturation (Gottle et al., 2015). In situ analysis of active MS lesions suggested that OPCs are more vulnerable to injury than mature oligodendrocytes within the same lesion site. *In vitro* and animal studies also indicated enhanced vulnerability of OPCs to proinflammatory mediators, including TNF-a, compared with more mature oligodendrocyte lineage cells (Moore et al., 2015).

Although, EAE recapitulates many critical events of MS pathogenesis including oligodendrocyte cell injury and death, traditional EAE has certain limitations. It cannot delineate oligodendrocyte response to injury or isolate its most intricate mechanisms (Patel and Balabanov, 2012). To date, various animal models are developed to study different aspects of oligodendrocytes remyelination including: lysolecithin and ethidium bromide focal injections, oral cuprizone administration, and inflammatory models. The inflammatory process is critical in inducing OPC activation and subsequent remyelination as several models of inflammation-induced demyelination show spontaneous remyelination. However, in MOG induced EAE remyelination is not very extensive, perhaps due to the dense infiltration of macrophages and microglia in the lesion over prolonged periods of time. The only indication of impressive levels of remyelination in EAE is observed in focal models of cortical demyelination involving immunization with subclinical doses of MOG and injection of pro-inflammatory mediators (Miron et al., 2011).

1.4 FGF/FGFR and MS

1.4.1 Fibroblast Growth Factors (FGF)

The fibroblast growth factor (FGF) family is a group of multifunctional signalling molecules which are involved in numerous cellular processes such as proliferation, migration, and differentiation and various physiological processes such as mitogenesis, angiogenesis, embryogenesis, regulating metabolism and wound healing (Teven et al., 2014). FGF growth factors have been identified in various multicellular organisms from the nematode to humans (Itoh, 2007). In mammals, the FGF family consist of 22 structurally related proteins (Woodbury and Ikezu, 2013). Based on the modes of action, mechanisms of secretion and ultimate biological consequences, these proteins have been further grouped into several subfamilies, each sharing both genetic and functional similarity. They include FGF1 subfamily (FGF1 and FGF2), FGF4 subfamily (FGF4, FGF5, FGF6), FGF7 subfamily (FGF3, FGF7, FGF10 and FGF22), FGF8 subfamily (FGF8, FGF17 and FGF18), FGF9 subfamily (FGF9, FGF16 and FGF20), FGF19 subfamily (FGF19, FGF21 and FGF23), and FGF homologous factor (FHF) subfamily (FGF11 (FHF3), FGF12 (FHF1), FGF13 (FHF2), and FGF14 (FHF4)) (Imamura, 2014). FGFs share a similar internal core and have a characteristically high binding affinity for both heparin and fibroblast growth factor receptors (FGFRs) (Teven et al., 2014). They exert their activities mainly *via* paracrine and/or autocrine modes of action by activating one or more cell surface receptor tyrosine kinases (Imamura, 2014).

FGF-binding protein (FGFBP) is a carrier protein that activates FGFs by releasing them from the extracellular matrix, where they are bound by heparan sulphate glycosaminoglycan (HSGAG). FGFBP has been shown to increase FGF2-dependent proliferation of fibroblast cells and may have an important role in the development of some cancers. Other activators of FGF signalling include fibronectin leucine-rich transmembrane protein 3 (FLRT3), which facilitates FGF8 activity through the MAPK pathway (Beenken and Mohammadi, 2009). FGFs are crucial to development of the CNS, which explains their importance in adult neurogenesis. During development, high levels of FGF2 are detected from neurulation onwards. Moreover, developmental expression of

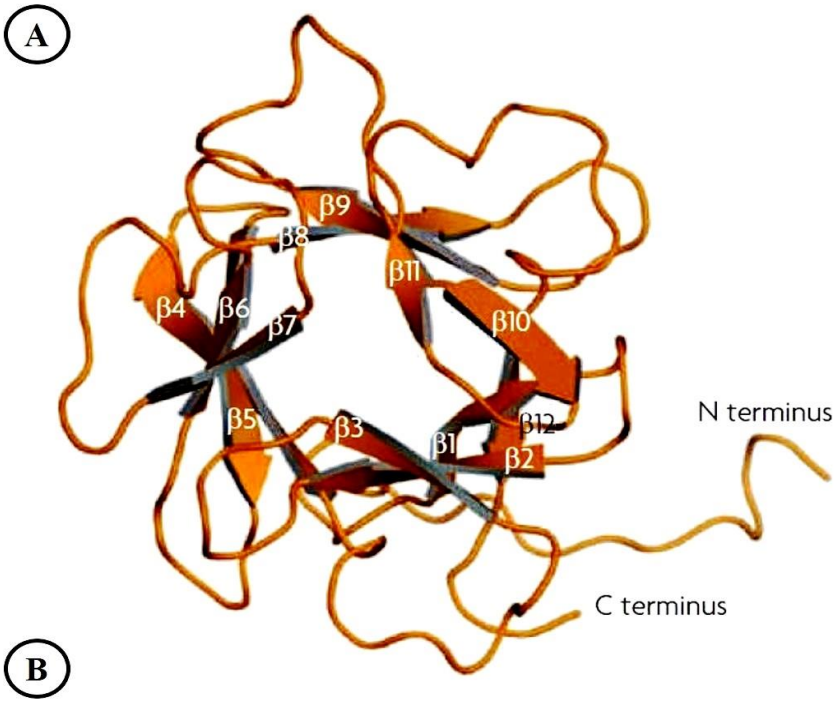

LIGANDS				RECEPTORS		
Scheme	Family		Members	FGFR	Isoforms	Scheme
SP HSPG binding domain	*cFGFs*	FGF4	FGF3	*1, 2*	IIIb	SP IgGI AB HSPG IgGII IgGIII TM KI KII
			FGF4	1, 2, *3*, 4	IIIc	
			FGF6	*1, 2*, 4		
		FGF5	FGF1	1, 2, 3, 4	IIIb, IIIc	
			FGF2	1, 2, 3, 4		
			FGF5	*1, 2*	IIIc	
		FGF8	FGF8	*1*, 2, **3, 4**	IIIc	
			FGF17	*1*, 2, 3, *4*		
			FGF18	*2, 3, 4*		
		FGF9	FGF9	*2*, 3	IIIb, IIIc	
			FGF16	*2, 3*	IIIc	
			FGF20	*1, 2*, 3, *4*	IIIb, IIIc	
		FGF10	FGF7	**2, 4**	IIIb	
			FGF10	*1, 2*		
			FGF22	*1, 2*		
	hFGFs	FGF15/19	FGF15/19	1, **2, 3, 4**	IIIb, IIIc	
			FGF21	*1*, 2, *3*, **4**		
			FGF23	*1*, 2, *3*, **4**		
	iFGFs	FGF11	FGF11			
			FGF12			
			FGF13			
			FGF14			

Figure 7. Structural features of FGF ligands and their specific receptors. A. FGF1, showing its 12 antiparallel β-sheets and amino and carboxyl termini (Beenken and Mohammadi, 2009). **B.** the 22 FGFs, grouped according to their subfamily. The family of FGF receptors contains four main members (FGFR1 to 4) and each receptor could be activated with more than a single ligand (Guillemot and Zimmer, 2011).

FGF2 and its receptors is temporally and spatially regulated, concurring with development of specific brain regions including the hippocampus and substantia nigra pars compacta (Woodbury and Ikezu, 2013). FGF2 regulates neural stem cells propagation both *in vitro* and *in vivo* (Gritti et al., 1996).

The involvement of FGF signalling in human disease is well documented. Deregulated FGF signalling can contribute to pathological conditions either through gain or loss of function. For instance, mutations in FGF23 (gain of function) in autosomal dominant hypophosphataemic rickets, in FGF10 (loss of function) in lacrimo-auriculo-dento-digital syndrome (LADD syndrome), FGF3 (loss of function) in deafness and FGF8 (loss of function) in Kallmann syndrome (Beenken and Mohammadi, 2009). FGFs are also involved in the inflammatory process. FGF-1 and FGF-2 upregulated in inflammatory disorders such as bowel syndrome, Crohn's disease, ulcerative colitis, and rheumatoid arthritis. Other reports have suggested that FGF-1 and FGF-2 are secreted by and may act as immunoregulators of infiltrating neutrophils, monocytes, macrophages, and T lymphocytes, often in tandem with powerful inflammatory cytokines (Haddad et al., 2011). FGF2 has been identified as a neuroprotective factor in preventing disease and in milder course of EAE (Woodbury and Ikezu, 2013). More severe EAE disease course was observed in FGF2(−/−) mice vs. FGF2(+/+) mice, specifically measured by increased infiltration of macrophages/microglia and CD8+ T-cells, increased nerve fibre degeneration, and decreased remyelination of axons, suggesting a protective role of FGF2 (Rottlaender et al., 2011).

1.4.2 FGF Receptors (FGFR)

The effects of FGF ligands are mediated by binding to four FGF receptors (FGFR1–4) and their splice variants (Jiang et al., 2015). FGFRs are tyrosine kinase receptors (RTK) that contain a heparin-binding sequence, three extracellular immunoglobulin (Ig)-like domains (D1eD3), an acidic box, a hydrophobic transmembrane domain, and a split intracellular tyrosine kinase domain (Teven et al., 2014). The IgIII domains of FGFR1–3 are encoded for by exons 7–9. Inclusion of exons 8 and 9 is mutually exclusive, producing

the IIIb and IIIc splice isoforms (Morita et al., 2014). This alternative RNA splicing of FGFRs 1–3 is an essential determinant of ligand binding specificity. The IIIb and IIIc splice forms are regulated in a tissue specific manner, such that the b isoform is restricted to epithelial lineages and the c isoform is preferentially expressed in mesenchymal lineages (Zhang et al., 2006). The diversity in FGF signalling is due, in part, to different FGF/FGFR combinations. Additionally, alternative splicing in the FGFR Ig-like domains generates additional receptor isoforms with novel ligand affinities (Haddad et al., 2011). Finally, effector cells will usually express different heparan-sulfates at their surface, which are responsible for stabilizing FGF/FGFR complexes and enhancing FGFR downstream signalling (Haddad et al., 2011).

FGF1 is known to activate all seven FGFR subtypes, while FGF2 shows greater receptor specificity, activating only FGFR1c, FGFR2c, FGFR3c, FGFR4 and, to a lesser degree, FGFR1b (Imamura, 2014). The FGFR activation is in a HSGAG-dependent manner. Upon binding of ligand and HSGAG, FGFRs dimerize, enabling the cytoplasmic kinase domains to transphosphorylate on “A” loop tyrosines to become activated. A loop phosphorylation is followed by phosphorylation of tyrosines in the C tail, kinase insert and juxtamembrane regions. The two main intracellular substrates of FGFR are phospholipase C (PLC) γ1 (also known as FRS1) and FGFR substrate 2 (FRS2). Phosphorylation of an FGFR-invariant tyrosine (Y766 in FGFR1) at the C tail of FGFR creates a binding site for the SH2 domain of PLCγ and is required for PLCγ phosphorylation and activation. Phosphorylation of FRS2 is essential for activation of the Ras–mitogen-activated protein kinase (MAPK) and phosphoinositide 3-kinase–AKT signalling pathways (Figure 8) (Beenken and Mohammadi, 2009).

FGF/FGFR interactions comprise a large signalling network, playing key roles in different physiological processes and functions including embryonic development and normal tissue homeostasis via ligand binding of the extracellular domains in FGFRs (Tchaicha et al., 2014). Germline gain-of-function mutations in FGFR contribute in many skeletal syndromes, Kallmann syndrome. Most of the FGFR mutations are ligand independent, but a few manifest only during ligand binding. Apert’s syndrome is the result of such mutation which enhances ligand binding of inappropriate ligands (Beenken and

Mohammadi, 2009). Most of the FGFR3 mutations found in cancer are identical to the FGFR2 mutations involved in skeletal disorders. Kinase domain loss-of-function mutations also occur in FGFR2 and FGFR3 in LADD syndrome and in FGFR2 in melanoma (Rohmann et al., 2006). Direct inhibition of FGFRs may prove to be of clinical value. Inhibitory molecules such as NDGA that target a specific subcellular compartment may be beneficial in the inhibition of activated receptors such as FGFR3 that signal from the same compartment (Meyer et al., 2008).

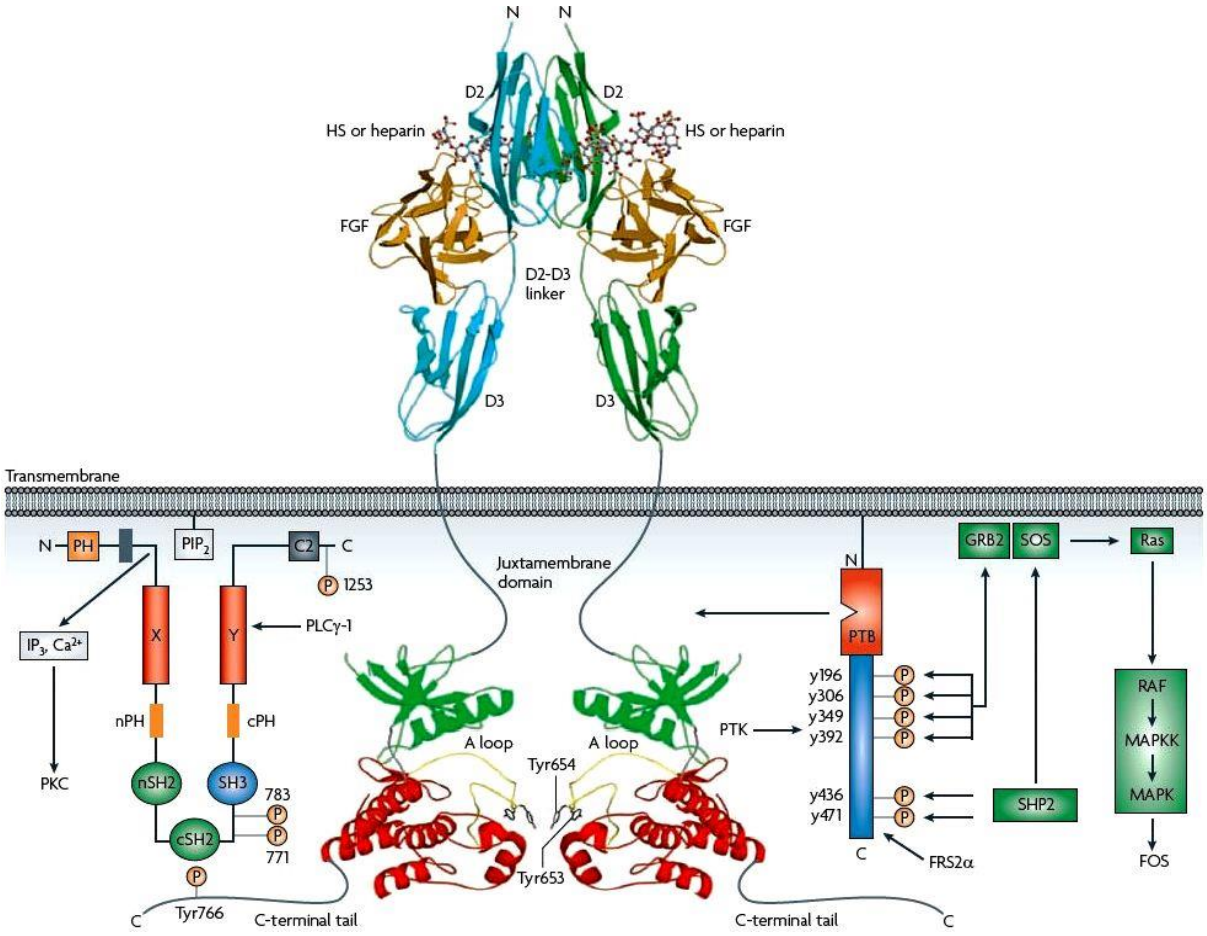

Figure 8. Fibroblast growth factor receptor (FGFR) signalling. Structurally unresolved regions are shown as grey lines. Amino-terminal and carboxy-terminal lobes of the kinase domain are coloured green and red, respectively. The two major intracellular targets, phospholipase (PLC)γ1 and FGFR substrate 2α (FRS2α), are shown. A loop, activation loop; GRB2, growth factor receptor bound 2; HS, heparan sulphate; IP3, inositol-1,4,5-trisphosphate; MAPK, mitogen-activated protein kinase; MAPKK, mitogen-activated protein kinase kinase; PH, pleckstrin homology domain; PIP2, phosphatidyl inositol-4,5- bisphosphate; PKC, protein kinase C; PTB, phosphotyrosine binding domain; PTK, protein tyrosine kinase; SH, Src homology domain (Beenken and Mohammadi, 2009).

1.4.3 FGFR2

Fgfr2 gene at human chromosome 10q26 encodes FGFR2b and FGFR2c isoforms due to alternative splicing (Katoh and Katoh, 2009). FGFR2b isoform is expressed in epithelial cells, and that the FGFR2c is expressed in mesenchymal cells (Orr-Urtreger et al., 1993). FGFR2b on epithelial cells is a high affinity receptor for FGF1, FGF3, FGF7, FGF10 and FGF22 while the FGFR 2c isoform on mesenchymal cells is a high affinity receptor for FGF1, FGF2, FGF4, FGF6, FGF9, FGF16 and FGF20. FGFR 2b and FGFR2c show distinct expression domain and ligand specificity (Zhang et al., 2006, Morita et al., 2014). The lineage-specific expression of the IIIb and IIIc isoforms of FGFRs enables interaction between the epithelial and mesenchymal layers during development in response to different FGFs (Eswarakumar et al., 2005). FGF7, FGF10, and FGF22 constitute a subfamily among the FGF family. FGF7, induced by PDGF, IL-1, IL-1ß or TNF-α, is secreted from fibroblast, smooth muscle cells, endothelial cells, skin dermis, and γδT cells to promote tissue repair (auf demKeller et al., 2004). FGF10 is secreted from mesenchymal cells to orchestrate morphogenesis of gastrointestinal tract, respiratory tract, limb, and other organs or tissues. FGF22 is secreted from cerebellar granule cells to regulate synapse formation. FGF7, FGF10 and FGF22 transduce signals through FGFR2b on epithelial cells to regulate embryogenesis and adult tissue homeostasis (Katoh and Katoh, 2009).

It has been shown that $Fgfr2^{-/-}$ mice die at E10.5 due to defects in the placenta. However, selective disruption of the FGFR2b isoform leads to severe impairment in the development of the lung, limbs and other tissues resulting in lethality immediately after birth. Disruption of the FGFR2c isoform, on the other hand, results in impairment in skull and bone development, but the mutant mice are viable (Eswarakumar et al., 2005). FGFR2b and FGFR2c function as FGF receptors transducing FGF signals to RAS-ERK and PI3K-AKT signalling cascades through FRS2, and also to DAG-PKC and IP3-Calmodulin signalling cascades through PLCγ. FGFR2b and FGFR2c with extracellular Ig-like domains and cytoplasmic tyrosine kinase domain are almost identical except the latter half of the third immunoglobulin-like domain (Katoh and Katoh, 2009).

1.4.4 FGFR2 related disorders

Fgfr2 mutations around the third Ig-like domain result in FGFR2 signalling activation due to the creation of autocrine FGF signalling loop. While mutations within tyrosine kinase domain results in FGFR2 signalling activation due to the release of FGFR2 from autoinhibition (Katoh and Katoh, 2009). Most of the Fgfr mutations are ligand independent, but a few such as Ser252Trp and Pro253Arg in the ectodomain of Fgfr2 manifest only during ligand binding. These mutations cause Apert syndrome by enhancing ligand binding affinity and promoting the binding of inappropriate ligands (Beenken and Mohammadi, 2009). Fgfr2 mutations that enhance receptor activity cause abnormal fusions of the bones within the skull and limbs in Apert, Crouzon, Jackson-Weiss and Pfeiffer syndromes (Eswarakumar et al., 2005). In contrast, Fgfr2 mutations that reduce receptor activity cause bone hypoplasia within the skull and limb in Lacrimo-auriculo-dento-digital (LADD) syndrome (Eswarakumar et al., 2005).

Severe defects in epithelial organogenesis occur in mice lacking Fgf10 or its receptor, FGFR2b, causing underdevelopment of many organs, such as salivary glands and lungs (Lombaert et al., 2013). Genetic studies in mouse show that Fgfr2 mutations disrupt skeletal development by altering the ability of the receptor to regulate osteoprogenitor cell proliferation and differentiation: increased FGFR2 function enhances proliferation and differentiation (Neben et al., 2014). FGFR2 and its ligands have been proved to play an important role in breast cancer development and progression. Genome-wide analysis has identified four SNPs (single nucleotide polymorphism) in the intron 2 of Fgfr2 gene, which were associated with a higher incidence of breast cancer. Moreover, the activation of FGFR2 triggered aggressive growth of breast cancer cells *in vivo*. FGFR2 is suggested to be essential for induction of self-renewal and cell maintenance of human breast tumour initiating cells (Czaplinska et al., 2014).

Protein kinases with conserved amino-acid sequence share the catalytic domain with similar three-dimensional structure. Small-molecule compounds fitting into the ATP-binding pockets of protein kinases have been developed for cancer therapeutics (Garber, 2006). PD173074, SU5402, AZD2171, and Ki23057 are representative small-molecule FGFR inhibitors (Katoh and Katoh, 2009). Several kinds of molecular-targeted therapies

to the FGFR2 signalling pathway have been reported in various cancers. Ki23057, which inhibits autophosphorylation of FGFR2 IIIb decreased the growth of biliary tract cancer cells. In endometrial cancer cells harbouring activated mutations of Fgfr2, knockdown of Fgfr2 using short hairpin (sh) RNA or treatment with a pan-FGFR inhibitor (PD173074) caused cell cycle arrest and cell death (Matsuda et al., 2012). Other therapeutics targeted to FGFR2 include human antibody, peptide mimetic, RNA aptamer, small interfering RNA (siRNA), and synthetic microRNA (miRNA) (Katoh and Katoh, 2009).

1.4.5 FGFR2 in oligodendrocyte and MS

FGF/FGFR interactions play diverse roles in proliferation, migration, differentiation, and survival of both neurons and glial cells including oligodendrocytes, the myelin-forming cells of the CNS (Furusho et al., 2011). A key feature of this regulation is the differential expression of three FGF receptors during oligodendrocyte development. FGFR1 is expressed at all stages of the oligodendrocyte lineage, FGFR2 appears only in differentiated oligodendrocytes, FGFR3 expression increases from the early to late progenitor stage and then is downregulated as oligodendrocytes begin terminal differentiation, and FGFR4 is not expressed by oligodendrocyte lineage cells (Furusho et al., 2015). Only in a short window of time during maturation the oligodendrocytes initiate myelin formation (Bryant et al., 2009). Stimulation of oligodendrocyte process outgrowth and myelin-like membrane formation occurs with selective activation of FGFR2 *in vitro* (Fortin et al., 2005). *In vivo* FGFR2 is expressed by oligodendrocytes in myelinated fiber tracts of adult rodent brain, spinal cord, and optic nerve and is present in purified myelin. The expression of FGFR2 by neurons and astrocytes is low or absent (Kaga et al., 2006).

The most abundant tyrosine-phosphorylated protein in oligodendrocytes is the 120-kd isoform of FGFR2 and it is phosphorylated even in the absence of FGF2, suggesting a potential ligand independent function for this receptor. Furthermore, FGFR2, but not FGFR1, is associated with lipid raft microdomains in oligodendrocytes and myelin (Bryant et al., 2009). Conditional knockout mice that lack Fgfr2 and the myelin protein CNP display dopamine-related hyperactive behavior (Kaga et al., 2006). Interestingly, down-

regulation of both CNP and Fgfr2 mRNA expression occurs in schizophrenia, a condition that also is intimately related to the brain dopamine system (Bryant et al., 2009).

Remyelination, which may restore nerve conduction and protect axons, is significantly greater in early stage of MS lesions than in chronic disease. Failed differentiation of oligodendrocyte lineage cells may contribute to poor remyelination in chronic MS lesions and prolonged neurological deficits. Multiple molecular signaling pathways inhibit differentiation of oligodendrocyte progenitor cells and limit remyelination in experimental models. Modifying inhibitory signals in lesion areas could potentially enhance functional recovery in MS patients by improving the remyelination capacity of immature oligodendrocytes that persist in MS lesions (Mierzwa et al., 2013).

Selective activation of FGFR2 leads to stimulation of oligodendrocyte process outgrowth and myelin-like membrane formation in cultures, whereas inhibition of FGFR2 function by blocking antibodies leads to attenuation of these responses (Fortin et al., 2005). During remyelination, FGF2 may play a role in directly regulating oligodendrocyte lineage cell responses and may also act through paracrine or autocrine effects on astrocytes, which are known to synthesize other growth factors and immunoregulatory molecules that influence oligodendrocyte lineage cells (Messersmith et al., 2000). FGF signaling plays a key role during the regeneration of oligodendrocytes and myelin. FGF2 and/or FGFR is upregulated in MS patients and in mouse models of demyelination (Clemente et al., 2011).

2 OBJECTIVES

The FGF/FGFR interactions regulate a broad spectrum of physiological and pathological processes. Various research studies attribute a critical role to FGFR2 in oligodendroglial organization and function. Therefore, we hypothesized that deletion of Fgfr2 in oligodendrocytes would lead to a more severe course of EAE, leading to higher inflammation and neurodegeneration. The aim of this study was to characterize the role of FGFR2 in experimental autoimmune encephalomyelitis, the most common animal of multiple sclerosis.

Study Objectives

1. To determine the proliferative and differentiate changes of oligodendrocytes in $Fgfr2^{ind-/-}$ mice.
2. To study the expression and regulation patterns of oligodendroglial Fgfr2 knockout downstream signaling pathway in $Fgfr2^{ind-/-}$ mice in different CNS regions.
3. To investigate the potential role of oligodendroglial FGFR2 in disease severity in acute and chronic experimental autoimmune encephalomyelitis.
4. To characterize the morphology and immunohistochemistry of MOG_{35-55}-EAE lesions in $Fgfr2^{ind-/-}$ mice.
5. To evaluate the oligodendroglial FGFR2 downstream signaling pathway in EAE.
6. To investigate the pharmacological effects of GA in MOG_{35-55}-EAE induced $Fgfr2^{ind-/-}$ mice.

3 MATERIALS AND METHODS

3.1 Materials

3.1.1 Mice

Mice line	Supplier	Animal facility
Fgfr2$^{fl/fl}$	Michael Sendtner, Würzburg (Blak et al., 2007)	JLU, Central Animal facility, Frankfurter strasse 110, Giessen, Germany.
PLP Cre^{ERT}	The Jackson Laboratories, Bar Harbor, ME, USA	
C57BL/6J		

3.1.2 Genetic background

Mouse strain	Treatment	Abbreviation	Genotype
Plp/CreERT:Fgfr2$^{fl/fl}$	Vehicle (sunflower oil + ethanol)	Control	Homozygous
Plp/CreERT:Fgfr2$^{fl/fl}$	Tamoxifen	Fgfr2$^{ind-/-}$	Homozygous
Plp/Cre^{-ve}:Fgfr2$^{fl/fl}$	Tamoxifen	-	Heterozygous

3.1.3 Kits

Kit	Manufacturer	Art. No.	Method
DirectPCR Lysis Reagent (Tail)	Peqlab, Erlangen, Germany	31-121-T	DNA isolation
BCA Protein Assay Kit	Pierce® Thermo Scientific, IL, USA	23225	Protein quantification

iTaqTM Universal SYBR® Green qPCR Master Mix	Bio-Rad, CA, USA	172-5124	PCR
SuperSignal® West Pico Chemiluminescent substrate	Thermo Scientific, Il, USA	34077	Western Blot
AceGlowTM Ultrasensitive Chemiluminescent substrate	PEQLAB, Erlangen, Germany	37-3420	Western Blot

3.1.4 Primers

Gene (Primer)	5' to 3' Sequence	
Fgfr2 lox	Forward	CTAGGCCAGCTGGACCAGAC
	Reverse	CATCTTCTCGGTGTTGGTCC
PLP Cre PCR	PLP transgene forward	GCGGTCTGGCAGTAAAAACTATC
	PLP transgene reverse	GTGAAACAGCATTGCTGTCACTT
	Cre Internal primer forward	CTAGGCCACAGAATTGAAAGATCT
	Cre Internal primer reverse	GTAGGTGGAAATTCTAGCATCATCC

3.1.5 Primary Antibodies

Name	Host	Reactivity	Mol. W.	Tech.	Art. No.	Manufacturer
Anti-pStat1	Rabbit	H, M, R	84/91 kDa	WB	9171s	Cell Signaling Tech, MA, USA
Anti-Stat1	Rabbit	H, M, R, MK	84/91 kDa	WB	9172	Cell Signaling Tech, MA, USA

Anti-CNPase	Mouse	H, M, R	46/48 kDa	WB	ab6319	Abcam, UK
Anti-MBP	Mouse	H, M, R, G	33 kDa	WB	ab62631	Abcam, UK
Anti-PLP	Rabbit	H, M	26/30 kDa	WB	ab28486	Abcam, UK
Anti-pERK p-44/42	Rabbit	H M R Hm Mk	44, 42	WB	4370s	Cell Signaling Tech, MA, USA
Anti-ERK 1/2	Rabbit	H, M, R, MK	42/44 kDa	WB	9102	Cell Signaling Tech, MA, USA
Anti-AKT	Rabbit	H, M, R, MK	60 kDa	WB	9272	Cell Signaling Tech, MA, USA
Anti-pAKT (Ser473)	Rabbit	H, M, R, MK	60 kDa	WB	4060s	Cell Signaling Tech, MA, USA
Anti-Flg (C-15) (FGFR1)	Rabbit	H, M, R	110 kDa	WB	sc-121	Santa Cruz Biotech, CA, USA
Anti-Bek (C-17) (FGFR2)	Rabbit	H, M, R	120 kDa	WB	sc-122	Santa Cruz Biotech, CA, USA
Anti-GAPDH	Mouse	Ca, H, M, R	38 kDa	WB	MAB374	Chemicon/ Millipore, CA; USA
Anti-Trk B (794):sc12	Rabbit	H, M, R	145 kDa	WB	sc-12	Santa Cruz Biotech, CA, USA
Anti-BDNF	Rabbit	H, M, R	17, 13 kD	WB	sc-546	Santa Cruz Biotech, CA, USA
Anti pFGFR1	Rabbit	H M, R	~145 kDa	WB	06-1433	Millipore, CA; USA
Mac 3 Clone M3/84	Rat	M	staining	IHC	553322	Pharmingen, USA
B220 clone RA3-6B2	Rat	H, M	staining	IHC	557390	Pharmingen, USA
CD3, clone CD3-12	Rat	M	staining	IHC	MCA 1477	Serotec, UK
Olig-2	Rabbit	M	staining	IHC	18953	IBL, Japan
Nogo A H300	Rabbit	H, M	staining	IHC	Sc 25660	Santa cruz Biotech, CA, USA
MBP	Rabbit	M, R	staining	IHC	62301	Dako, Germany
SMI 32	Mouse	H, M.	staining	IHC	SMI32	SMI

3.1.6 Secondary Anibodies

Antibody	Host	Art. No.	Manufacturer
Anti-Rabbit-HRP	Goat	sc-2004	Santa Cruz Biotech, CA, USA
Anti-Mouse-HRP	Donkey	sc-2318	Santa Cruz Biotech, CA, USA

3.1.7 PCR Ladders

Marker	Manufacturer
PageRulerTM Plus Prestained Protein Ladder	Fermentas, Invitrogen, Carlsbad, USA
Fluorescent Long Range DNA Ladder	Jena Bioscience, Jena, Germany

3.1.8 Chemicals and Solutions

Compound	Manufacturer
10x PBS for cell culture (DPBS)	Lonza, Köln, Germany
2-Mercaptoethanol	Sigma-Aldrich, Steinheim, Germany
2-Propanol	Sigma-Aldrich, Steinheim, Germany
3% Hydrogen peroxide	Carl Roth, Karlsruhe, Germany
Acetic acid	Merck, Darmstadt, Germany
Agarose	Bioline GmbH, Luckenwalde, Germany
Ammonium Persulphate (APS)	Carl Roth, Karlsruhe, Germany
Bovine Serum Albumin (BSA)	Merck, Darmstadt, Germany
Bromophenol Blue	Neolab, Heidelberg, Germany

Citric acid	Merck, Darmstadt, Germany
complete Freund´s adjuvant	Sigma, Steinheim, Germany
Destilled water (Ecostrain®)	Braun, Melsungen, Germany
Dimethylsulfoxide (DMSO)	Carl Roth, Karlsruhe, Germany
Disodium-hydrogen-phosphate	Merck, Darmstadt, Germany
DNase	Qiagen, Hilden, Germany
EDTA	Carl Roth, Karlsruhe, Germany
Eosin	Merck, Darmstadt, Germany
Eosin	Carl Roth, Karlsruhe, Germany
Ethanol 100%	Sigma-Aldrich, Steinheim, Germany
FBS	PAA Laboratories, Pasching, Austria
Glycerol	Carl Roth, Karlsruhe, Germany
Glycin	Merck, Darmstadt, Germany
Glyzerin	Carl Roth, Karlsruhe, Germany
Hematoxylin	Carl Roth, Karlsruhe, Germany
Isopropanol	Merck, Darmstadt, Germany
Ketamine	Inersa Arzneimittel GmbH, Freiberg, Germany
Luxol-Fast-Blue	Sigma-Aldrich, Steinheim, Germany
Magnesiumsulfate ($MgSO_4$)	Sigma Aldrich, Tachfkirchen, Germany
Methanol	Merck, Darmstadt, Germany
MOG_{35-55}	Charité Berlin, Berlin, Germany
Mycobacterium tuberculosis	Difco Microbiology, Michigan, USA
NP40	US Biologicals, MA, Germany
Paraformaldehyde (PFA)	Sigma Aldrich, Taufkirchen, Germany
Pertussis Toxin	Calbiochem, Darmstadt, Germany

Ply L Lysine	Sigma-Aldrich, Steinheim, Germany
Potassium chloride (KCL)	Merck, Darmstadt, Germany
Potassiumdihydrogenphosphate	Merck, Darmstadt, Germany
Protease Inhibitor cocktail	Roche, Manheim, Germany
Proteinase K	Sigma-Aldrich, Missouri, USA
RNAse free water	Millipore corporation, MA, USA
Rotiphorese Gel (30% acrylamide mix)	Carl Roth, Karlsruhe, Germany
Sodium chloride (NaCl)	Carl Roth, Karlsruhe, Germany
Sodium-dihydrogen-phosphate	Merck, Darmstadt, Germany
Sodium hydrogen carbonate ($NaHCO_3$)	Merck, Darmstadt, Germany
Sodiumdodecylsulfate (SDS)	Neolab, Heidelberg, Germany
Soiumazid (NaN_3)	Merck, Darmstadt, Germany
Sunflower oil	Sigma-Aldrich, Steinheim, Germany
Tamoxifen	Sigma-Aldrich, Steinheim, Germany
TEMED	Carl Roth, Karlsruhe, Germany
Tris HCl	Carl Roth, Karlsruhe, Germany
Tris.acetat-EDTA buffer (TAE) 10x	Carl Roth, Karlsruhe, Germany
Trishdroxymethyl aminomethan (Tris)	Carl Roth, Karlsruhe, Germany
Tryphanblue	Carl Roth, Karlsruhe, Germany
Trypsin (2.5g/l)	Gibco, Invitrogen, Carlsbad, USA
Tween 20	Merck, Darmstadt, Germany
Xylazin 2%	CEVA Tiergesunheit GmbH, Düsseldorf, Germany

3.1.9 Consumables

Consumables	Manufacturer
Cell scrapper	GreinerBioOne, Frickenhausen, Germany
Cellstar® 125 cm^2 Cell cultur flasks	GreinerBioOne, Frickenhausen, Germany
Cellstar® 6 Well and 24 well Cell Culture Plate	GreinerBioOne, Frickenhausen, Germany
Cellstar® 75 cm^2 Cell cultur flasks	GreinerBioOne, Frickenhausen, Germany
Cellstar® Flat bottom with Lid, TC-Plate, 96 well, sterile	GreinerBioOne, Frickenhausen, Germany
Cellstar® Plastikpipettes (5 ml, 10 ml)	GreinerBioOne, Frickenhausen, Germany
Cellstar® U-shape with Lid, TC-Plate, 96 well, sterile	GreinerBioOne, Frickenhausen, Germany
Cryobox 136x136x130 mm	Ratiolab GmbH, Dreieich, Germany
Cryo TubeTM vials (1,8 mL; 4,5 mL)	Sarstedt AG & Co, Nümbrecht, Germany
DPX Mountant	Sigma Aldrich, Taufkirchen, Germany
Eppendorf tubes 1,5 mL, 2mL	Eppendorf Vertrieb Deutschland GmbH, Wesseling-Berzdorf, Germany
Eppendorf tubes 1,5 mL, 2mL (PCR clean- pyrogen & DNase free)	Nerbe Plus GmbH, Winsen (Luhe), Germany
Falcon® Plastic pipettes 10ml, 5ml	Becton Dickinson, Heidelberg, Germany
Falcon tubes (15ml, 50ml)	Becton Dickinson, Heidelberg, Germany
Glass Pasteur pipettes 150 mm	Brand, Wertheim, Germany
Glasswares (different sorts)	Fisherbrand; IDL; Schott&Gen; Simax
Butterfly needle	DKS LOVERSAN INDUSTRIA BIOMEDICA SPA, Gemonio, Italy
Ministart single use filter (0,2 µm, 0,45 µm)	Sartorius Stedim Biotech GmbH, Göttingen, Germany
Nitra-Tex® powder free gloves	B. Braun Melsungen AG, Germany
Nitrocellulose membrane	GE Healthcare, Amersham™ Hybond ECL, Buckinghamshire, UK

Parafilm	Pechiney Plastic packaging, Menasha, WI
PCR Tube, cap-strips	Applied Biosystems, Darmstadt, Germany
Pipette tips without filter (10 µL, 100 µL, 1000 µL)	Sarstedt AG & Co, Nümbrecht, Germany
Sterile PCR- clean pyrogen & DNase free with filter (10, 100, 200, 1000µl)	Nerbe Plus GmbH, Winsen (Luhe), Germany
Syringe 25ml for BSA	B. Braun Melsungen AG, Germany
Tissue culture dishes sterile 35,0 /10mm	GreinerBioOne, Frickenhausen, Germany

3.1.10 Instruments

Instrument	Manufacturer
Arpege 75, Liquid nitrogen tank	Air Liquide Medical GmbH, Düsseldorf, Germany
Axioplan 2 Fluorescence Microscope	Carl Zeiss, Jena, Germany
BEP 2000 Advance (ELISA-Reader)	Dade Behring Marburg GmbH, Marburg, Germany
Centrifuge type 2-6 Easia shaker Medgenix diagnostics	Sigma-Aldrich Chemie GmbH, Taufkirchen, Germany
Centrifuge Universal 32 R	Hettich GmbH, Kirchlengen, Germany
ELISA-Reader Multiscan EX	Thermo electron corporation, Langenselbold, Germany
Fusion FX7 chemiluminescence system	Peqlab Biotechnologie GmbH, Erlangen, Germany
Hettich centrifuge (cooling)	Hettich GmbH, Kirchlengen, Germany
Light Microscope for cell culture	Carl Zeiss Microscopy GmbH, Oberkochen Germany
Magnetic stirrer	IKA® Werke GmbH, Staufen, Germany
Nalgene™ Cryo 1°C Freezing container	Nalgene®, Germany

Nanophotometer	Implen GmbH, München, Germany
Neubauer improved cell chamber	Brand, Wertheim, Germany
Neubauer improved Haemocytometer	Brand, Wertheim, Germany
Nuaire™ Biological Safety Cabinets Class II type A/B3 (Sterilbank)	INTEGRA Biosciences GmbH, Fernwald, Germany
pH-Meter	Mettler Toledo GmbH, Giessen, Germany
Pipette boy	INTEGRA Biosciences GmbH, Fernwald, Germany
Power pack	Peqlab Biotechnologie GmbH, Germany
Refrigerators and freezers	Different companies
Rotamax 120 (Shaker)	Heidolph Instruments GmbH & Co. KG, Schwabach, Germany
Sanyo Incu-safe incubator for cell culture	Ewald Innovationstechnik GmbH, Bad Nenndorf, Germany
SmartSpecTM Plus Spectrophotometer	BioRad, München, Germany
StepOne® Real-Time PCR system	Applied Biosystems, Darmstadt, Germany
Surgical instruments	Various companies
Table top centrifuge EBA 20	Hettich GmbH, Kirchlengen, Germany
Table top centrifuge micro 120	Hettich GmbH, Kirchlengen, Germany
TissueRuptor	Qiagen Instruments, Hombrechtikon, Switzerland
Thermomixer® comfort	Eppendorf, Hamburg, Germany
Trans-Blot® SD Semi-dry transfer cell	BIO RAD, München, Germany
Trans-Blot® SD Semi-dry transfer cell	BioRad, München, Germany
Vortexer vortex-Genie2	Heidolph Instruments GmbH & Co. KG, Schwabach, Germany
Water bath	Memmert GmbH + Co.KG, Germany
Weighing balance	Sartorius Stedim Biotech GmbH, Göttingen, Germany
Western blotting system	BioRad, München, Germany

3.1.11 Buffers

Buffer	Components	Volume
Lysis Buffer (250ml) **pH 7.4**	NaCl Tris EDTA Glycerol NP40 NaN_3	2.19 g 0.61 g 0.07 g 25 ml 2.5 ml 0.025 g
10% Ammonium Persulfate (APS)	APS ddH_2O	1 g 10 ml
10% Sodiumdodecylsulfate (SDS)	SDS ddH_2O	1 g 10 ml
10x PBS (1 Liter) **pH 7.4**	137 mM NaCl 2 mM KH_2PO_4 2.7 mM KCl 10 mM Na_2HPO_4 H_2O	80 g 2.4 g 2 g 14.4 g 1000 ml
6x SDS-PAGE Loading Buffer	60 mM Tris-HCl (pH 6.8) 2% SDS 0.01% Bromophenol blue 10% Glycerol ddH_2O β-Mercaptoethanol	36 ml 60 ml 60 mg 60 ml 144 ml 65 µl/ml
10x Trypsin EDTA	10x Trypsin ddH_2O	5 ml 45 ml
SDS-PAGE Transfer buffer (1 Liter)	10x Running buffer Methanol ddH_2O	100 ml 200 ml 700 ml
Blocking buffer (5% BSA) **Bovine Serum Albumin**	BSA fraction V TBST	5 g 100 ml
10x TBS (1 Liter) **pH 7.2 to 7.6**	Tris NaCl H_2O	24.2 g 87.7 g 1000 ml
1x TBS-Tween (TBST) **(1 Liter)**	1x TBS 0.1% Tween®20	100 ml 1 ml

3.1.12 Software

Software	Company
Fusion BioID software	Peqlab, Erlangen, Germany
Graph Pad Prism Software Version 5.01	GraphPad Software, Inc. CA, USA
Image J software	Image J 1.47d, National Institute of Health, USA
Microsoft Office Professional 2013	Microsoft corporation, USA
TierBase Client 4Dm v11	University of Heidelberg, Heidelberg, Germany

3.2 Methods

3.2.1 Mice

The Fgfr2$^{flox/flox}$ mouse was received from Michael Sendtner's laboratory, Würzburg which was generated on C57BL/6J background (Blak et al., 2007) and crossbred with B6.Cg-Tg(Plp1-cre/ERT)3Pop/J to generate inducible oligodendrocyte Fgfr2 conditional knock-out mice. Mice were bread and grown in JLU-central animal facility, Frankfurter Strasse 110, Giessen, Germany. All animal experiments were carried out in JLU central animal facility and analyzed in the Neurochemical laboratory, Department of Neurology, Giessen, Germany.

3.2.2 Mice Genomic DNA preparation

The tail pieces (3 mm) and/or ear marks of 3 week old mice were collected under anesthesia. The tissue was suspended in Eppendorf tube with 200 µl DirectPCR lysis reagent containing freshly prepared Proteinase K (0.2-0.4 µg/µl, Sigma-Aldrich, St. Louis, USA). It was incubated in rotating thermomixer (Thermomixer® comfort, Eppendorf, Hamburg, Germany) at 55 °C with 400 RPM for 5-10 hours (until no tissue clumps were observed). Proteinase K was inactivated by incubating the lysates at 85 °C for 45 minutes. The tissue debris and hair were precipitated by centrifuging the lysate for 30 seconds and the crude lysate was stored in -20 °C. The lysates were amplified with PCR for Fgfr2^{lox} and Plp^{cre} locus confirmation and were subjected to agarose gel electrophoresis.

3.2.3 PCR Protocol

To determine the genotype, 1 µl of genomic DNA of each sample was diluted in SYBR Green PCR Master Mix along with the target amplification primers (Fgfr2 or PLP/Cre primers) (Table 3). The PCR thermal profile for each genetic locus was established and standardized (Table 4). The PCR products were run and separated in 1.5% agarose gel electrophoresis in 120 V for 50 min (BioRad electrophoresis chamber). The bands were detected using Fusion Fx7 chemiluminescence system (PEQLAB, Erlangen, Germany). The database recording, breeding and documentation of animal experiments was managed using TierBase program (University of Heidelberg, Heidelberg, Germany).

Table 3. PCR Master Mix (for each sample)

Fgfr2 Locus	**PLP Cre Locus**
10 µl SYBR Green master mix	10 µl SYBR Green master mix
1 µl Forward Primer (Fgfr2)	1 µl Forward Primer (PLP)
1 µl Reverse Primer (Fgfr2)	1 µl Reverse Primer (PLP)
1 µl genomic DNA	1 µl genomic DNA
7 µl H_2O	5 µl H_2O
	1 µl Forward Primer (CRE)
	1 µl Reverse Primer (CRE)
20 µl TOTAL	**20 µl TOTAL**

Table 4. PCR Thermal profile

	Fgfr2 Locus			**PLP Cre Locus**		
	Temp.	**Time**	**Cycles**	**Temp.**	**Time**	**Cycles**
Denaturing	95° C	5 min	**40 X**	95° C	5 min	**35 X**
Denaturing	95° C	30 s		95° C	30 s	
Annealing	62.5° C	30 s		51° C	1 min	
Elongation	72° C	45 s		72° C	1 min	
				72° C	2 min	

3.2.4 Fgfr2 conditional knockout Induction

The conditional oligodendrocyte specific Fgfr2 knock out (referred to as *Fgfr2*$^{ind-/-}$) was induced at 4-5 week old female *Plp*$^{cre+}$*: Fgfr2*$^{flox/flox}$ littermates by 5 consecutive daily intraperitoneal Tamoxifen injections (1 mg of Tamoxifen in 100 µl sunflower oil/ethanol) (Sigma-Aldrich, Steinheim, Germany). The control littermates were injected with the same solution excluding Tamoxifen and received the same treatments in time and place. The spinal cord and hippocampus were taken 2 weeks after Tamoxifen administration and Fgfr2 expression was analyzed to confirm the knockout efficiency. Animal experiments were approved by the local state authorities of Hesse, Giessen, Germany (GI 20/23-Nr. 31/2008) (Figure 8).

3.2.5 Induction and evaluation of MOG_{35-55}-induced EAE

At 12-13 weeks the oligodendrocyte $Fgfr2^{ind-/-}$ and control mice were anesthetized with isoflurane (20-40 seconds) prior to EAE immunization. This was achieved by 4 flank subcutaneous injections (300 µg in total) of myelin oligodendrocyte glycoprotein peptide (MOG_{35-55}; MOG peptide amino acids - MEVGWYRSPFSRVVHLYRNGK; Charité Hospital, Berlin, Germany) emulsified in complete Freund´s adjuvant (Sigma, Steinheim, Germany) containing 10 mg Mycobacterium tuberculosis (Difco, Michigan, USA). Intraperitoneal pertussis toxin (Calbiochem, Darmstadt, Germany) was administered on days 0 and 2 post immunization (300 ng/mouse). Mice were blindly evaluated for the clinical course of EAE (up to day 25 daily and later every other day) according to a 5-scale score criteria; 0 to 5: 0 = normal, 0.5 = distal tail weakness, 1 = complete tail weakness, 1.5 = mild hind limb weakness, 2 = ascending hind limb weakness, 2.5 = severe hind limb weakness, 3 = hind limb paralysis, 3.5 = hind limb paralysis and moderate forelimb weakness, 4 = hind limb paralysis and severe forelimb weakness, 4.5 = tetraplegia and incontinence, to 5 = moribund/death. Mice were sacrificed and tissues were collected in the acute (on day 18-20 p.i.) and chronic phase of EAE (day 60-65 p.i.) (Figure 8).

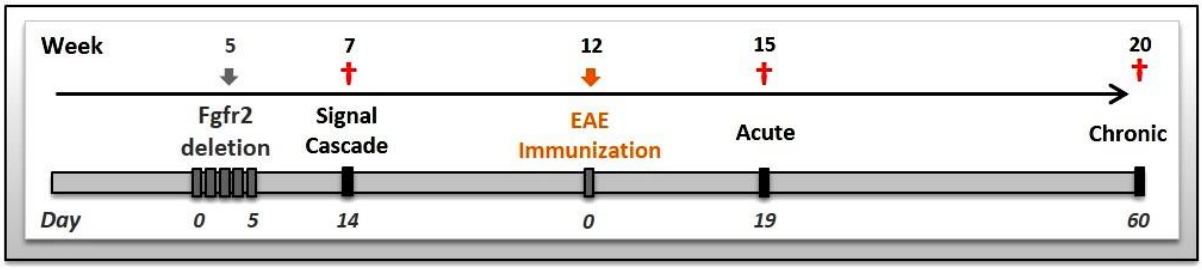

Figure 9. Experimental design of the knock out and the KO-EAE study. In the **Knock out** study the OLs Fgfr2 conditional KO was induced in 4-5 week old female mice by 5 consecutive IP Tamoxifen injections. In the first set of studies the OLs specific Fgfr2 knock out downstream signalling was investigated by sacrificing (†) the mice 2 weeks after Tamoxifen induction. Different CNS region tissues were collected and subjected to the protein analysis. **In the KO-EAE study**, the *Fgfr2*$^{ind-/-}$ and control mice were immunized by MOG_{35-55}-EAE in 12-13 weeks of age. Here the mice were sacrificed at acute (week 15) and chronic (week 20) of immunization and the CNS tissues were collected to investigate protein biochemistry as well as histopathology and immunohistochemistry of EAE.

3.2.6 Glatiramer acetate (GA) treatment in MOG_{35-55}-induced EAE

The MOG_{35-55}-EAE immunized *Fgfr2*$^{ind-/-}$ and control mice (described in the previous paragraph) have received a prevention regimen of GA (COPAXONE® 20 mg/ml, Teva Pharmaceutical Industries). GA was administered with 8 consecutive daily subcutaneous injections, starting on the immunization day. The clinical score of EAE was blindly assessed until day 30 when the mice were perfused and the tissues were collected for histological studies (Figure 9).

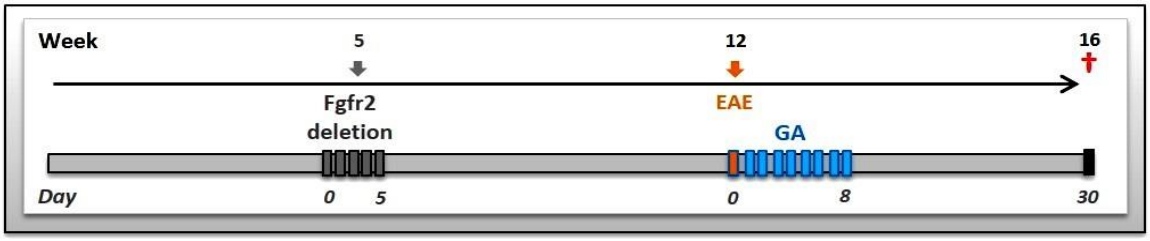

Figure 10. Experimental design of GA treatment study. The prevention regimen of GA was administered to the *Fgfr2*$^{ind-/-}$ and control mice on the day of MOG_{35-55}-EAE immunization. The mice were treated with 8 daily doses of GA (2 mg in 100 µl per injection) and the clinical course of the disease was monitored until the day of euthanization (day 30).

3.2.7 Protein extraction

In each study (oligodendrocyte Fgfr2 knock out downstream signaling as well as acute and chronic EAE) the mice were sacrificed by CO_2 inhalation at the termination criteria of the respective experiments (described above). The tissues from different CNS regions (spinal cord, hippocampus, cortex, cerebellum, and brain stem) were collected carefully and immediately kept in 4 °C protein lysis buffer (150 mM NaCl, 20 mM Tris HCl, 1 mM EDTA, 10% glycerol, 1% NP40, 0.01% sodium azide).The tissues were homogenized in lysis buffer with Tissue rupture (Qiagen Instruments, Hombrechtikon, Switzerland) and the tissue debris were precipitated by centrifuging in 4 °C for 20 minutes at 14000 rpm. The supernatant was collected and the protein content was measured using BCA assay according to manufacturer instructions (Pierce® BCA Protein Assay Kit, Thermo Scientific, IL, USA). In brief 25 µl of 1:10 diluted protein samples were poured into 96 well flat bottom plate in 3 replicates. 200 µl of Reaction Reagent was added to each well and after mixing thoroughly, incubated for 30 minutes at 37 °C. The absorbance was

measured at 540 nm in room temperature with an ELISA reader. The protein level was normalized to 2 µg/µl concentration in lysis buffer and stored at -20° C until it was used for SDS-PAGE western blot protein analysis.

3.2.8 Western Blot (WB) Analysis

The loading buffer (200 mM Tris-Cl (pH 6.8), 400 mM DTT, 8% SDS, 0.4% bromophenol blue, and 40% glycerol) was added to the normalized protein lysate (2 µg/µl concentration) and was incubated at 95 °C for 5 minutes to achieve protein denaturation. Samples were loaded (30 µl of protein lysate, 60 µg protein) on 10% SDS-PAGE (Rotiphorese® Gel 30, 10x SDS-PAGE, Carl Roth Gmbh, Karlsruhe, Germany) and ran until the target protein bands were separated. Using semidry unit (Trans Blot, Semi dry Transfer cell, BioRad) the proteins were transferred to a nitrocellulose membrane (GE Healthcare, AmershamTM Hybond ECL, Buckinghamshire, UK) and were blocked with 5% BSA (diluted in 1x TBST buffer) for 1 hour. The membranes were incubated overnight at 4 °C with standardized dilution of each primary antibody in 1x TBST-BSA 5% solution. The membranes were washed (3X) with 1XTBST for 5 min each. The secondary antibody was administered for 1 hr and washed 3 times with TBST. The membranes were developed using SuperSignal West Pico chemiluminescent substrate (Thermo, Pierce Biotechnology, Rockford, IL, USA) and AceGlow chemiluminescence Substrate (PEQLAB, Erlangen, Germany) in Fusion Fx7 chemiluminescence system (PEQLAB, Erlangen, Germany). Finally, the membrane was incubated with GAPDH (1:5000, Merck Millipore, Massachusetts, USA) as loading control. The captured proteins signals were analyzed using Fusion Bio1D software (PEQLAB, Erlangen, Germany).

3.2.9 Mice Perfusion

To obtain a rapid and uniform fixation of tissues in order to preserve them in a life-like state for further histological and immunohistochemical analysis, the paraformaldehyde perfusion via vascular system was chosen. The *Fgfr2*$^{ind-/-}$ and control mice in acute and chronic EAE were anesthetized by intraperitoneal injection of Ketamine (Inersa

Arzneimittel GmbH, Freiberg, Germany) and Xylazine (CEVA Tiergesundheit GmbH, Düsseldorf, Germany) prior to transcardial perfusion with 4% paraformaldehyde. The depth of anesthesia was confirmed with pinch-response method. Following standard surgical procedures the abdominal cavity was exposed and the diaphragm was opened to reach thoracic cavity. While holding the heart steady with a pair of small forceps (it should be still beating), a butterfly needle (DKS LOVERSAN INDUSTRIA BIOMEDICA SPA, Gemonio, Italy) (gauge 21) was inserted directly into protrusion of left ventricle with care to not penetrate the cardiac septum. A cut made quickly in the right atrium with sharp scissors to insure the free flow of the solutions and blood drain (Figure 10). The valve was released to allow slow and steady flow of around 20 ml/min of saline solution (1X PBS). As soon as the out-flow solution turned clear and liver color changed to pale-yellow the flow was switched to 4% paraformaldehyde solution (Sigma Aldrich, Taufkirchen, Germany). Continuous perfusion carried on for about 5-10 min until the tail and the four limbs of the mouse become stiff. The brain, spinal cord, spleen, and liver were dissected and placed in the 4% paraformaldehyde solution overnight. The following day the tissues were fixed in paraffin blocks and slides were cut by microtome for histopathological and immunohistochemical analysis.

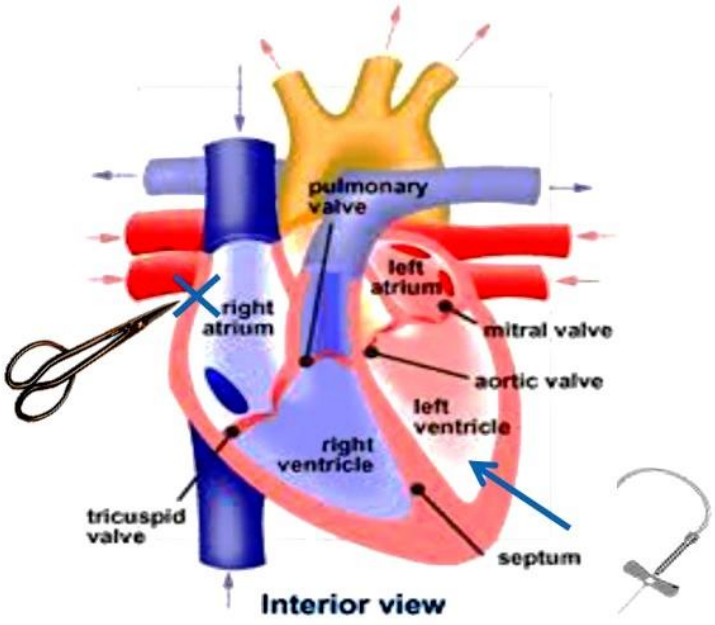

Figure 11. The schematic view of heart during perfusion. The location of butterfly needle insertion into the left ventricle protrusion and the in the right atrium cut during perfusion are showed.

3.2.10 Hematoxylin and Eosin (H&E) staining

Hematoxylin and eosin stainings of spinal cord in acute and chronic EAE were performed to determine the inflammation. The 1 µm thick slides of spinal cord were kept in 35 ˚C overnight and deparaffinized by suspending in xylene. Slides were passed through several changes of alcohol to remove xylene and rinsed with water. The rehydrated slides were then stained with hematoxylin (a nuclear stain, blue to violet), differentiated (remove excess background) with 2 deeps of HCL/EtOH and rinsed under tap water for weak alkaline solution treatment existing in the tap water. Here eosin (pink to red) counterstain was applied, slides were rinsed and dehydrated, cleared and mounted with coverslip (Figure 11).

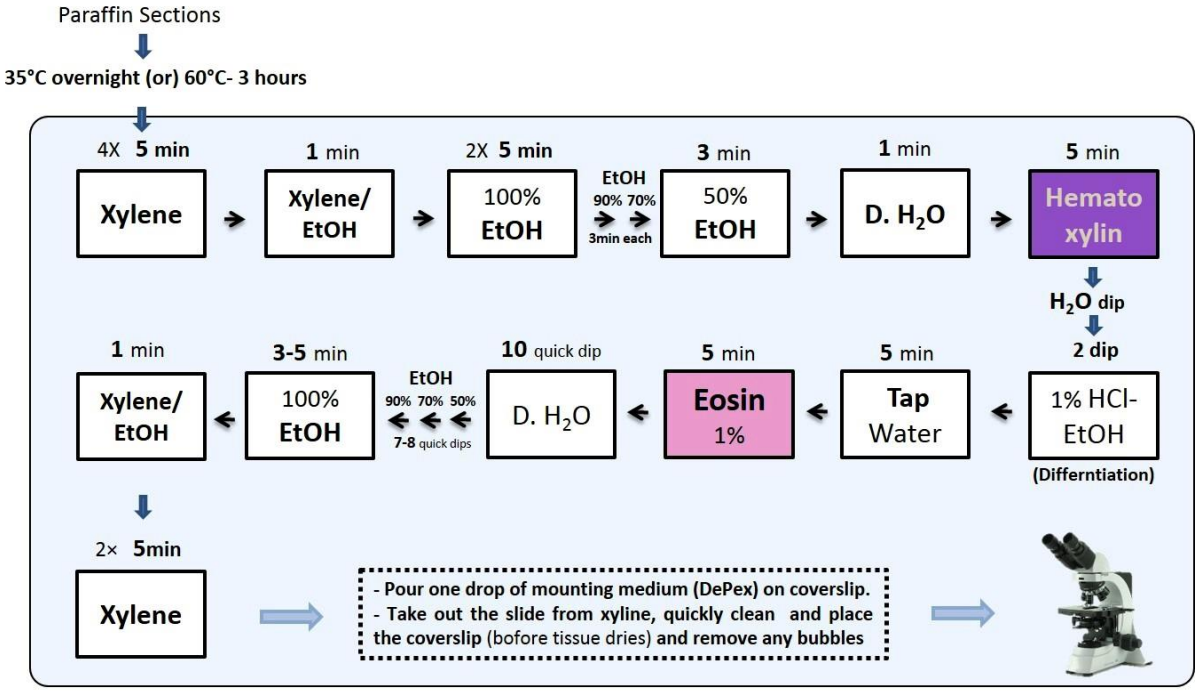

Figure 12. The schematic procedure of Hematoxylin and Eosin (H&E) staining

3.2.11 Luxol fast blue/periodic acid-Schiff stain (LFB/PAS)

The LFB/PAS stainings of spinal cord in acute and chronic EAE were performed to determine the demyelination rate. The 1 µm thick slides of spinal cord were kept in 35 ˚C overnight and deparaffinized by suspending in xylene. Slides were passed through several changes of alcohol to remove xylene and incubated in a tightly sealed container of luxol fast blue at 56°C overnight. The following day the slides went through 95% ethanol

change to remove excess stain. Slides went through a brief differentiation with lithium carbonate solution, rinsed with 70% ethanol and ethanol washed away by distilled water. The slides could be either counter stained (myelin is blue and background colorless) or followed up with PAS staining. In the latter case, the slides were exposed to 1% periodic acid solution for 5 min and rinsed with tap water. Exposed sections to Schiff's reagent for 20 min and washed in running tap water for 5 min. They were counterstained with hematoxylin for approx. 2 min and differentiated (if necessary), dehydrated, cleared and mounted with coverslip (Figure 12).

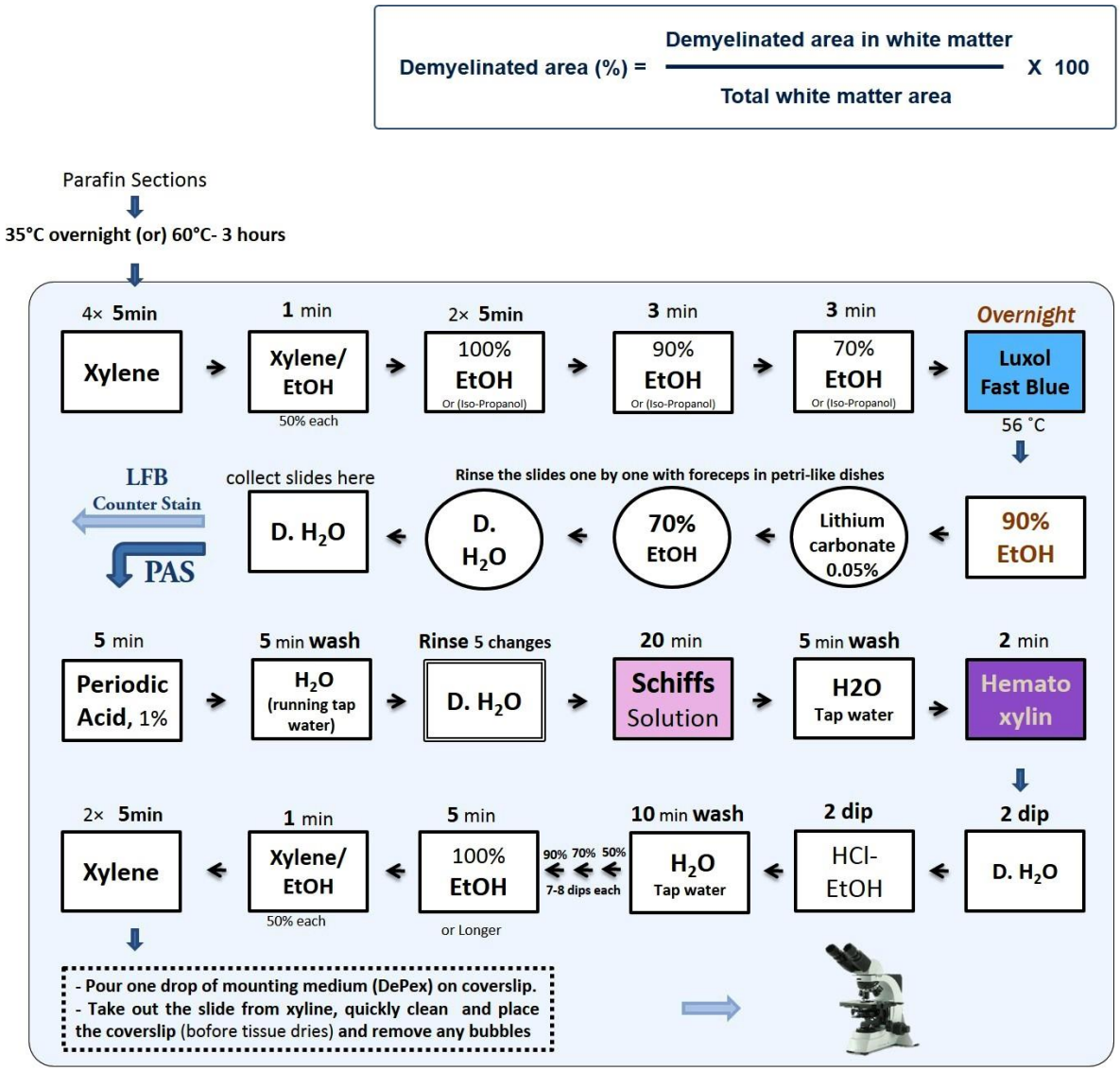

Figure 13. The schematic procedure Luxol fast blue/periodic acid-Schiff stain (LFB/PAS)

3.2.12 Bielschowsky's silver staining

The Bielschowsky's silver staining of spinal cord in acute and chronic EAE were performed to determine the axonal density. In principal the nerve fibers are sensitized with a silver solution and when the sections are treated with ammoniacal silver they are reduced to a visible metallic silver. The slides were kept overnight in 35 ˚C and deparaffinized and rehydrated. Sections were incubated in 20% silver nitrate ($AgNO_3$ diluted in DH_2O) for about 20 mins until they become light brown color (thicker sections may look dark brown). The silver nitrate was poured in a conical flask and concentrated ammonium hydroxide (32% Ammonia) was added drop by drop (meanwhile preserve slides with H_2O). The precipitate forms at first an ugly brown and we continue adding ammonium hydroxide until its color turns just clear (add 2 drops extra). This solution was poured back to the slides and incubated for 15 minutes in 40˚C in dark (or until sections become dark brown). The slides were placed directly (without washing) in developer working solution for about 1 minute or less (the incubation time is determined depending on the reaction intensity after checking under microscope). The reaction was stopped with distilled water and slides were incubated in 2% sodium thiosulfate and washed briefly under tap water. Finally the slides were dehydrated, cleared and mounted the coverslips.

3.2.13 Immunohistochemistry (IHC)

The immunohistochemistry of spinal cord in acute and chronic EAE were performed to analyze protein expression and localization in the context of tissue morphology through specific antibody binding. IHC technique exploits the specific binding of an antibody to its target epitope in combination with a chromogenic or fluorescent readout. The deparaffinized spinal cord sections were rehydrated and the antigens were retrieved by boiling the sections in the appropriate buffer (CD3, Mac-3, B220, MBP and NogoA in citrate buffer; Olig2 in TE buffer) (10 mM, pH 6). The endogenous peroxidases were blocked with 3% hydrogen peroxidase for 30 min and was followed by 10% FCS blocking for 1 hr. The overnight incubation with primary antibodies for macrophages/activated microglia (Mac 3, clone M3/84, 1:200, Pharmingen, San Diego, CA, USA), activated B

cells (B220, clone RA3-6B2, 1:200, Pharmingen, San Diego, CA, USA), T cells (CD3, clone CD3-12, 1:150, Serotec, Oxford, UK), Myelin Basic Protein (MBP, A0623, 1:1000; Dako), Olig2(+) and Nogo-A(+) oligodendrocyte (Olig 2, 1:300, IBL, Gunma, Japan; Nogo-A(+), 1:50, Santa Cruz Biotechnology, CA, USA) were performed in 4°C. Next day the sections were incubated with biotinylated secondary antibodies (goat anti-rat; Mac 3, B220 and goat anti-rabbit; CD3, MBP, Olig2, Nogo-A) and signals were detected with avidin-biotin complex by DAB. To determine the cells, a brief nucleus stain with hematoxylin was performed (Figure 13). Images were captured on a digital camera (Olympus DP71, Olympus America Inc., Center Valley PA, USA) using a light microscope (Olympus BX51, Hamburg, Germany). The demyelination of MBP(+) area was analyzed using Image J software (ImageJ 1.47d, National Institute of Health, USA). The axonal density was counted with a 25-point-grid ocular at 1000x magnification (oil immersion). CD3(+), B220(+), Mac3(+), Olig2(+), and Nogo-A(+) cells were counted at 400x magnification with an ocular morphometric grid.

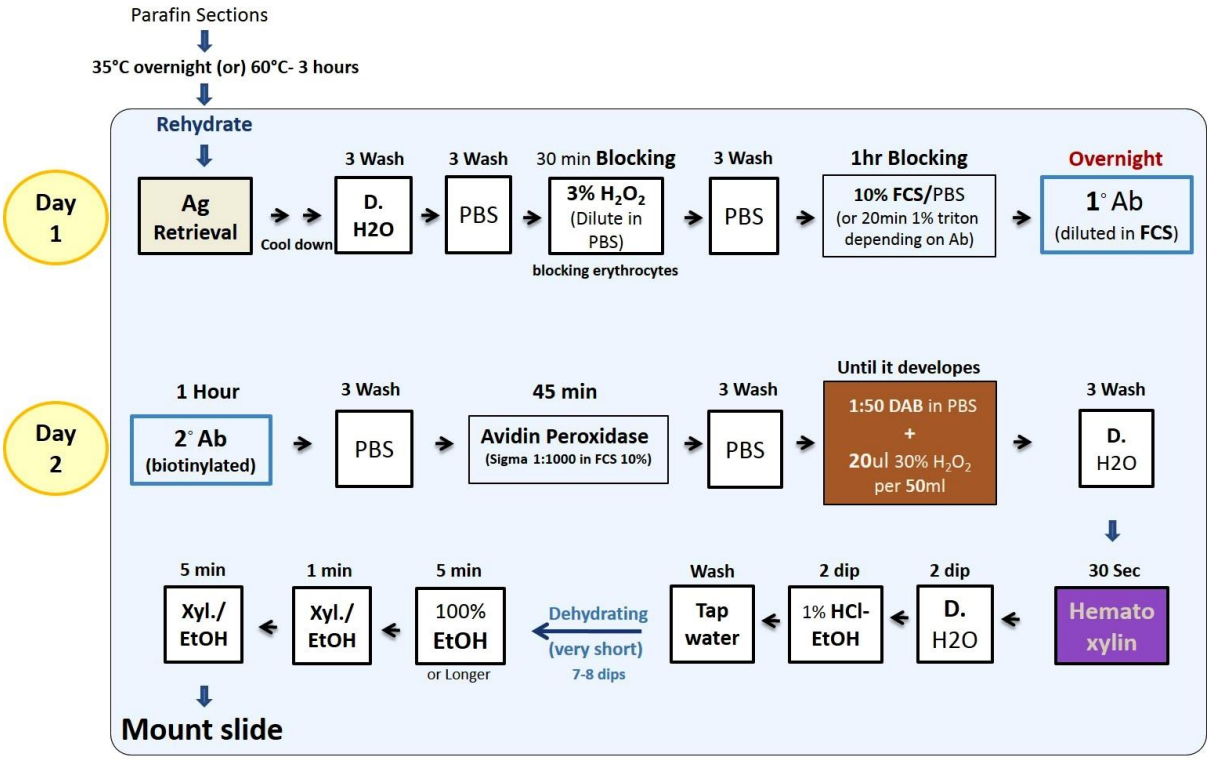

Figure 14. The schematic procedure of Immunohistochemistry

3.2.14 Statistical analysis

All analysis were performed genotype blinded and no samples were excluded from the analysis. The appropriate statistical analyses were chosen for each experiment. The EAE clinical score (three independent experiments were included for each acute and chronic EAE) differences between the genotypes and histological data analysis were performed using Mann-Whitney U test. Other experiments were analysed using unpaired T-test (The statistical significance was set at $P \leq 0.05$). Statistical analysis and graph preparations were achieved using GraphPad Prism 6.0 software for windows (GraphPad Software, San Diego, California, USA) and the values are expressed as mean ± standard error of mean. The magnitude of *P* values were resembled with stars: * $P < 0.05$, ** $P < 0.005$, *** $P < 0.001$.

4 RESULTS

4.1 Oligodendrocyte specific Fgfr2 knockout study

4.1.1 Genotype confirmation

The Fgfr2 complete knockout mice die at E10.5 due to defects in the placenta. Selective disruption of the FGFR2b isoform causes severe impairment in the development, resulting in lethality immediately after birth. Disruption of the FGFR2c isoform, although not lethal, results in impairment in skull and bone development (Eswarakumar et al., 2005). Hence, we used Cre-Lox system of DNA modification to target Fgfr2 gene in oligodendrocytes after mice CNS development. As explained in the methods, the Fgfr2 floxed mice was crossed with transgenic Cre expressing (under PLP promoter which is specific for oligodendrocytes) mice. The genotype of mice was confirmed with PCR, using PLP Cre and Fgfr2 loxP primers (Figure 14). No effects of mortality, body weight or other phenotype changes were observed in oligodendrocyte specific Fgfr2 conditional knockout mice.

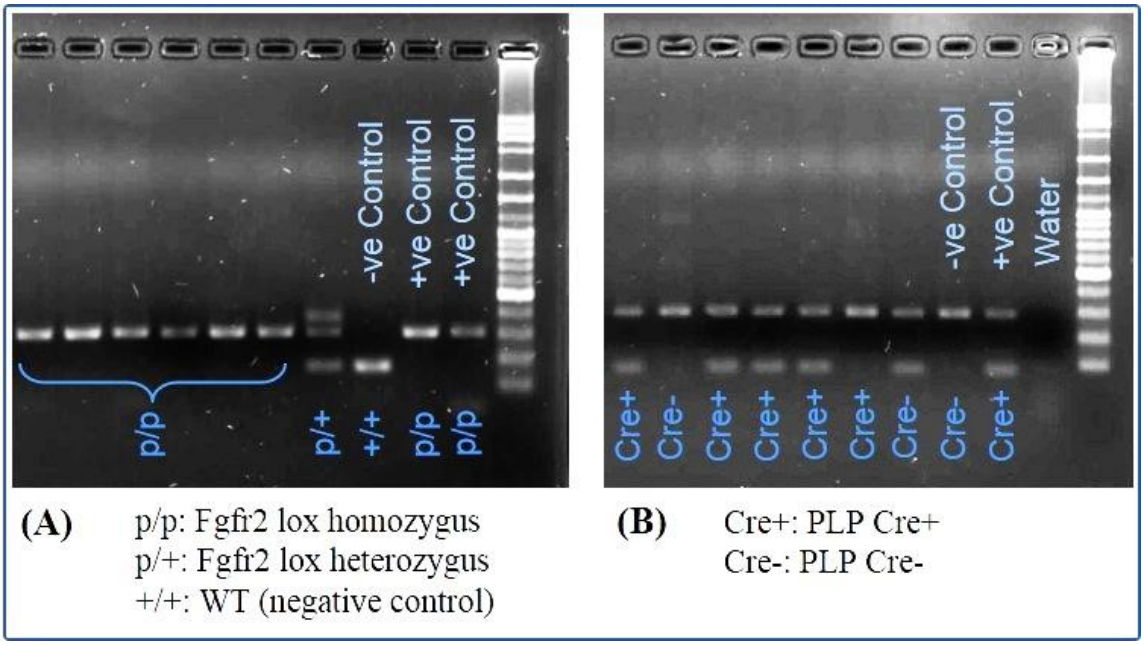

Figure 15. **Genotyping.** To determine and select the appropriate genotype, mice tail lysates were amplified by PCR, Fgfr2 lox **(A)** and PLP Cre locus **(B)** were confirmed. PCR amplified products were separated with agarose gel electrophoresis. The representative agarose gel images are shown. (-ve control: wild type).

4.1.2 Oligodendrocyte specific Fgfr2 knockout confirmation

The efficacy of oligodendrocyte specific Fgfr2 Tamoxifen inducible Cre mediated deletion was confirmed by western blot analysis in 6 week old female mice (2 weeks after Tamoxifen induction). The expression levels of the heavy splicing variant of FGFR2 (120 kDa) was significantly downregulated in spinal cord ($p = 0.013$) and brain rest ($p = 0.028$). There was no regulation in hippocampus and cortex in the heavy splicing variant of FGFR2. The expression level of FGFR2 light chain (110 kDa) was significantly downregulated in spinal cord ($p = 0.001$) and brain rest ($p \leq 0.001$). However, there was no significant regulation in hippocampus and cortex of $Fgfr2^{ind-/-}$ mice. This finding indicate that the conditional oligodendrocytes FGFR2 downregulation is dependent on the oligodendrocytes population and therefore, it is only significantly downregulated in the oligodendrocytes rich regions of CNS (spinal cord and total brain lysates) (Figure 15, 16).

4.1.3 Oligodendrocyte specific Fgfr2 knockout does not affect FGFR1 regulation

To investigate whether Fgfr2 knockout induction will lead to FGFR1 regulation as a compensatory mechanism, the protein lysates were evaluated for FGFR1 expression using WB analysis. The protein analysis of different brain regions (spinal cord, Hippocampus, cortex, and brain rest) in $Fgfr2^{ind-/-}$ mice and controls after knockout induction showed no statistically significant regulation in FGFR1 protein (Figure 17).

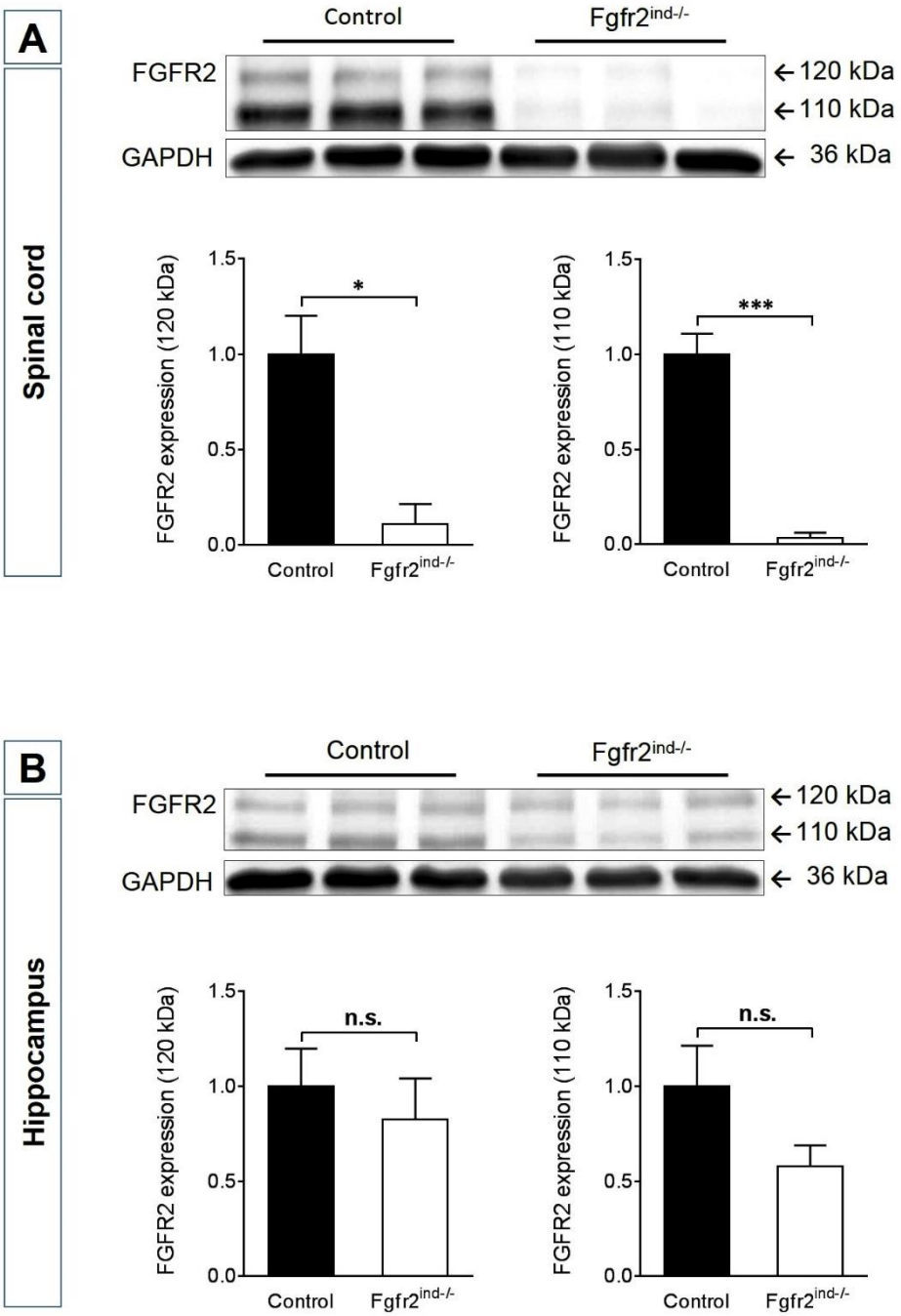

Figure 16. **Fgfr2 expression in Fgfr2$^{ind-/-}$ mice in spinal cord and hippocampus.** To determine the knockout efficacy of OL Fgfr2 Tamoxifen inducible mice, the different CNS lysates were evaluated by WB analysis. **(A) Spinal cord.** Fgfr2 was downregulated in the heavy (120 kDa) and the light (110 kDa) splicing variants of Fgfr2$^{ind-/-}$ mice (p = 0.013, p = 0.001). **(B) Hippocampus.** Both splicing variants of Fgfr2 were downregulated in hippocampus after Tamoxifen induction, however, the regulations were not statistically significant (p = 0.497, p = 0. 063). Values are expressed as mean ± SEM (n = 3).

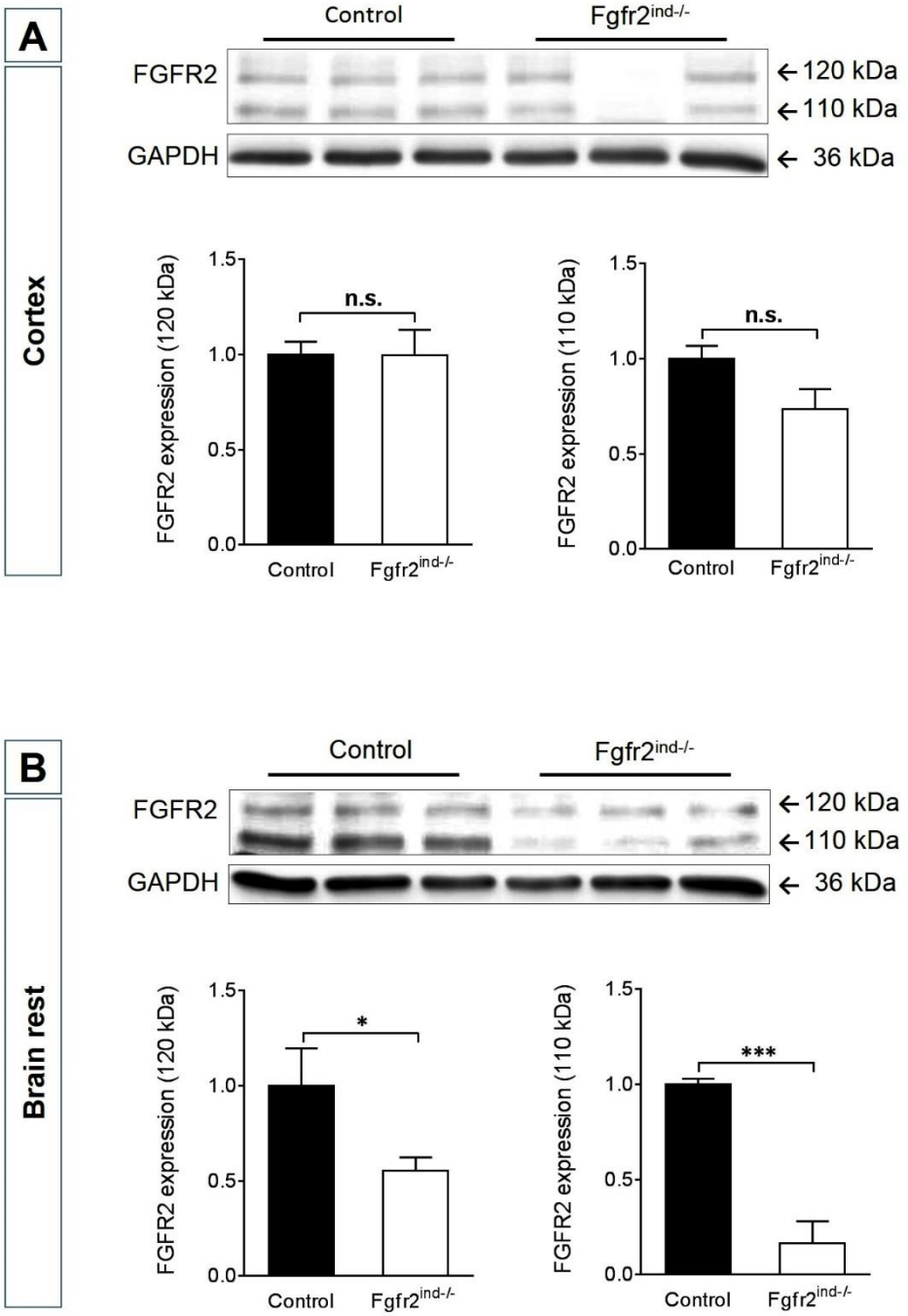

Figure 17. **Fgfr2 expression in Fgfr2$^{ind-/-}$ mice in cortex and brain rest.** To determine the KO efficacy of OL Fgfr2 Tamoxifen inducible mice, the different CNS lysates were analyzed by WB. **(A) Cortex.** Neither of the Fgfr2 splicing variants were regulated in cortex after Tamoxifen induction ($p = 0.972$, $p = 0.085$). **(B) Brain rest.** Fgfr2 was downregulated in the heavy and the light chains of Fgfr2$^{ind-/-}$ mice ($p = 0.028$, $p \leq 0.001$). Values are expressed as mean ± SEM (n = 3).

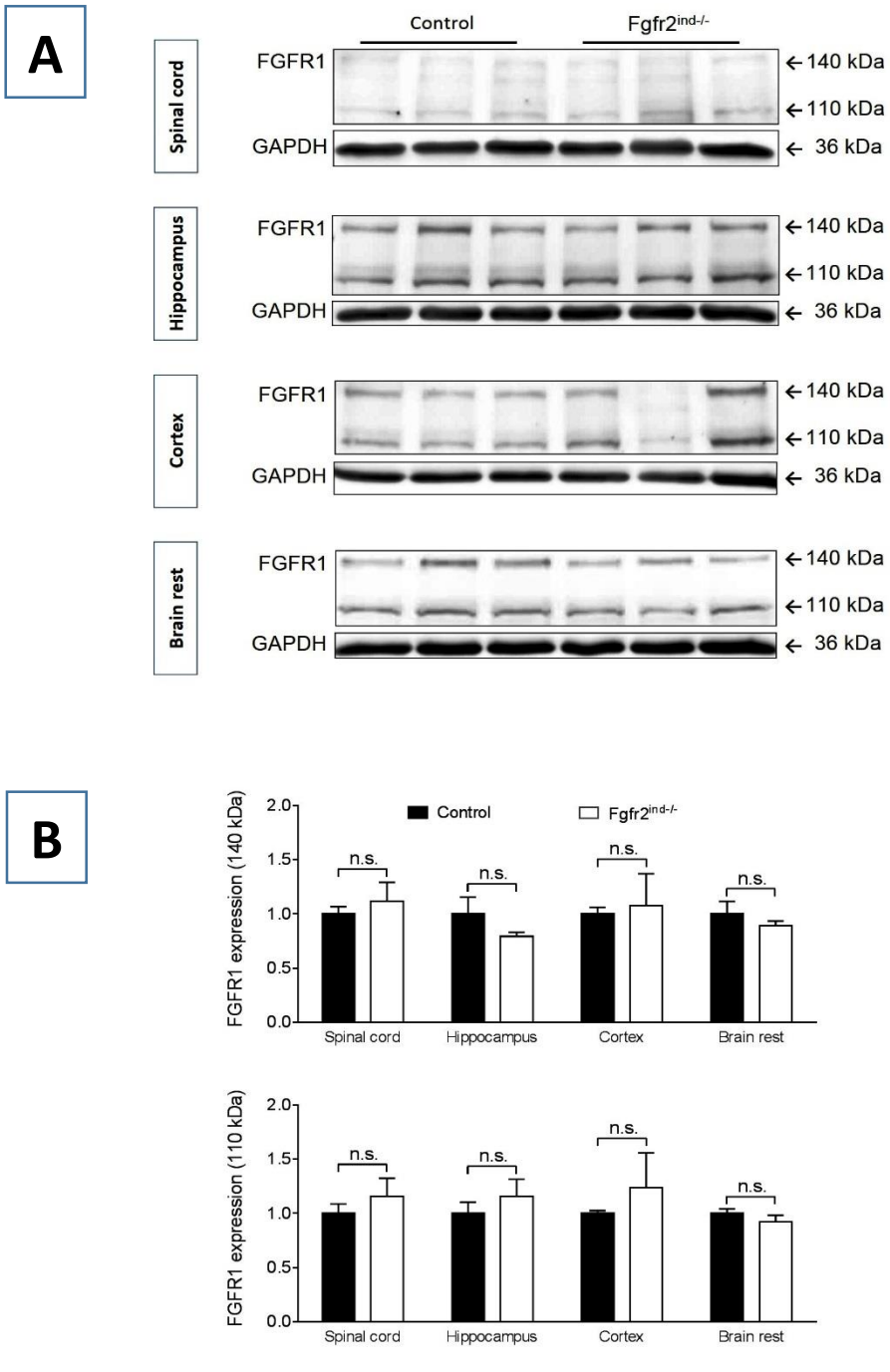

Figure 18. **Fgfr1 expression in Fgfr2$^{ind-/-}$ mice. (A)** The representative protein bands of Fgfr1 expressed in Fgfr2$^{ind-/-}$ mice and controls in different CNS regions. **(B)** The statistical analysis of Fgfr1 expression levels showed no significant regulation of heavy splicing variant of Fgfr1 (140 kDa) in spinal cord (p = 0.547), hippocampus (p = 0.269), cortex (p = 0.802), and brain rest (p = 0.436). Fgfr1 light splicing variant (110 kDa) evaluation also showed no significant regulation in spinal cord (p = 0.450), hippocampus (p = 0.440), cortex (p = 0.502), and brain rest (p = 0.362). Values are expressed as mean ± SEM (n = 3).

4.1.4 Characterization of oligodendrocyte specific FGFR2 downstream signaling

FGFR2 triggers a series of critical and complex protein downstream signaling. We studied the expression and regulation pattern of FGFR2 downstream signaling pathways involved in the inflammatory response as well as neuronal growth and development. The WB protein analysis of different brain regions (spinal cord, Hippocampus, cortex, and brain rest) in $Fgfr2^{ind-/-}$ mice and its controls were investigated 2 weeks after oligodendrocytes knockout induction.

4.1.4.1 Oligodendrocyte Fgfr2 ablation effect on AKT phosphorylation

To analyze the influence of oligodendrocyte specific Fgfr2 on AKT phosphorylation, whole protein lysates of cortex, spinal cord, hippocampus and brain rest from control and $Fgfr2^{ind-/-}$ were analyzed by western blot. AKT, a serine/threonine kinase, is one of the major FGFR2 mediators which regulates a variety of cellular functions by phosphorylating numerous downstream mediators in a cell specific manner. AKT pathway participate in various critical biological functions such as cell proliferation and survival by phosphorylating a variety of substrates. The WB analysis of pAKT expression showed higher phosphorylation level in $Fgfr2^{ind-/-}$ mice in spinal cord ($p \leq 0.001$), hippocampus ($p = 0.023$), cortex ($p = 0.002$), and brain rest ($p = 0.005$) (Figure 20).

4.1.4.2 Oligodendrocyte Fgfr2 ablation effect on ERK1/2 phosphorylation

ERK1 (44 kDa) and ERK2 (42 kDa) are related protein-serine/threonine kinases that participate in the Ras-Raf-MEK-ERK signal transduction cascade. They regulate a wide range of processes including cell adhesion, cell cycle progression, cell migration, cell survival, differentiation, metabolism, proliferation, and transcription. The WB analysis of pERK expression levels showed no significant regulation of pERK1 (44 kDa) in spinal cord ($p = 0.859$), hippocampus ($p = 0.269$), cortex ($p = 0.296$), and brain rest ($p = 0.743$). The evaluation of pERK2 (42 kDa) showed downregulation in spinal cord ($p = 0.012$), hippocampus ($p = 0.009$), cortex ($p = 0.035$), and brain rest ($p = 0.008$) (Figure 21).

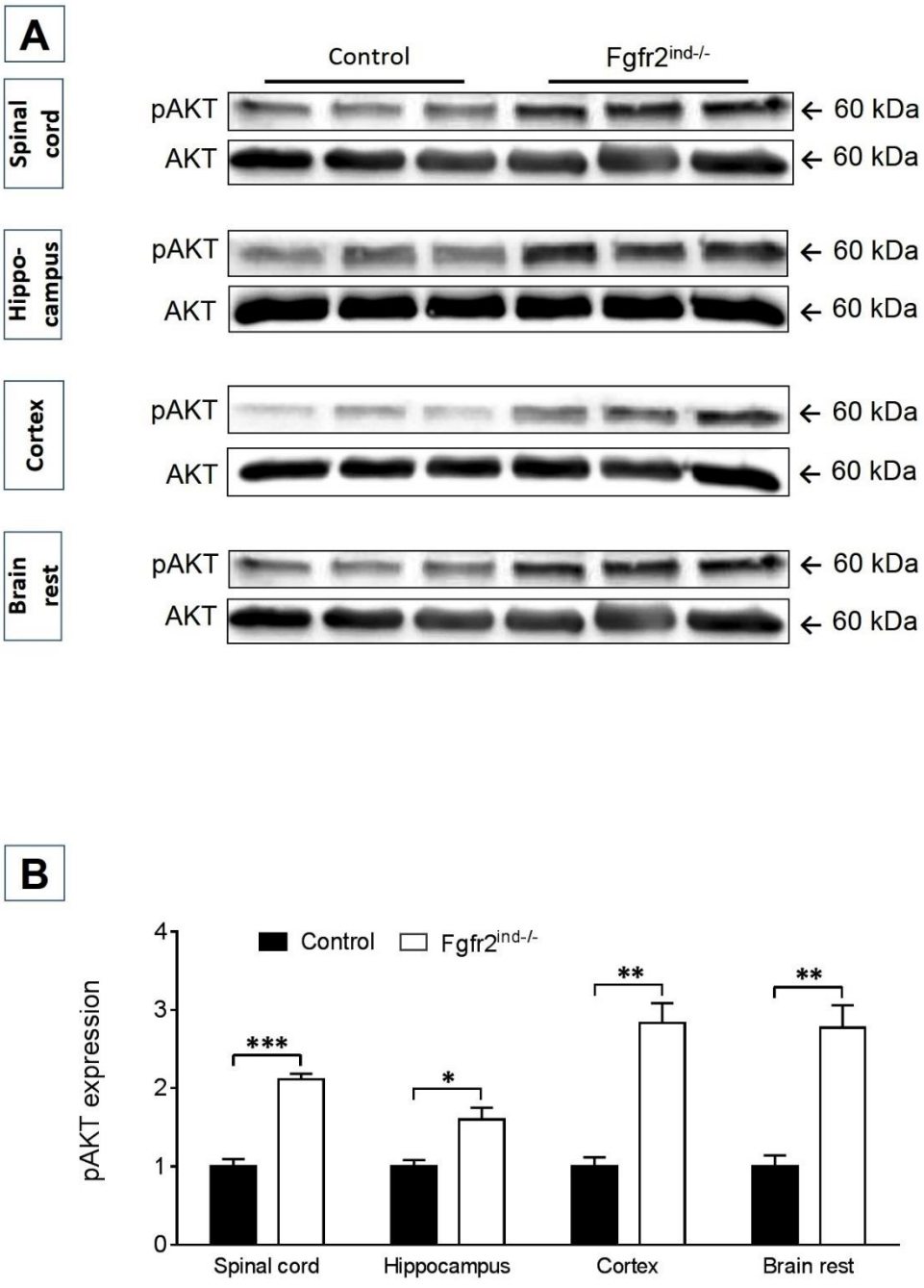

Figure 19. **AKT phosphorylation in Fgfr2$^{ind-/-}$ mice. (A)** The representative protein bands of pAKT expressed in Fgfr2$^{ind-/-}$ mice and controls in different CNS regions. **(B)** The statistical analysis of pAKT expression showed higher phosphorylation level in Fgfr2$^{ind-/-}$ mice in spinal cord ($p \leq 0.001$), hippocampus ($p = 0.023$), cortex ($p = 0.002$), and brain rest ($p = 0.005$).

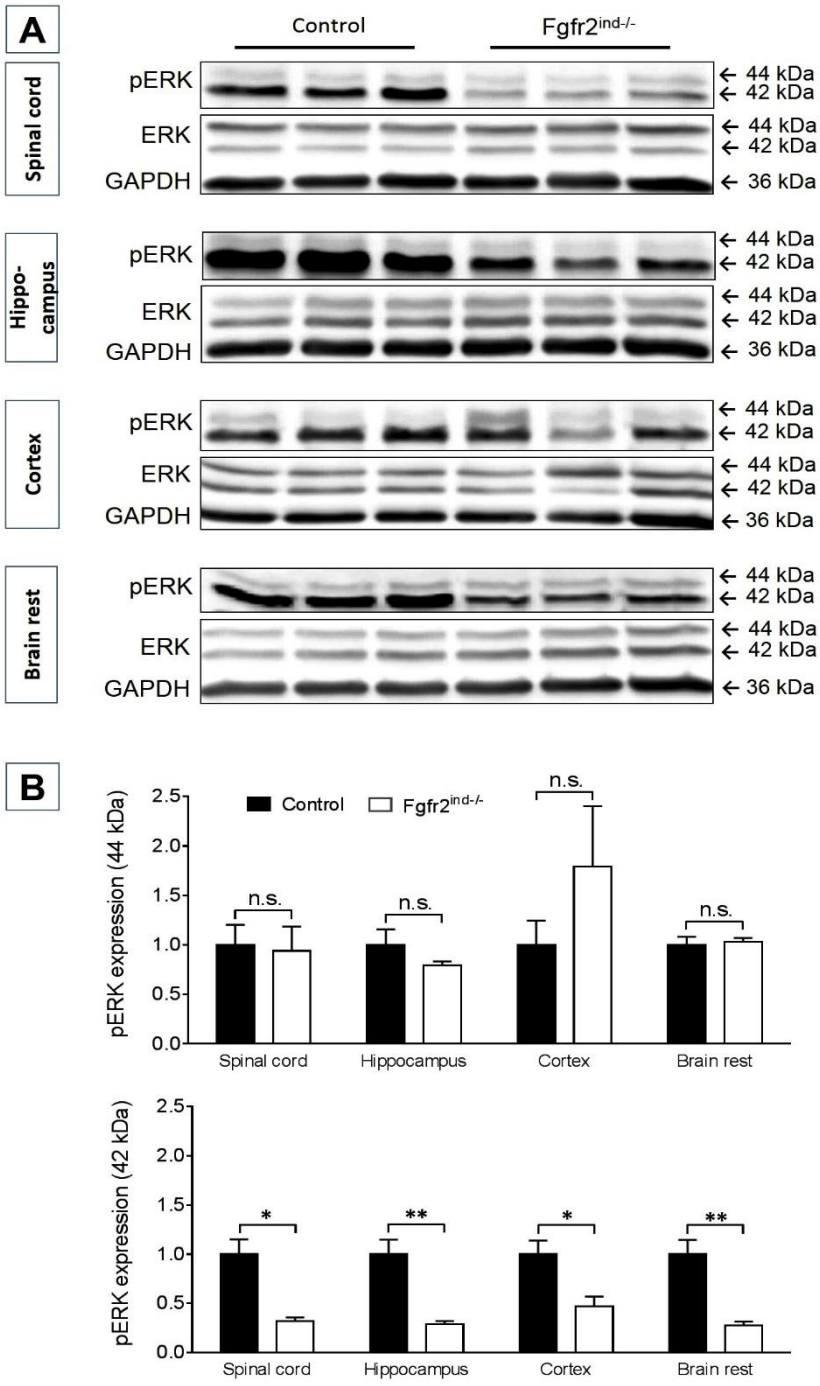

Figure 20. **ERK phosphorylation in Fgfr2$^{ind-/-}$ mice. (A)** The representative protein bands of pERK expressed in Fgfr2$^{ind-/-}$ mice and controls in different CNS regions. **(B)** The statistical analysis of pERK expression levels showed no significant regulation of heavy splicing variant of pERK (44 kDa) in spinal cord (p = 0.859), hippocampus (p = 0.269), cortex (p = 0.296), and brain rest (p = 0.743). The evaluation of pERK light chain (42 kDa) showed downregulation in spinal cord (p = 0.012), hippocampus (p = 0.009), cortex (p = 0.035), and brain rest (p = 0.008). Values are expressed as mean ± SEM (n = 3).

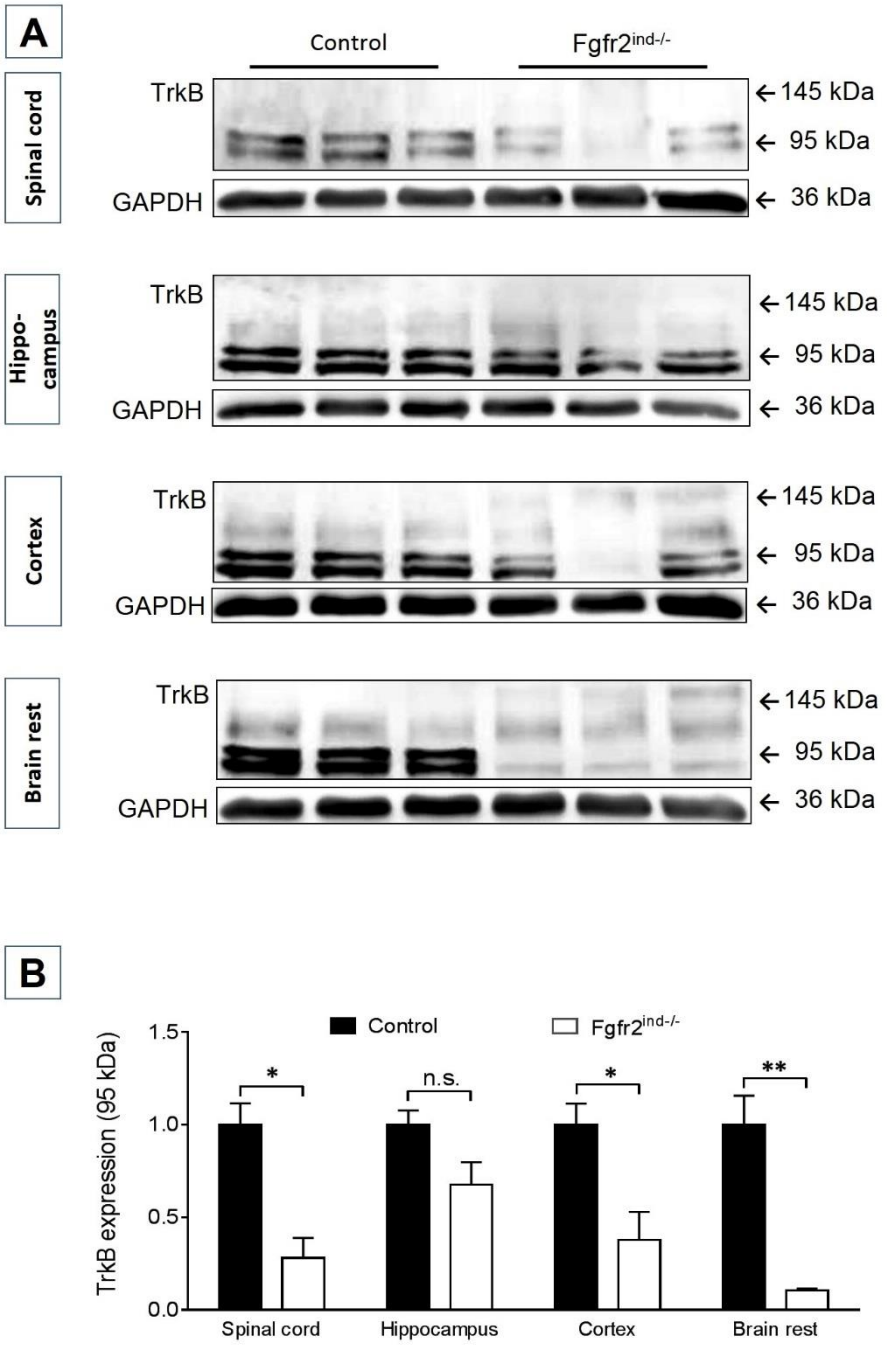

Figure 21. **TrkB expression in Fgfr2$^{ind-/-}$ mice.** The representative protein bands of TrkB expressed in Fgfr2$^{ind-/-}$ mice and controls in different CNS regions. **(B)** The statistical analysis of TrkB expression levels showed no significant regulation of heavy splicing variant of TrkB (145 kDa). The evaluation of TrkB light chain (95 kDa) showed downregulation in spinal cord (p = 0.011), hippocampus (p = 0.090), cortex (p = 0.031), and brain rest (p = 0.005). Values are expressed as mean ± SEM (n = 3).

4.1.4.3 The effect of oligodendrocytes Fgfr2 ablation on other downstream mediators

The expression pattern of various other FGFR2 downstream signalling protein mediators, potentially involved in the inflammatory response and neuronal growth and development were investigated from different CNS regions using WB analysis. The expression level of Stat1/2, DCLK, BDNF, CREB, P38, PCNA, and MBP proteins showed no statically significant regulation in $Fgfr2^{ind-/-}$ mice when compared to controls (n=3).

4.1.5 TrkB is downregulated upon Fgfr2 knockout induction

To analyze the influence of oligodendrocyte specific FGFR2 on TrkB expression, whole protein lysates of cortex, spinal cord, hippocampus and brain rest from control and $Fgfr2^{ind-/-}$ mice were analyzed by western blot. The heavy splicing variant of TrkB (145 kDa) was not detected in spinal cord and hippocampus protein lysates and it was not regulated in cortex and brain rest. The light chain of TrkB (95 kDa) was downregulated in spinal cord ($p = 0.011$), cortex ($p = 0.031$), and brain rest ($p = 0.005$) in $Fgfr2^{ind-/-}$ mice but not in hippocampus ($p = 0.090$) (Figure 21).

4.1.6 The Fgfr2 ablation does not affect the oligodendrocyte population

FGF receptors are known to play profound roles in neurons and oligodendrocyte proliferation, migration and maturation as well as central nervous system myelination. Here we investigated the effect of oligodendrocytes specific Fgfr2 conditional knockout on oligodendrocyte cell population in $Fgfr2^{ind-/-}$ and controls. Therefore, the Olig2(+) and NogoA(+) cells in spinal cord were quantified by immunohistochemistry. These analyses indicate the population of oligodendrocyte progenitors (Olig2(+)) or mature oligodendrocytes (NogoA(+)) were not altered in $Fgfr2^{ind-/-}$ when compared to WT controls (Figure 22).

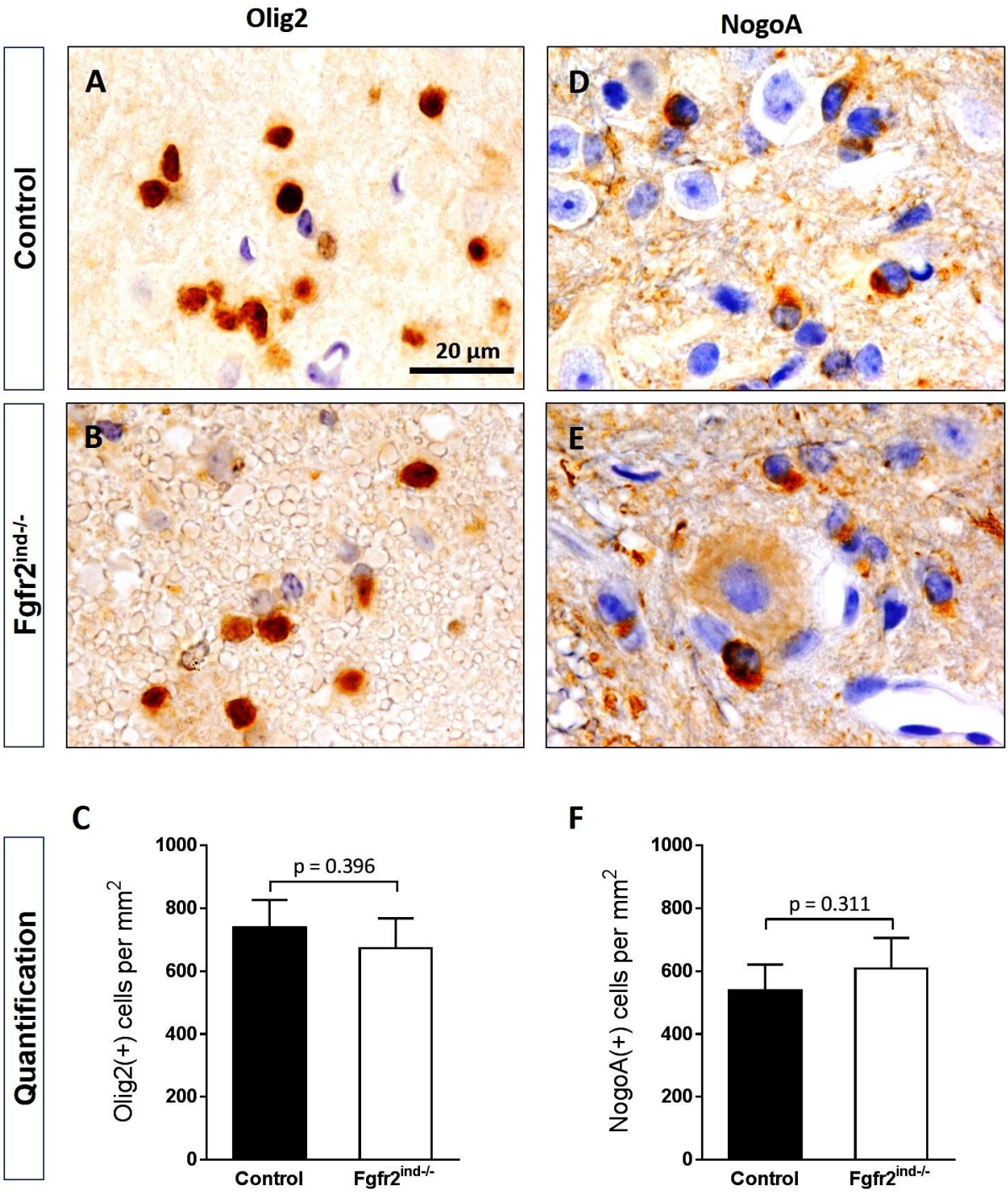

Figure 22. **Immunohistochemistry of oligodendrocyte populations in 8 week old mice.** The number of Olig2(+) (A, B, and C) and NogoA(+) (D, E, and F) oligodendrocytes in spinal cord cross-sections in controls and *Fgfr2*$^{ind-/-}$ mice 2 weeks after knockout induction. The representative spinal cord sections are shown. The number of OLs was not altered due to Fgfr2 deletion. Values are expressed as mean ± SEM (n = 4).

4.2 EAE in Fgfr2$^{ind-/-}$ mice

4.2.1 EAE clinical score

The Fgfr2$^{ind-/-}$ and control mice were immunized with MOG_{35-55} peptide and were monitored for their EAE clinical symptoms (Figure 23). The EAE scores were evaluated as described in methods (section 3.2.5).

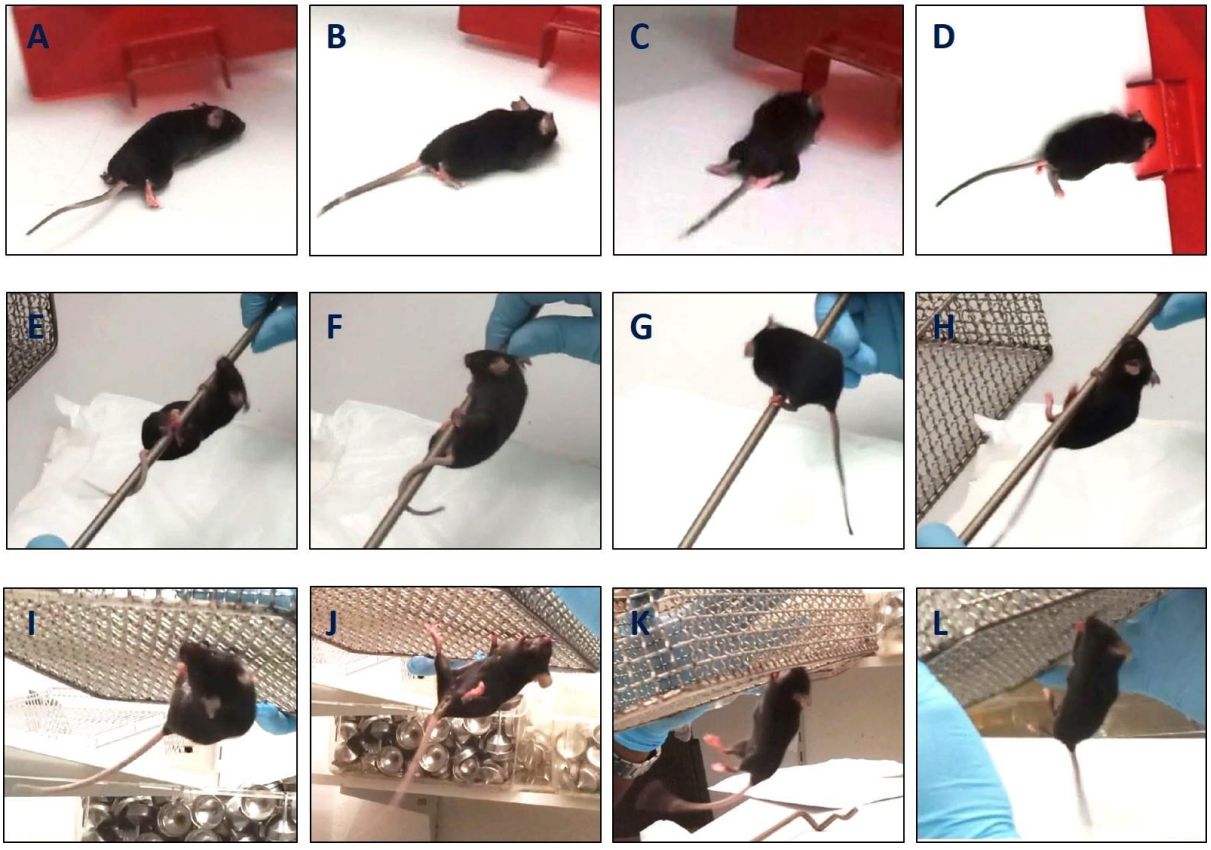

Figure 23. **Clinical symptoms of MOG_{35-55} peptide induced EAE in Fgfr2$^{ind-/-}$ mice.** Healthy mice showed with active tail while walking (A), spiral tail around the rod (E), and hanging on 4 limbs on the net (I). The slightly affected mice with complete tail weakness (clinical score 0.5-1.0) are showed while walking, standing on the rod and hanging on the net (B, F, J). The mice with ascending to severe hind limb weakness (clinical score 1.5-2.5) are shown (C, G, K). The last column shows the representative figures of mice with hind limb paralysis and forelimb weakness (clinical score 3-4) (D, H, and L).

4.2.2 Fgfr2$^{ind-/-}$ mice show a milder EAE disease course

The disease course of MOG_{35-55}-induced EAE was investigated in the acute and chronic phases of EAE (Figure 24). At 11-12 weeks of age, EAE was induced in female Fgfr2$^{ind-/-}$ and their control littermates (n=13) in a total of 3 independent experiments. The onset of disease was on day 9 p.i. in both study groups. On days 16 and 19 p.i. the EAE score was significantly reduced in Fgfr2$^{ind-/-}$ (p = 0.036, p = 0.042). From days 24 until day 60 (with the exception of day 45) Fgfr2$^{ind-/-}$ mice displayed a milder course of EAE compared to controls (p < 0.05). At the chronic phase of EAE, Fgfr2$^{ind-/-}$ mice had a mild paraparesis whereas controls suffered from a severe paraparesis. Body weight did not differ between the two groups. Fgfr2 gene deletion in oligodendrocytes did not increase mortality.

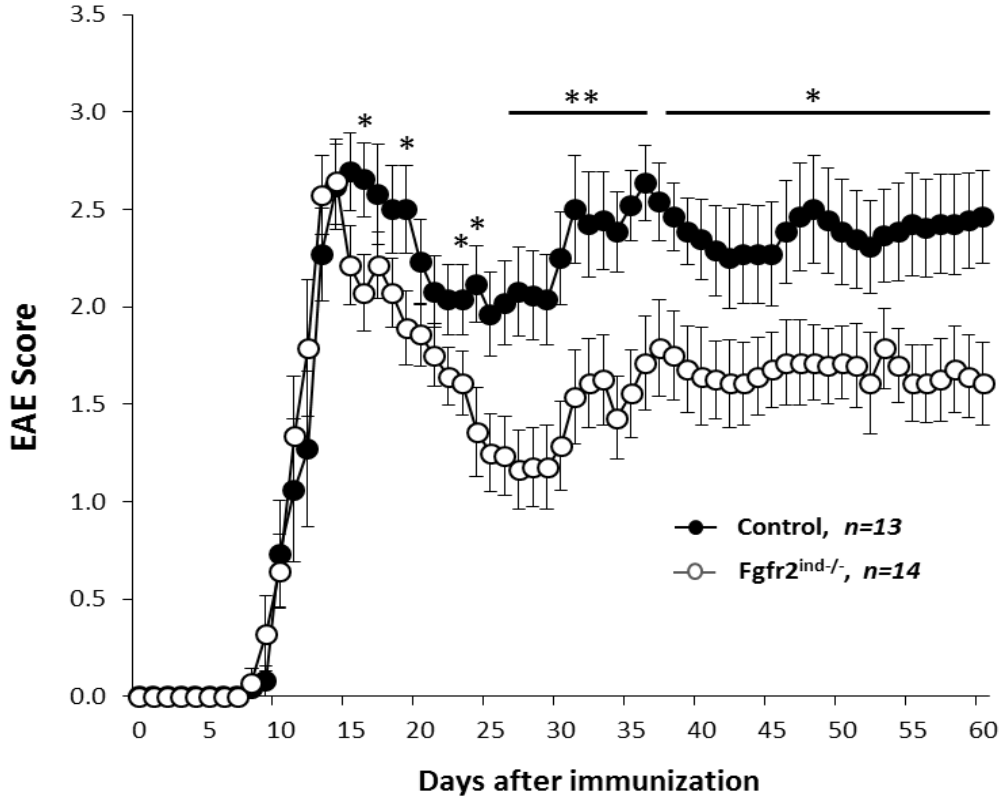

Figure 24. **Clinical course of EAE.** The onset of symptoms was not different between Fgfr2$^{ind-/-}$ mice and controls. The EAE score was decreased on days 16 and 19 in *Fgfr2$^{ind-/-}$* mice. From day 24 to day 60 (with the exception of day 45) Fgfr2$^{ind-/-}$ mice displayed a milder course of EAE. In this phase *Fgfr2$^{ind-/-}$* mice presented with a mild paraparesis whereas controls still had a moderate paraparesis. (* indicate p < 0.05, ** indicate p < 0.01) n= 13, data are presented as mean ± SEM

4.2.3 The inflammatory index is lower in Fgfr2$^{ind-/-}$ mice in chronic EAE

In alignment with the clinical course of EAE, the histological differences between Fgfr2$^{ind-/-}$ mice and controls were more evident in the chronic EAE. The inflammatory index was investigated in spinal cord white matter of acute and chronic EAE using H & E staining. There was no significant difference between the 2 groups in the acute EAE (p = 0.675), however, the infiltration rate was 33% less in Fgfr2$^{ind-/-}$ mice in chronic EAE (p = 0.002) (Figure 25).

4.2.4 The myelin loss is less in Fgfr2$^{ind-/-}$ mice in chronic EAE

The susceptibility of Fgfr2$^{ind-/-}$ mice to demyelination and MBP loss in spinal cord white matter were investigated using LFB/PAS and MBP staining respectively. The demyelination rate did not differ in acute EAE (p = 0.132), however, it was 43% lower Fgfr2$^{ind-/-}$ mice in chronic EAE (p = 0.002) (Figure 26). MBP staining showed a higher preservation of myelin (63%) in Fgfr2$^{ind-/-}$ mice only in chronic EAE (p = 0.016) (Fig. 27).

4.2.5 The nerve fibers are better preserved in Fgfr2$^{ind-/-}$ mice in chronic EAE

The axonal density was investigated with Bielschowsky's Silver Staining in spinal cord white matter of acute and chronic EAE. The analysis showed no statistically significant difference between the 2 groups in the acute phase of the disease (p = 0.119). In the chronic EAE the axonal density in Fgfr2$^{ind-/-}$ mice was 46% higher than controls (p = 0.001) (Figure 28).

Table 5. Histopathological analysis of EAE spinal cord

Pathology	Acute		*p*-value	Chronic		*p*-value
	Control	Fgfr2$^{ind-/-}$		Control	Fgfr2$^{ind-/-}$	
Inflammatory Index	4.70 ± 0.33	3.67 ± 0.48	0.133	3.98 ± 0.22	2.66 ± 0.24	0.004
Demyelination (%)	24.60 ± 1.39	18.26 ± 3.37	0.132	37.20 ± 2.81	21.00 ± 2.12	0.002
Myelin expression (%)	10.03 ± 0.45	8.62 ± 1.82	0.484	9.76 ± 1.54	3.53 ± 0.33	0.016
Axonal density (%)	41.65 ± 1.17	45.65 ± 1.85	0.119	34.14 ± 1.87	49.86 ± 2.47	0.001

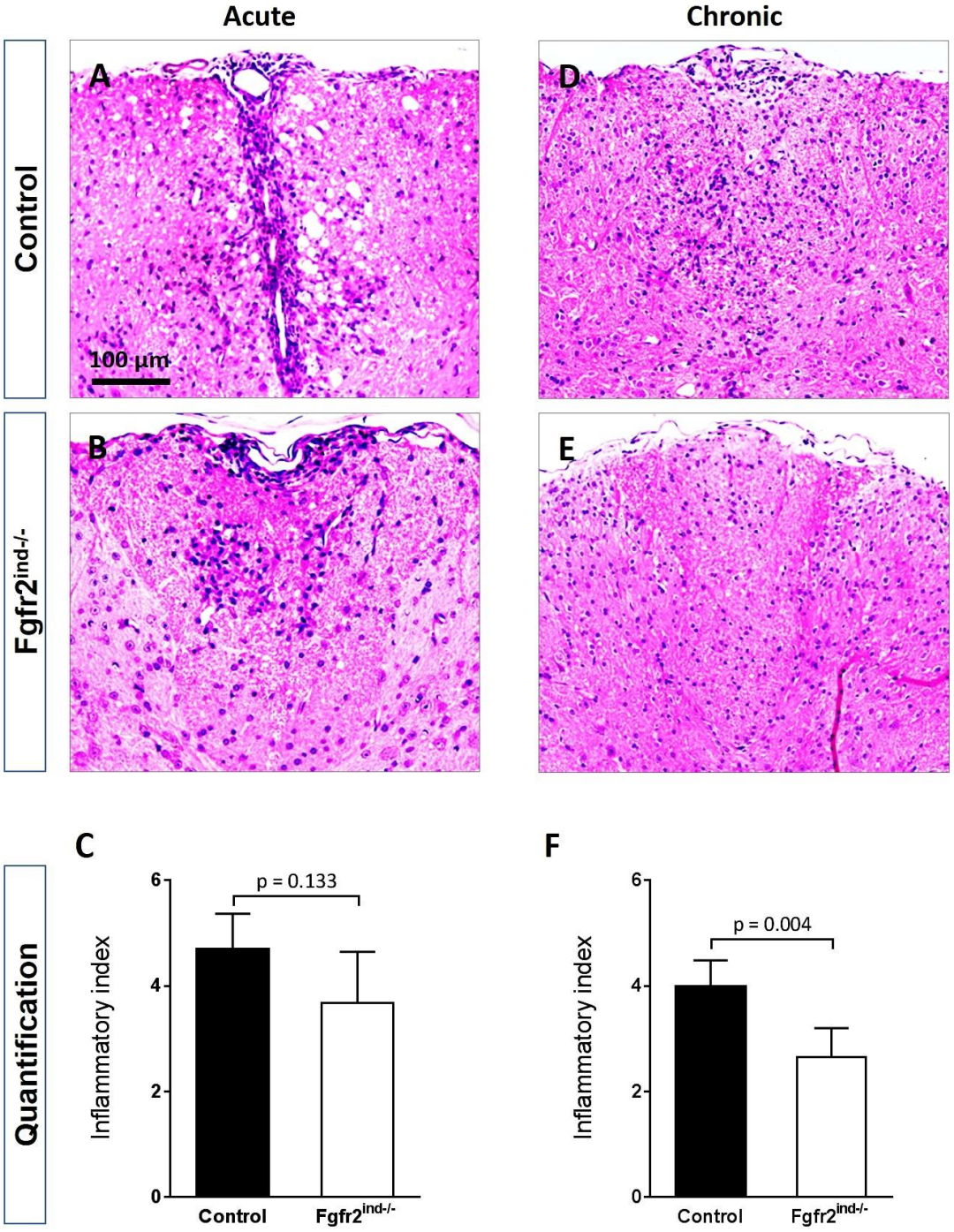

Figure 25. **The inflammatory index of EAE was investigated with H & E staining** in the spinal cord sections of acute (A, B, and C) and chronic (D, E, and F) phases of the disease. The representative spinal cord sections are shown. The inflammatory index (C and F) was less in Fgfr2$^{ind-/-}$ mice in the chronic EAE. n = 4, data are presented as mean + SEM

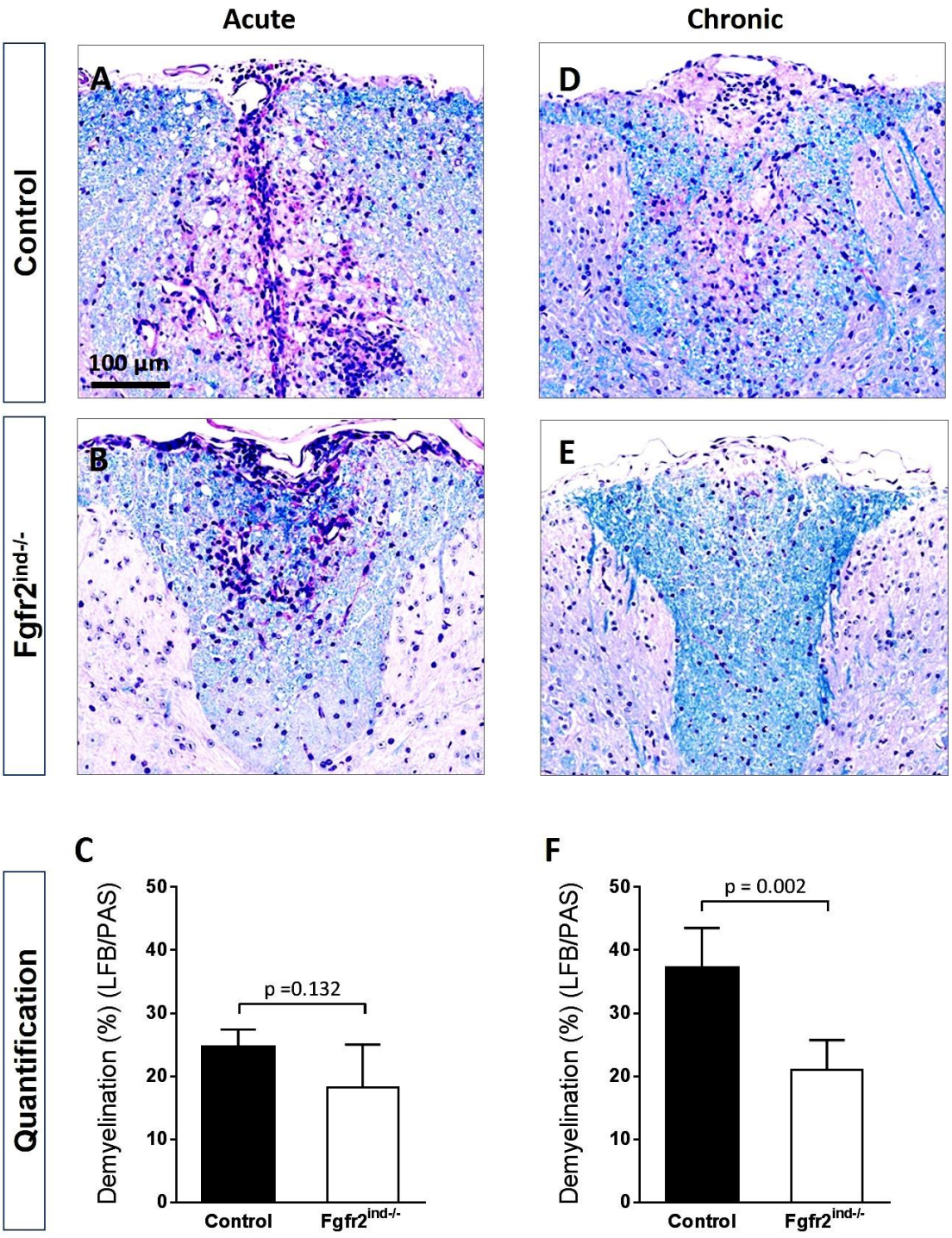

Figure 26. **The demyelination of EAE was investigated with LFB/PAS staining** in the spinal cord sections of acute (A, B, and C) and chronic (D, E, and F) phases of the disease. The representative spinal cord sections are shown. The demyelination rate (C and F) was less in $Fgfr2^{ind-/-}$ mice only in the chronic EAE. n = 4, data are presented as mean + SEM

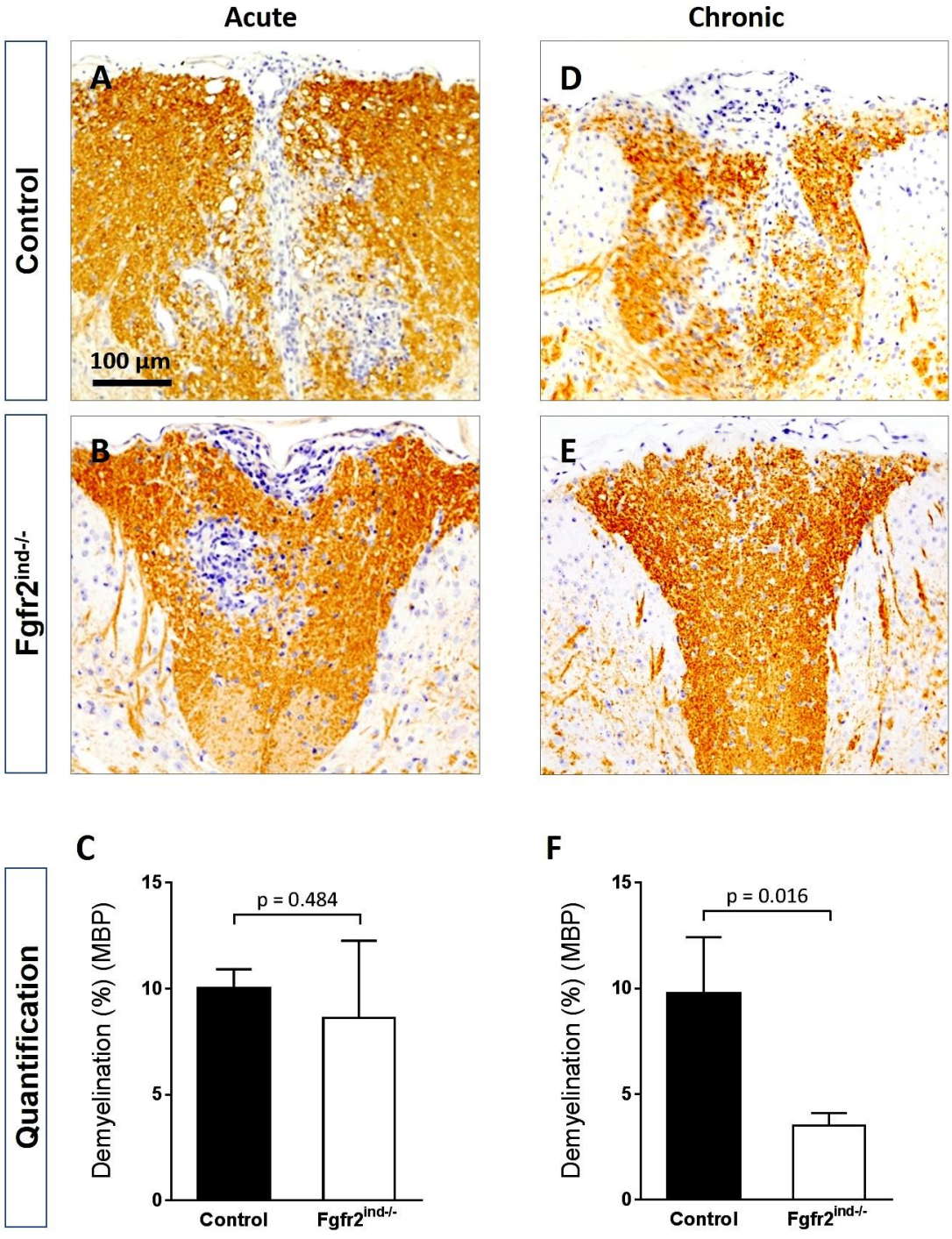

Figure 27. **The demyelination of EAE was investigated with MBP immunostaining** in the spinal cord sections of acute (A, B, and C) and chronic (D, E, and F) phases of the disease. The representative spinal cord sections are shown. The demyelination rate (C and F) was less in Fgfr2$^{ind-/-}$ mice only in the chronic EAE. n = 4, data are presented as mean + SEM

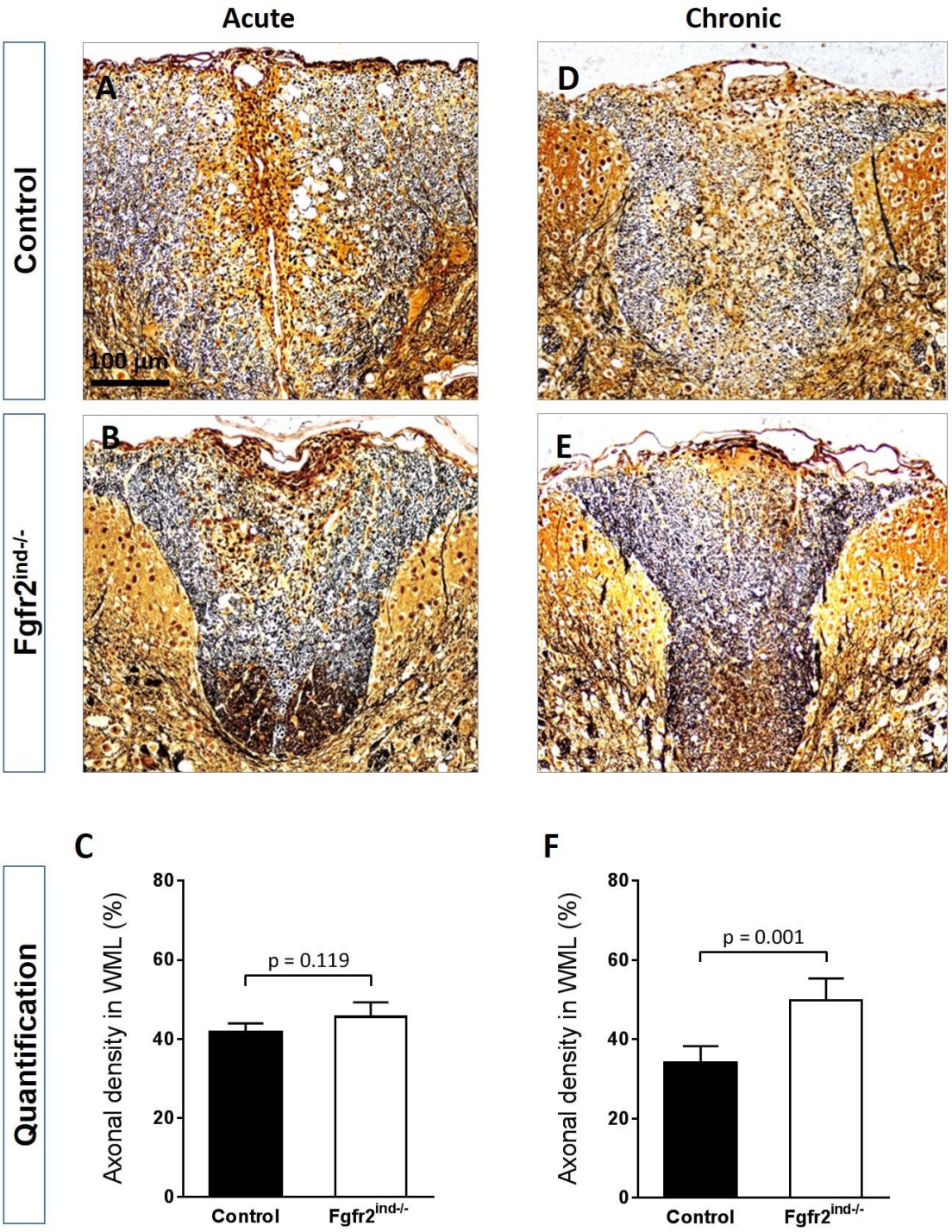

Figure 28. **The axonal density of EAE was investigated with Bielschowsky's Silver Staining** in the spinal cord sections of acute (A, B, and C) and chronic (D, E, and F) phases of the disease. The representative spinal cord sections are shown. The axonal density (C and F) was higher in Fgfr2$^{ind-/-}$ mice only in the chronic EAE. n = 4, data are presented as mean + SEM

4.2.6 Altered composition of the inflammatory infiltrate in Fgfr2$^{ind-/-}$ mice

Immunohistochemical analysis were performed to further investigate the composition of infiltrates in spinal cord EAE lesions. Histological studies addressing inflammatory index (H&E staining) determined a lower immune infiltration as well as demyelination (LFB/PAS staining) in Fgfr2$^{ind-/-}$ mice. Immunostaining for CD3(+), B220(+) and Mac3(+) cells were performed and quantified to achieve specific illustration of cellular infiltrate composition in spinal cord white matter lesions. The number of CD3(+) T cells were not affected by Fgfr2 deletion in acute EAE (p = 0.578) however, it was significantly lower in chronic stage in Fgfr2$^{ind-/-}$ mice (p = 0.002) (Figure 29). In the acute phase of EAE Mac3(+) cells (p = 0.045) and B220(+) B cells (p = 0.002) were reduced in Fgfr2$^{ind-/-}$ mice. In the chronic phase of EAE Mac3(+) cells (p = 0.007) and B220(+) B cells (p = 0.005) were reduced in Fgfr2$^{ind-/-}$ (Figure 30 and 31).

4.2.7 The oligodendrocytes population is not affected after EAE immunization

To investigate whether the changes in demyelination we observed between Fgfr2$^{ind-/-}$ and controls was caused by altered oligodendrocyte populations we quantified Olig2(+) cells and NogoA(+) cells in spinal cord sections by immunohistochemistry. Quantifications of Olig2(+) showed no difference between Fgfr2$^{ind-/-}$ and controls in either the acute (p = 0.590) or chronic phase of EAE (p = 0.203) (Figure 32). Fgfr2 deletion did not affect NogoA(+) cells (mature oligodendrocytes) in the acute (p = 0.386) or chronic phase of EAE (p = 0.251) (Figure 33).

Table 6. Immune cell infiltration analysis of EAE spinal cord

Pathology	**Acute**		***p*-value**	**Chronic**		***p*-value**
	Control	Fgfr2$^{ind-/-}$		Control	Fgfr2$^{ind-/-}$	
CD3 (+) T cells	380 ± 55	336 ± 53	0.578	235 ± 24	124 ± 11	0.002
Mac3 (+) Macrophages	666 ± 95	398 ± 46	0.045	298 ± 17	180 ± 15	0.007
B220 (+) B cells	241 ± 15	149 ± 10	0.002	93 ± 10	47 ± 7	0.005

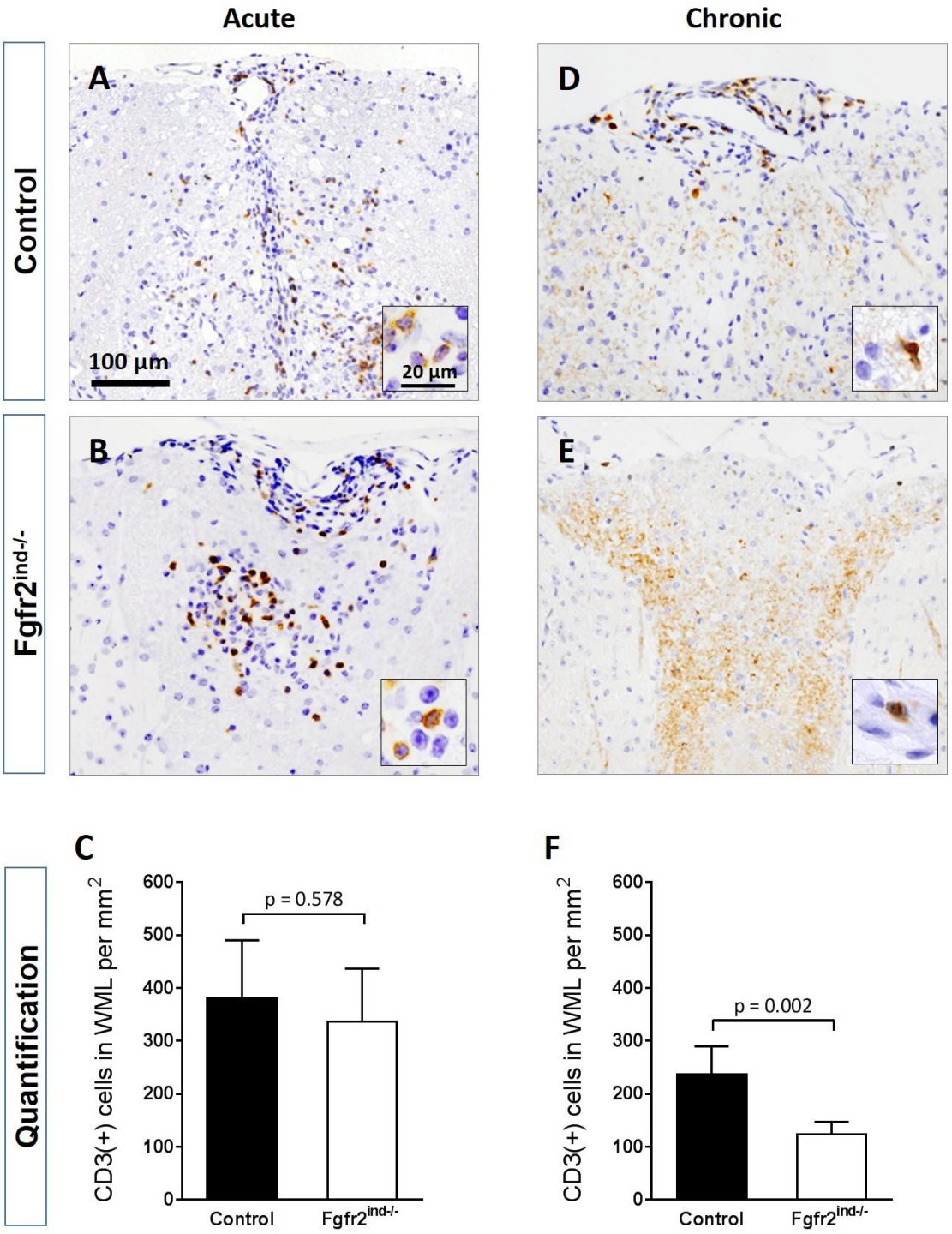

Figure 29. **The T cell infiltration in white matter** lesions was investigated by CD3(+) immunostaining of spinal cord cross-sections in Fgfr2$^{ind-/-}$ and control mice. The representative spinal cord sections of acute (A, B, and C) and chronic (D, E, and F) EAE are shown. The T cell infiltration (C and F) was reduced in Fgfr2$^{ind-/-}$ mice only in the chronic EAE. n = 4, data are presented as mean + SEM

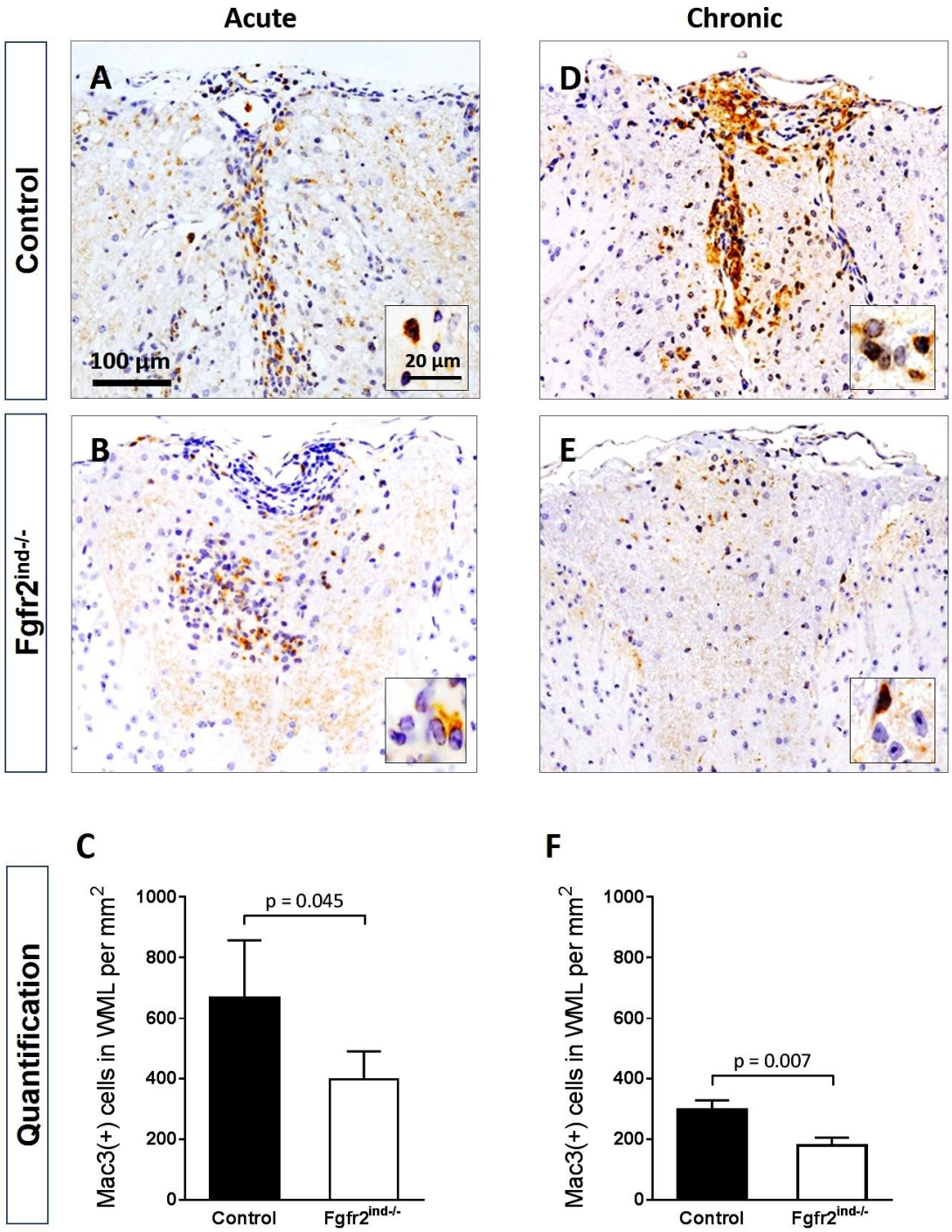

Figure 30. **The macrophages/microglia infiltration in white matter lesions** was investigated by Mac3(+) immunostaining of spinal cord cross-sections in Fgfr2$^{ind-/-}$ and control mice. The representative spinal cord sections of acute (A, B, and C) and chronic (D, E, and F) EAE are shown. The macrophage infiltration (C and F) was lower in Fgfr2$^{ind-/-}$ mice in the acute and chronic EAE. n = 4, data are presented as mean + SEM

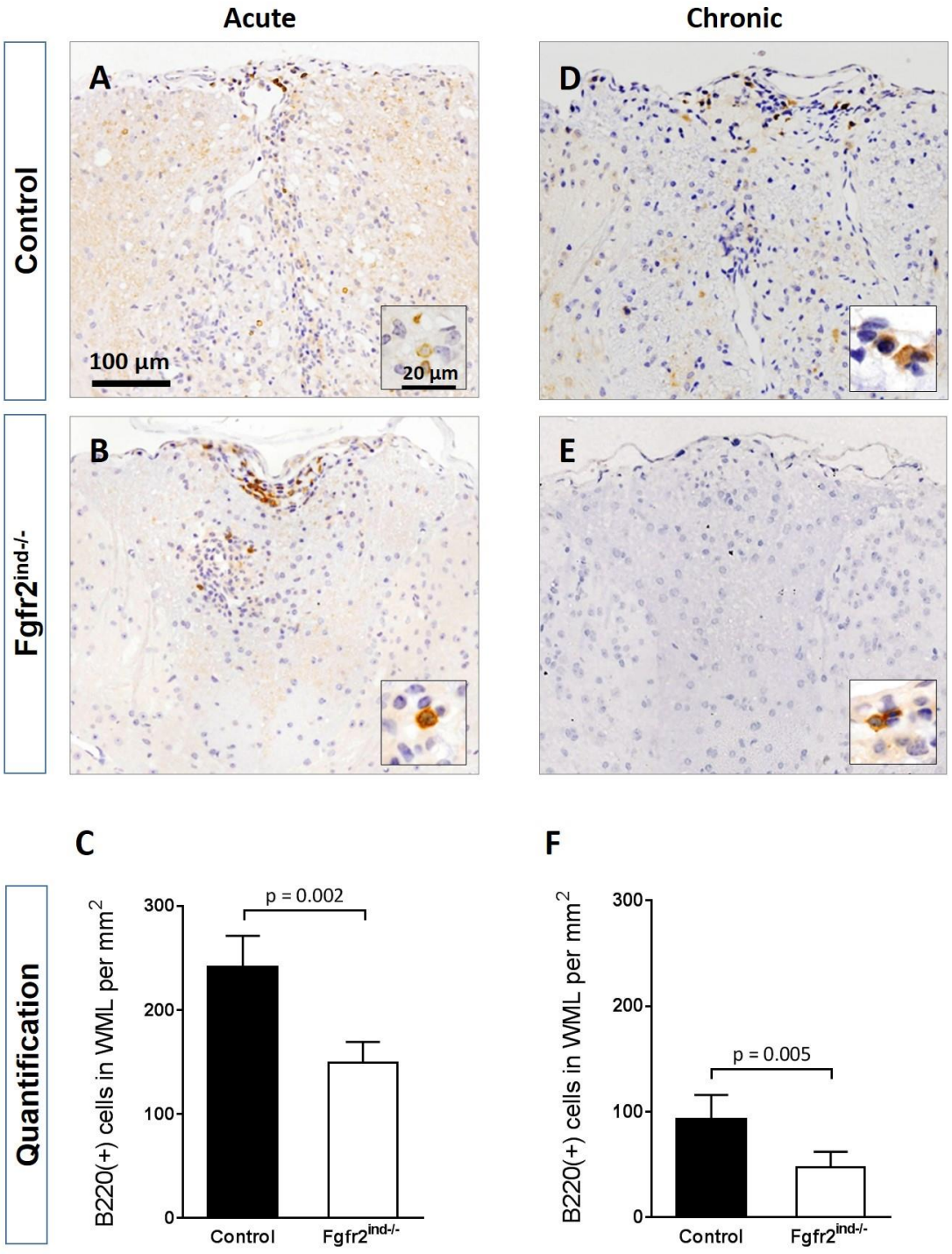

Figure 31. **B cell infiltration in white matter lesions** was investigated by B220 immunostaining of spinal cord cross-sections in Fgfr2$^{ind-/-}$ and control mice. The representative spinal cord sections of acute (A, B, and C) and chronic (D, E, and F) EAE are shown. The macrophage infiltration (C and F) was lower in Fgfr2$^{ind-/-}$ mice in the acute and chronic EAE. n = 4, data are presented as mean + SEM

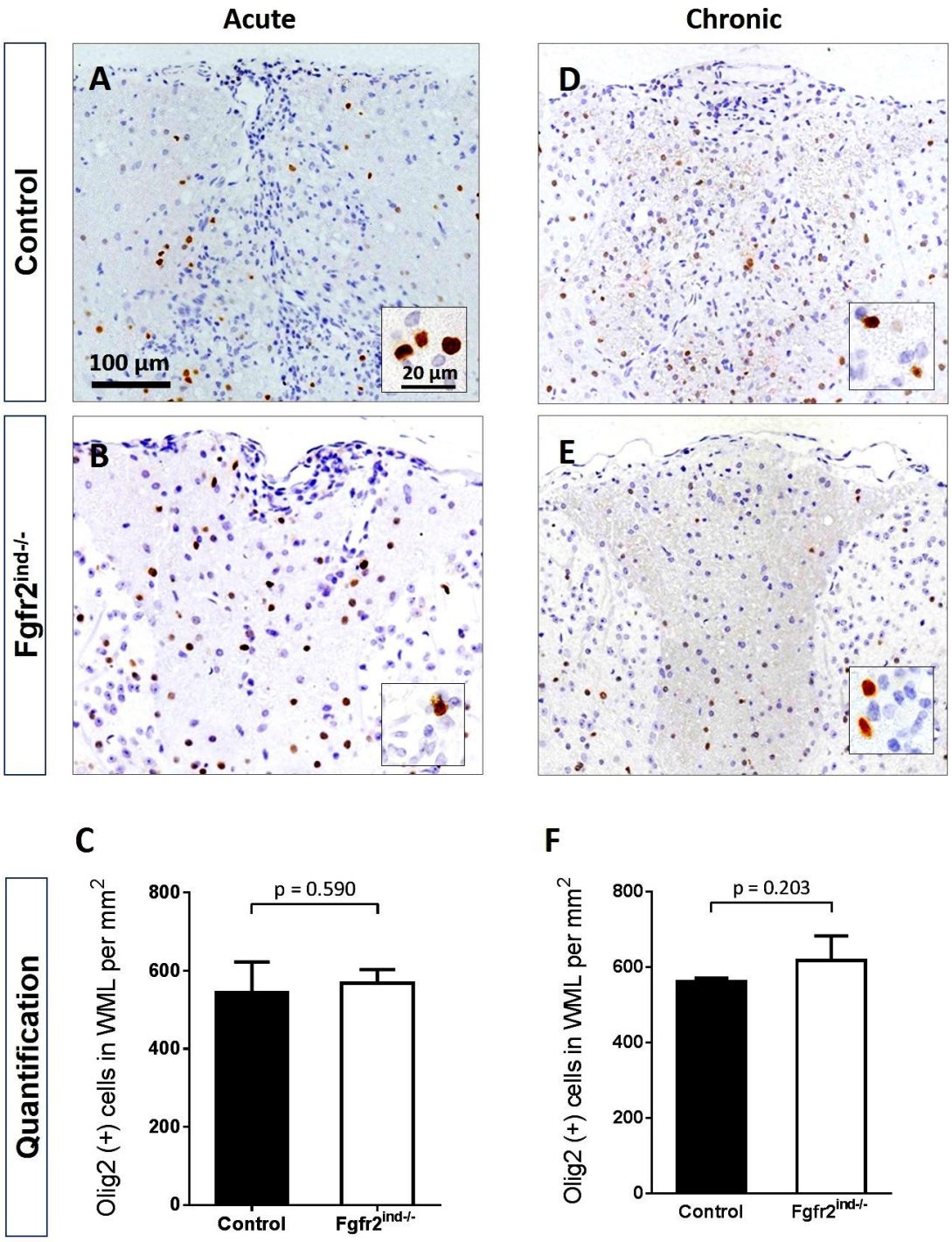

Figure 32. **Immunohistochemistry of oligodendrocyte progenitor cells in white matter lesions** was investigated by Olig2 immunostaining of spinal cord cross-sections in Fgfr2$^{ind-/-}$ and control mice. The representative spinal cord sections of acute (A, B, and C) and chronic (D, E, and F) EAE are shown. The oligodendrocyte number did not alter in acute or chronic EAE in Fgfr2$^{ind-/-}$ when compared with controls. n = 4, data are presented as mean + SEM

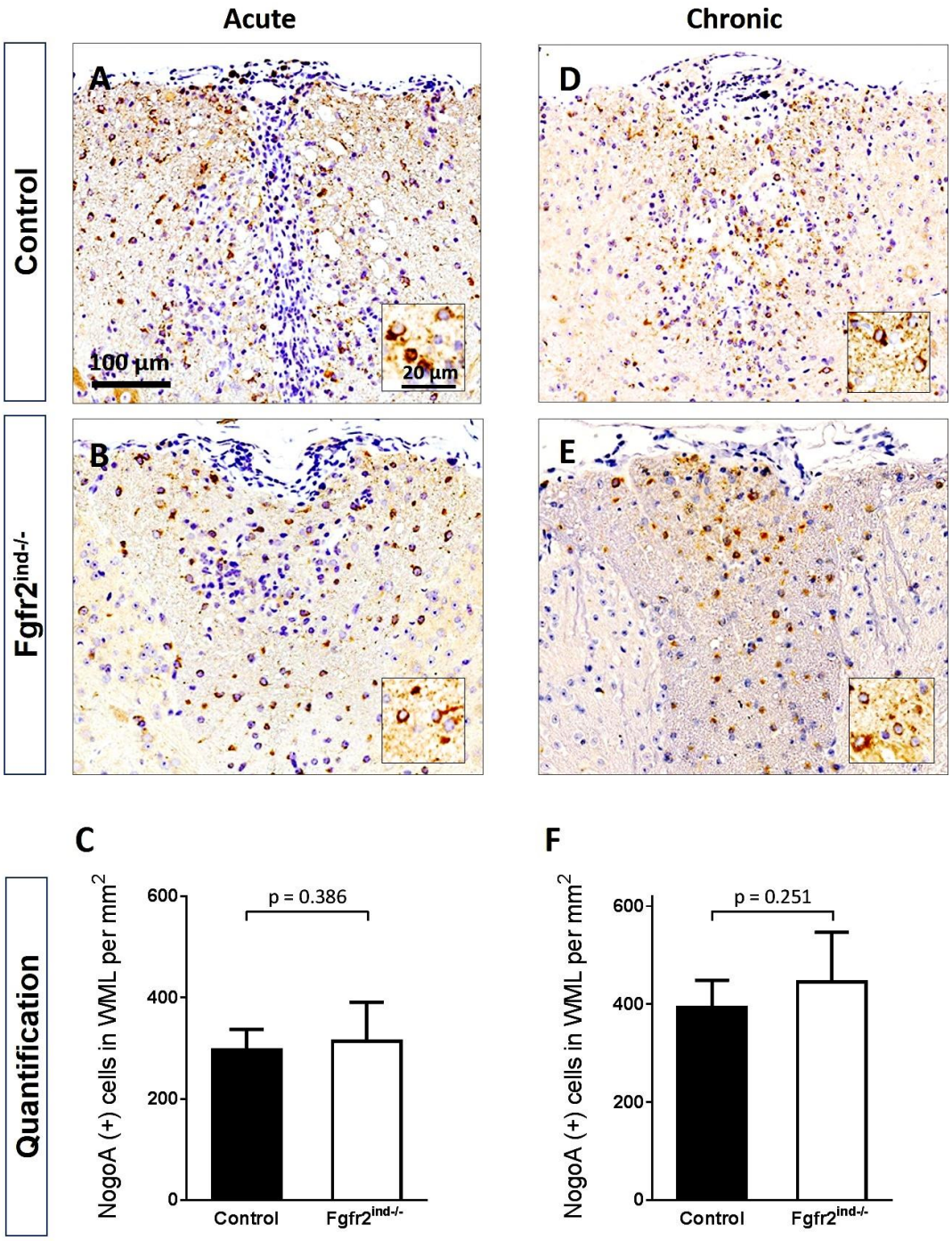

Figure 33. **Immunohistochemistry of mature oligodendrocyte population in white matter lesions** was investigated by NogoA immunostaining of spinal cord cross-sections in Fgfr2$^{ind-/-}$ and control mice. The representative spinal cord sections of acute (A, B, and C) and chronic (D, E, and F) EAE are shown. The mature oligodendrocyte number did not alter in acute or chronic EAE in Fgfr2$^{ind-/-}$ when compared with controls. n = 4, data are presented as mean + SEM

4.2.8 Fgfr2 deletion modulates ERK and AKT phosphorylation and TrkB Expression

To characterize the underlying mechanisms of oligodendrocyte Fgfr2 deletion in EAE, FGFR2-dependent downstream signaling was investigated in the spinal cord and hippocampus in both the acute phase (day 18-20) and chronic phase (day 60-65) of EAE (Figure 34, 35). Western blot analysis of FGFR2 in spinal cord and hippocampus showed no regulation in acute EAE ($p = 0.961$, $p = 0.842$), however, it was significantly reduced in chronic stage of the disease in spinal cord protein lysate ($p = 0.001$) (Figure 35 A). It appears that ablation of FGFR2 leads to upregulation of TrkB in both acute and chronic phase of EAE, however, it is statistically significant only in chronic EAE in hippocampus ($p = 0.028$) (Figure 35 D).

The phosphorylated form of AKT was upregulated in $Fgfr2^{ind-/-}$ mice in acute hippocampus ($p = 0.002$) (Figure 34 F) and in chronic spinal cord ($p = 0.014$) (Figure 35 E). The level of ERK phosphorylation was downregulated in the chronic spinal cord and hippocampus, however, it was statistically significant only in spinal cord ($p \leq 0.031$) (figure 35 G).

We also confirmed that the expression levels of Stat1, Stat3, IkB, P38, BDNF, CREB, DCLK and PCNA proteins were not significantly regulated in any stages of EAE.

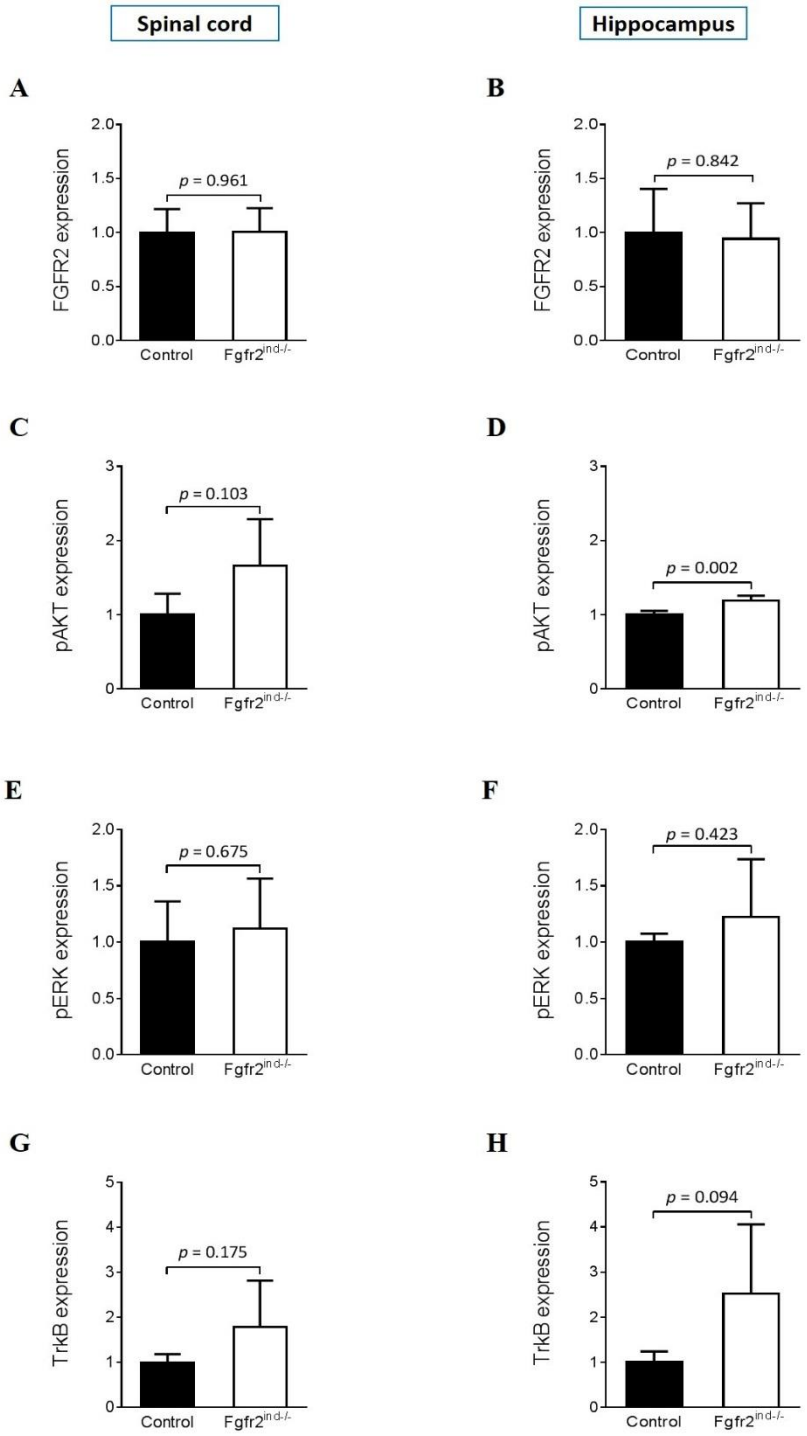

Figure 34. FGFR2 downstream signaling in Fgfr2$^{ind-/-}$ in the acute EAE. (A, B) The expression level of FGFR2 was not regulated in spinal cord and hippocampus in Fgfr2$^{ind-/-}$ mice when compared to controls. **(C, D)** The expression level of pAKT in Fgfr2$^{ind-/-}$ was upregulated in spinal cord and hippocampus, however, it was statistically significant only in hippocampus. **(E, F)** The pERK expression in Fgfr2$^{ind-/-}$ was not regulated. **(G, H)** The protein expression of TrkB in Fgfr2$^{ind-/-}$ mice was upregulated only in hippocampus. Values are expressed as mean ± SEM (n = 5).

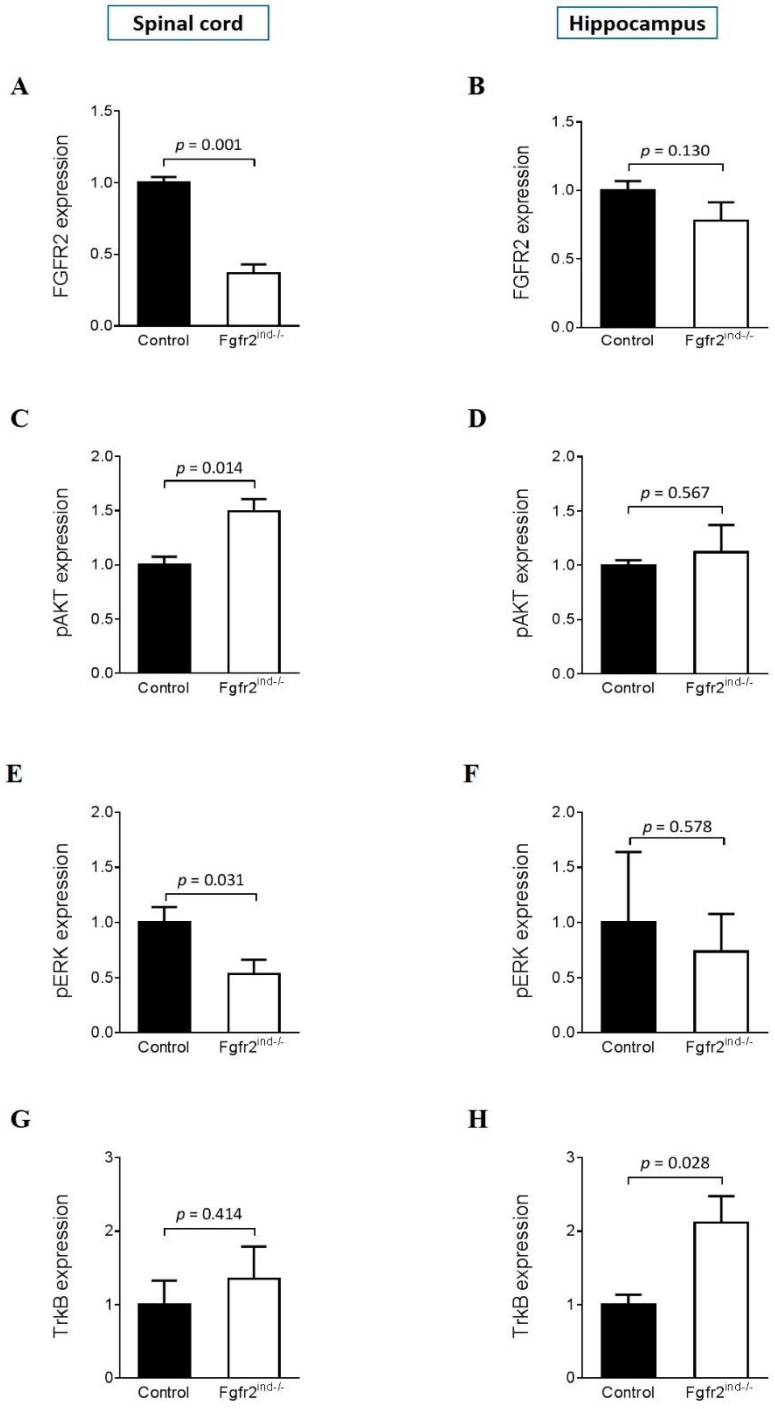

Figure 35. FGFR2 downstream signaling in Fgfr2$^{ind-/-}$ in the chronic EAE. (A, B) The expression level of FGFR2 was regulated only in the spinal cord of Fgfr2$^{ind-/-}$ when compared to controls. **(C, D)** The expression level of pAKT in Fgfr2$^{ind-/-}$ was upregulated in spinal cord but not in hippocampus. **(E, F)** The pERK expression in Fgfr2$^{ind-/-}$ was downregulated in both spinal cord and hippocampus. **(G, H)** The TrkB expression in Fgfr2$^{ind-/-}$ was upregulated in both spinal cord and hippocampus, however, it was statistically significant only in hippocampus. Values are expressed as mean ± SEM (n = 3).

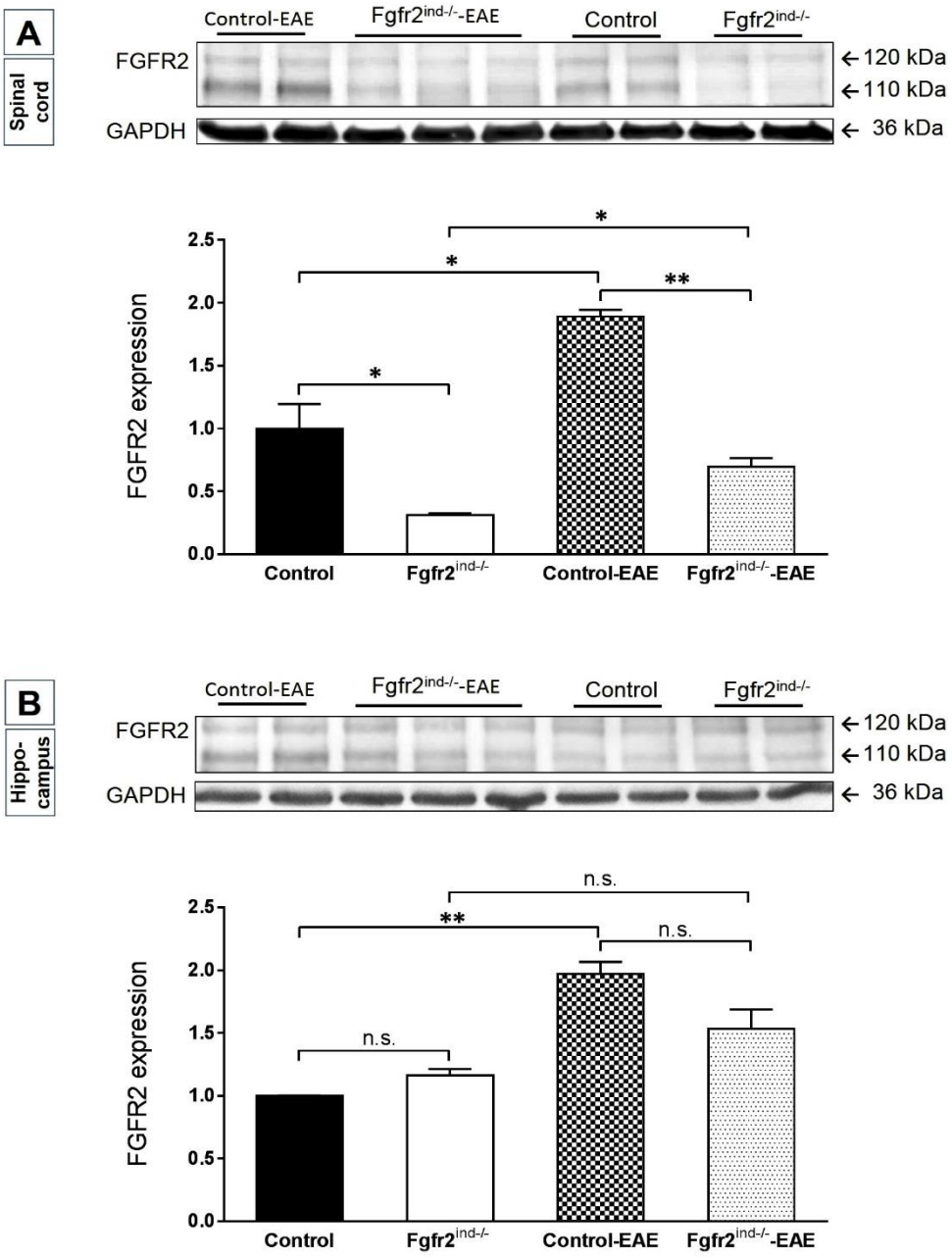

Figure 36. **FGFR2 expression in chronic EAE.** To determine the FGFR2 expression pattern due to EAE immunization, the non-EAE groups of control and Fgfr2$^{ind-/-}$ mice were included. **(A) Spinal cord.** FGFR2 was upregulated in the control and Fgfr2$^{ind-/-}$ mice when compared to the respective EAE immunized groups (p = 0.026, p = 0.021). In both EAE and non-EAE groups the Fgfr2$^{ind-/-}$ mice expressed a lower level of FGFR2 (p = 0.039, p = 0.001). **(B) Hippocampus.** FGFR2 was upregulated in the control and Fgfr2$^{ind-/-}$ mice when compared to the respective EAE immunized groups, however, it was statistically significant only in the control group (p = 0.001, p = 0.16). Fgfr2 was not regulated within EAE and non-EAE groups. Values are expressed as mean ± SEM.

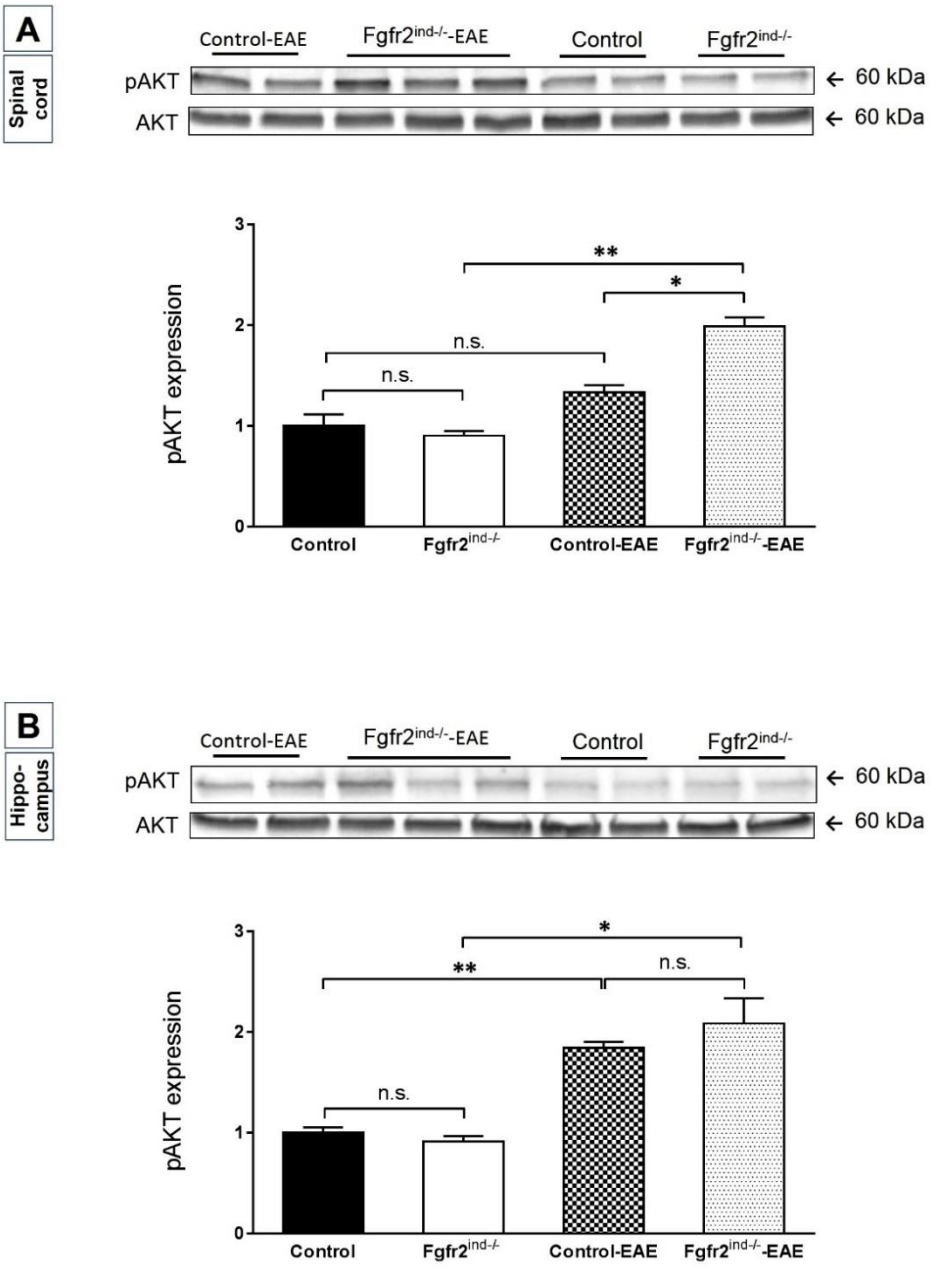

Figure 37. **pAKT expression in chronic EAE.** To determine the pAKT expression pattern due to EAE immunization, the non-EAE groups of control and Fgfr2$^{ind-/-}$ mice were included. **(A) Spinal cord.** pAKT was upregulated in Fgfr2$^{ind-/-}$ mice when compared to the respective EAE immunized Fgfr2$^{ind-/-}$ mice (p = 0.003). In EAE group the expression of pAKT was upregulated in Fgfr2$^{ind-/-}$ mice (p = 0.014). **(B) Hippocampus.** pAKT was upregulated in the control and Fgfr2$^{ind-/-}$ mice when compared to the respective EAE immunized groups (p = 0.007, p = 0.036). pAKT was not regulated in Fgfr2$^{ind-/-}$ mice within the EAE or non-EAE groups when compared to their respective controls. Values are expressed as mean ± SEM.

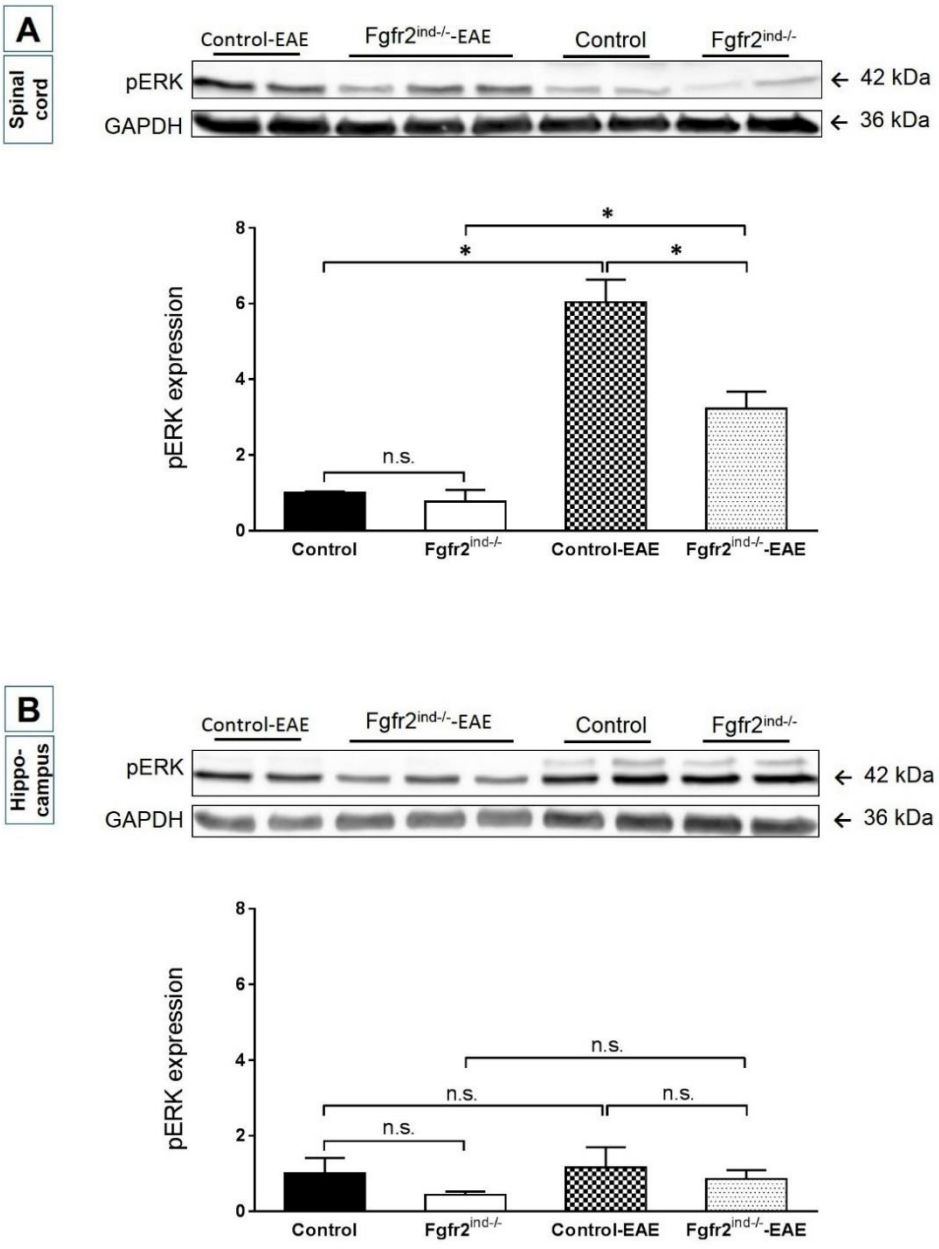

Figure 38. **pERK expression in chronic EAE.** To determine the pERK expression pattern due to EAE immunization, the non-EAE groups of control and Fgfr2$^{ind-/-}$ mice were included. **(A) Spinal cord.** pERK was upregulated in the control and Fgfr2$^{ind-/-}$ mice when compared to the respective EAE immunized groups (p = 0.014, p = 0.029). In EAE group the Fgfr2$^{ind-/-}$ mice expressed a lower level of pERK (p = 0.031). **(B) Hippocampus.** pERK was not regulated in the control and Fgfr2$^{ind-/-}$ mice when compared to the respective EAE immunized mice (p = 0.809, p = 0.256). pERK was downregulated in Fgfr2$^{ind-/-}$ mice within EAE and non-EAE groups, however, it was not statistically significant (p = 0.758, p = 0.204). Values are expressed as mean ± SEM.

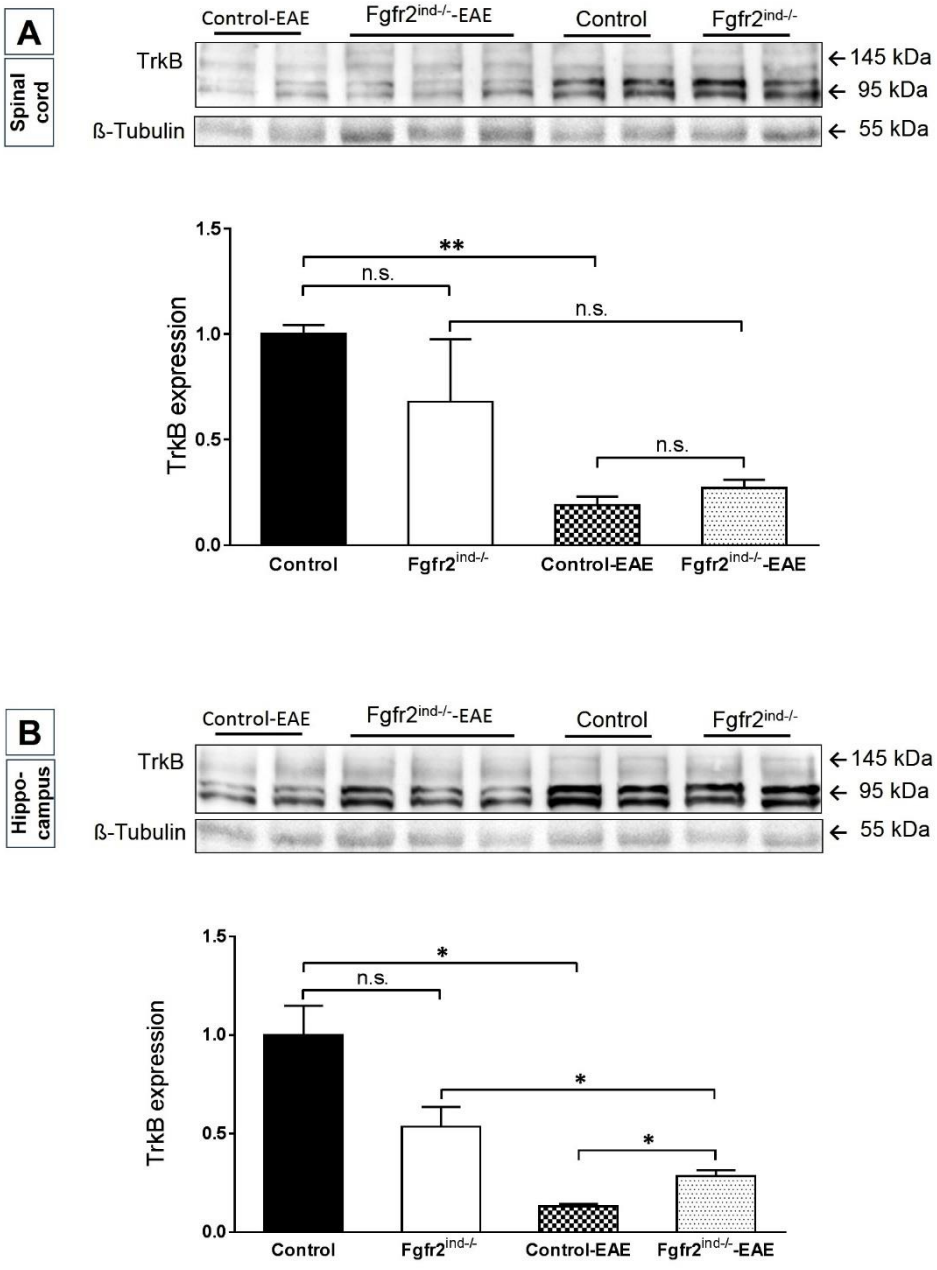

Figure 39. **TrkB expression in chronic EAE.** To determine the TrkB expression pattern due to EAE immunization, the non-EAE groups of control and Fgfr2$^{ind-/-}$ mice were included. **(A) Spinal cord.** TrkB was downregulated in the control but not Fgfr2$^{ind-/-}$ mice when compared to the respective EAE immunized groups (p = 0.004, p = 0.088). In EAE group the Fgfr2$^{ind-/-}$ mice expressed a higher level of TrkB, however, it was not statistically significant (p = 0.274). **(B) Hippocampus.** TrkB was downregulated in the control and Fgfr2$^{ind-/-}$ mice when compared to the respective EAE immunized mice (p = 0.015, p = 0.032). TrkB was upregulated in Fgfr2$^{ind-/-}$ mice within EAE immunized group (p = 0.033). Values are expressed as mean ± SEM.

4.3 Glatiramer acetate treatment

Treated with GA, the Fgfr2$^{ind-/-}$ mice exhibited a milder course of EAE

To characterize the potential association of FGFR2 with anti-inflammatory and neuroprotective effects of glatiramer acetate in MOG$_{35-55}$-induced EAE, the Fgfr2$^{ind-/-}$ and control mice were treated with GA pretreatment regimen. GA is one of the well-known immunomodulatory drugs currently used to treat multiple sclerosis. Although the immunomodulatory effects of GA are not quite understood, they are mainly attributed to its capacity in stimulating specific Th2/3 cells which enter CNS and express IL-10 and TGF- β as well as neurotrophic factors such as BDNF the ligand of TrkB which is upregulated in Fgfr2$^{ind-/-}$ mice. The blind-assessed clinical score of EAE shows that GA prevention regimen delays the EAE manifestation in both knockout and controls (3-4 days) but significantly reduces the disease severity only in Fgfr2$^{ind-/-}$ mice (Figure 36).

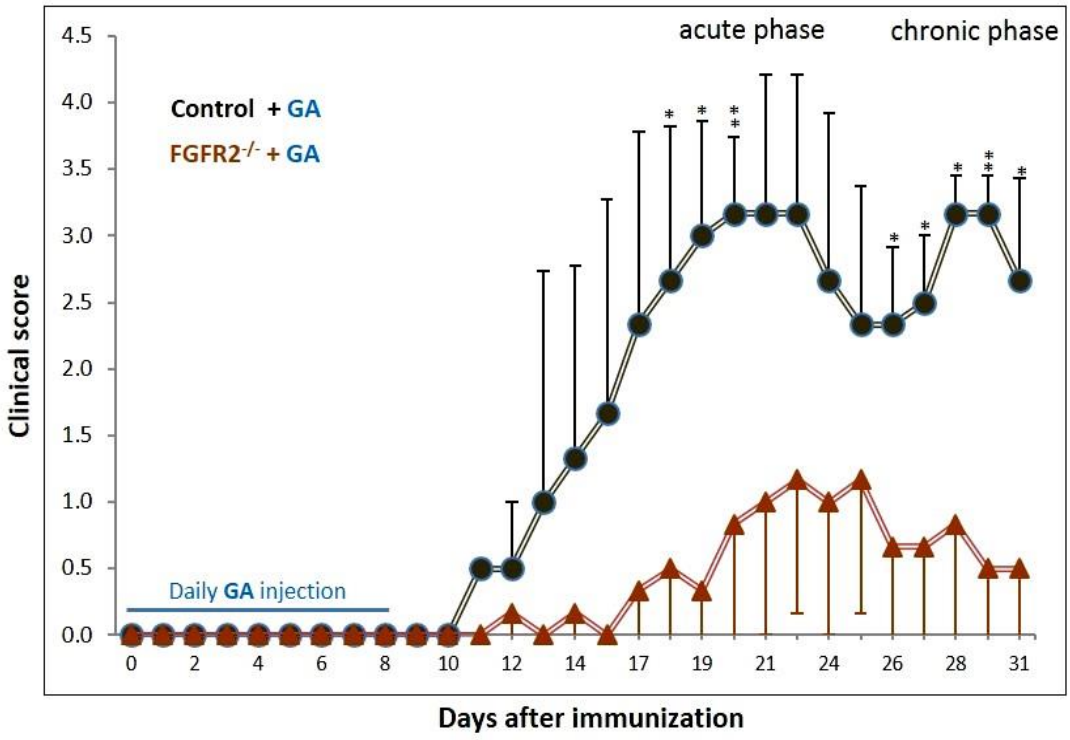

Figure 40. Pretreatment regimen of GA in MOG$_{35-55}$-induced EAE.

The onset of symptoms was not delayed in Fgfr2$^{ind-/-}$ mice when compared to controls. The disease peak was significantly lower in the in Fgfr2$^{ind-/-}$ mice in acute EAE and the difference was retained through the chronic phase of EAE. The clinical score was assessed genotype-blinded. n = 3, data are presented as mean + SEM.

5 DISCUSSION

Identifying and interrupting the key regulatory signalling mechanisms involved in demyelination are of great importance in treating demyelinating diseases such as multiple sclerosis. FGF/FGFR interactions are complex and regulate diverse functions of oligodendrocyte lineage cells, the myelin producing cells in the CNS (Furusho et al., 2015). Present study aims at better understanding the FGF/FGFR2 interactions *in vivo*, utilizing an oligodendrocyte specific Fgfr2 conditional knockout mice. To characterize the role of oligodendroglial FGFR2 in demyelinating conditions, the clinical course of MOG_{35-55}-EAE was investigated in $Fgfr2^{ind-/-}$ mice. Contrary to our hypothesis we observed a milder disease course of MOG_{35-55}-EAE in $Fgfr2^{ind-/-}$ mice. The pathological analysis showed decreased lymphocyte and microphage/microglia infiltration in spinal cord. The degree of demyelination was lower in $Fgfr2^{ind-/-}$ mice and axons were better preserved while the oligodendrocyte progenitor cells and mature oligodendrocyte populations did not alter. In $Fgfr2^{ind-/-}$ mice TrkB expression and AKT phosphorylation were upregulated while ERK phosphorylation was reduced.

5.1 $Fgfr2^{ind-/-}$ mice have normal phenotype

FGF/FGFR interactions exert various physiological effects including cellular proliferation, migration, differentiation, and survival (Furusho et al., 2011). The complete Fgfr2 depletion leads to embryonic lethality at E10.5 due to defects in the placenta while the selective disruption of the FGFR2b isoform causes severe impairment in the development of the lung, limbs and other tissues resulting in lethality immediately after birth. Fgfr2 mutations that enhance receptor activity cause abnormal fusions of the bones within the skull and limbs in Apert, Crouzon, Jackson-Weiss and Pfeiffer syndromes (Eswarakumar et al., 2005, Beenken and Mohammadi, 2009). Moreover, FGFR2 has been proven to play an important role in breast cancer development, being essential for induction of self-renewal and cell maintenance of human breast tumour initiating cells (Czaplinska et al., 2014). Therefore and to avoid developmental or other functional complications, we utilized a Tamoxifen inducible Cre mediated approach to delete Fgfr2 in oligodendrocyte

lineage cells. Our investigation on Fgfr2$^{ind-/-}$ mice revealed that the conditional deletion of Fgfr2 under PLP promoter does not result in any behavioural or phenotypical changes in Fgfr2$^{ind-/-}$ mice when compared to its C57BL/6J background controls.

5.2 FGFR2 signaling pathway

5.2.1 FGFR2 is downregulated in the white matter regions of Fgfr2$^{ind-/-}$ mice

In vitro FGFR2 is highly expressed by mature oligodendrocytes (not progenitors) coincidentally with major myelin proteins and its ligand binding leads to enhanced growth of oligodendrocyte processes and the formation of myelin-like membranes (Fortin et al., 2005). *In vivo* FGFR2 is expressed by oligodendrocytes in myelinated fibre tracts of adult rodent brain, spinal cord, and optic nerve and is present in purified myelin, however, its expression is low or not expressed in neurons and astrocytes (Fortin et al., 2005, Bansal et al., 2003). In our study the whole protein lysates showed downregulation of FGFR2 in spinal cord, and brain rest in Fgfr2$^{ind-/-}$ mice (but not in cortex and hippocampus). Since this conditional knockout system targets oligodendrocytes specifically, it could draw the speculation that CNS white matter regions composite a higher proportion of oligodendrocytes. Hence, the white matter rich regions of Fgfr2$^{ind-/-}$ mice appear to receive stronger influence by Tamoxifen induction, leading to significant FGFR2 downregulation.

5.2.2 FGFR1 is not compensated due to oligodendroglial Fgfr2 knockout

FGF family members insert their various impacts in CNS mainly through FGFR1 and FGFR2 receptors. Furthermore, FGFR1 and 2 share many common ligands such as FGF-2 (main ligand for FGFR1) and FGF-10 (main ligand for FGFR2) (Guillemot and Zimmer, 2011). One of the main processes involved in oligodendrocyte progenitor cell migration and maturation is the mitogenic and chemokinetic effects of FGF-2 exerted via FGFR1 activation. FGF-2 could be involved in oligodendrocyte response during demyelination and remyelination, however, the effects exerted by FGF-2 are controversial (Butt and Dinsdale, 2005, Clemente et al., 2011). In MS patients FGFR1 expressing oligodendrocyte progenitor cell subpopulations are increased in active plaques and

chronic inactive peri-plaques where remyelination normally occurs, suggesting an ameliorating role for FGF/FGFR1 interaction in MS recovery (Clemente et al., 2011). Considering the numbers of ligands that FGFR1 and 2 share and the overlapping functions they exert in oligodendrocyte homeostasis and myelination, it is fundamental to determine whether oligodendrocyte Fgfr2 knockout could be compensated by FGFR1 upregulation. Our findings show that the loss of oligodendroglial FGFR2 signalling *in vivo* has no impact on FGFR1 expression in spinal cord and different brain regions.

5.2.3 AKT phosphorylation was upregulated in Fgfr2$^{ind-/-}$ mice

In this study the whole protein lysate of spinal cord and different brain regions (hippocampus, cortex, and brain rest) showed increased AKT phosphorylation in Fgfr2$^{ind-/-}$ mice. AKT, a serine/threonine kinase and a downstream of FGFR2, regulates a variety of cellular functions by phosphorylating numerous downstream mediators in a cell specific manner. AKT signalling is known to influence cell survival, proliferation, and differentiation (Brazil et al., 2004). Although AKT is often considered to be a key cell survival regulatory mediator, in the oligodendrocyte lineage, AKT overexpression appears to have little impact on oligodendrocyte cell number (Flores et al., 2008). This is in line with our findings which indicate that oligodendroglial FGFR2 ablation induced p-AKT expression, does not affect oligodendrocyte progenitor cells or mature oligodendrocyte numbers. Transgenic mice with over activation of phosphatidylinositol-3-phosphate kinase (PI3K)/AKT pathway display increased myelin thickness (Ishii et al., 2012). Conversely, mTOR inhibition (a downstream target of PI3K/AKT), led to attenuation of this increase (Narayanan et al., 2009). Enhanced CNS myelination in oligodendroglial overexpressing p-AKT achieved with no changes in the proliferation or survival of oligodendrocyte progenitors or mature cells (Narayanan et al., 2009). This could suggest that the myelin sheath thickness might have altered in Fgfr2$^{ind-/-}$ mice in spite of no significant change in oligodendrocyte populations (precursor or mature). In our study western blot analysis of MBP showed no regulation in different CNS regions of Fgfr2$^{ind-/-}$ mice, however, we did not generate data on the myelin sheath thickness.

5.2.4 ERK phosphorylation is downregulated in Fgfr2$^{ind-/-}$ mice

Our analysis of the whole protein lysates showed that ERK2 but not ERK1 phosphorylation was decreased in spinal cord and different brain regions (hippocampus, cortex, and brain rest) of Fgfr2$^{ind-/-}$ mice. One of the three major subgroups of MAPKs, ERK1/2, play crucial roles in cellular processes including proliferation, stress response, apoptosis, and immune response. The signals that lead to ERK activation are usually initiated on the cell surface, primarily by various membrane-bound receptors (Liu et al., 2007). Ligand binding activates the intracellular kinase domain of FGF receptors resulting intermolecular transphosphorylation of the tyrosine kinase domains, initiating downstream signalling through four major pathways namely RAS/MAPK, PI3K-AKT, JNK and STAT (Huang et al., 2015). However, Miraoui's group brought more attention to MAPK signalling in FGFR2 downstream pathway by showing that FGFR2 activation in mesenchymal stem cells induces ERK1/2 but not JNK or PI3K/AKT activation (Miraoui et al., 2008). Our study downgraded the relevence of the fourth major downstream pathway of FGFR2, STAT signalling, since oligodendroglial FGFR2 knockout did not affect STAT expression in spinal cord. Further support for our finding in suggesting a positive relation between FGFR2 and ERK phosphorylation comes from Schuller's study. They showed *in vitro*, FGFR2 overexpression increased ERK phosphorylation in MCF-7 (Huang et al., 2015). Others showed that the gain of function point mutations in FGFR2 enhances ERK1/2 phosphorylation in PC12 cells (neuronal precursor-like cells) (Schuller et al., 2008).

Negative feedbacks regulate FGFR signalling at different levels by receptor internalization or induction of negative regulators such as FGFRL1, SEF, and MAPKs. While FGFRL1 and SEF regulators interrupt ligand binding, MAPK pathway mainly modulates the intracellular signalling (Turner and Grose, 2010). *In vitro*, Ser779 cytoplasmic domains of FGFR1 and FGFR2 (but not FGFR3 or 4) is required for the sustained activation of Ras and ERK (Lonic et al., 2013). Exogenous human recombinant FGF2 activates FGFR/MEK/ERK pathway, which induces cell growth and inhibits apoptosis. Conversely, inhibiting FGF receptor, interrupts mesoderm stimulation and angiogenesis (Hu et al., 2014). *In vitro* studies show that blockade of ERK pathway enhances apoptosis in tumour

cells (Sakamoto et al., 2013). However, in our study p-ERK2 downregulation in CNS of Fgfr2$^{ind-/-}$ mice did not affect the progenitor or mature oligodendrocyte population. A possible explanation for this finding could emerge from a work done by Yao's group. They demonstrated that ERK2 cannot compensate for all mediated functions of ERK1 since *Erk1-deficient* mice despite being viable and fertile, have defective thymocyte maturation. Yet, *in vitro* ERK1 can compensate for ERK2 loss (Yao et al., 2003).

5.2.5 TrkB but not BDNF is regulated in Fgfr2$^{ind-/-}$ mice

Bioactivity of BDNF has been demonstrated in neuronal cultures, with its expression enhanced upon stimulation. BDNF and FGF receptor signalling regulate cell migration of neuroblasts along rostral migratory steam (Zhou et al., 2015). BDNF belongs to the neurotrophin family of growth factors and modulates axonal growth, neuronal activity, and activity-dependent synaptic and dendritic plasticity (Hohlfeld et al., 2000, Hohlfeld et al., 2006). Like FGF receptors the high-affinity receptor for BDNF, TrkB, is also a receptor tyrosine kinase. In our study BDNF itself was not regulated, however, its receptor TrkB was downregulated in Fgfr2$^{ind-/-}$ mice. This could indirectly affect the functions which are attributed to BDNF signaling in the central nervous system. Upon ligand binding, various signalling pathways such as mitogen-activated protein kinase, phosphatidylinositol 3-kinase and Fyn-mediated actin polymerization are stimulated through TrkB receptors (Harada et al., 2011). TrkB and FGFR2 share similar and possibly overlapping patterns of cellular distribution in inferior colliculus, hippocampus and cerebellum of F344 rats (Sato et al., 2001). Application of FGF-2, a major ligand for FGFR1/ 2, up-regulates BDNF and TrkB in ganglion cells of frog optic nerve after axotomy (Soto et al., 2006). Earlier studies conducted in our group showed TrkB was upregulated in spinal cord of oligodendrocyte specific Fgfr1 knockout mice (Rajendran, 2014). However, in contrary, oligodendrocyte specific Fgfr2 deletion resulted in TrkB downregulation in spinal cord, and brain rest with no regulation of BDNF in Fgfr2$^{ind-/-}$ mice. This suggest TrkB signaling and synthesis could have a close association to FGFR2 biogenesis. The discrepancy of TrkB regulation associated to each FGFR1 and FGFR2 is not clearly understood and needs to be further investigated.

5.3 Oligodendroglial Fgfr2 depletion leads to a milder course of EAE

The current study is the first to investigate and characterize the role of oligodendroglial FGFR2 signaling in the course of $MOG_{35–55}$-EAE. Our data demonstrate that interrupting oligodendrocyte specific FGFR2 signaling leads to a milder disease course in chronic EAE. The onset of EAE did not differ between the two groups and during acute EAE, although presenting the trend, $Fgfr2^{ind-/-}$ mice did not show a statistically significant milder disease course. Various studies in different experimental paradigms have proposed contrary roles for FGF signaling in remyelination and clinical recovery. Beneficial roles were reported from gene therapy, stating that introducing FGF2 by viral vectors reversed the clinical and pathological signs of chronic EAE (Ruffini et al., 2001). Furthermore, systemic deletion of FGF2 showed more severe symptoms of EAE, decreased remyelination, and increased nerve fiber degeneration (Rottlaender et al., 2011). Conversely, others reported mice lacking FGF2 or FGFR1 manifest increased oligodendrocyte population and improved remyelination of cuprizone-induced lesions. This proposes an inhibitory role for FGF signaling in oligodendrocyte differentiation and remyelination. These conflicts partially might be due to the fact that FGF signaling elicits various responses in different cell types (Furusho et al., 2015).

In MS patients FGF2 and FGFR1 are upregulated in oligodendrocyte progenitors in active plaques and in chronic inactive peri-plaques, where remyelination normally occurs (Clemente et al., 2011). However, it has been unclear whether this upregulation around demyelinated lesions is indicative of enhanced or interrupted repair capacity (Furusho et al., 2015). Our protein analysis of spinal cord in chronic EAE show that FGFR2 is upregulated upon EAE immunization, proposing a negative role for FGFR2 in the course of EAE. Therefore, it is legitimate to see $Fgfr2^{ind-/-}$ mice with a lower FGFR2 expression, show milder signs of EAE clinical symptoms. Putting together, we conclude a negative role for oligodendroglial FGFR2 signaling in the pathology of $MOG_{35–55}$-EAE.

5.4 Reduced immune infiltration in Fgfr2$^{ind-/-}$ mice

In our study the impaired oligodendroglial FGFR2 signaling which led to milder clinical symptoms of $MOG_{35–55}$-EAE, was associated with decreased spinal cord infiltration of macrophages and/or activated microglia as well as B220 (+) B cells in both acute and chronic EAE. In addition to progenitor and mature oligodendrocytes, other FGFR expressing cells such as reactive astrocytes and microglia, are also likely to be affected by modulation of FGF2 in the lesions (Furusho et al., 2015). During induction and peak phases of EAE, massive infiltration of peripheral macrophages is seen in acute lesions of EAE (Linker and Lee, 2009). In spinal cord of EAE induced mice the activated microglia show increased FGF2 and FGFR1 expression (Liu et al., 1998). The elevated capacity of activated macrophages into CNS is correlated to pro-inflammatory chemokines and their receptors (Jiang et al., 2014). In cuprizone model the production of FGF2 in microglia has peaked during demyelination. Conversely, the microglial FGF2 expression was downregulated during remyelination (Voß et al., 2012).

In our study the CD3 (+) T cell infiltration was significantly reduced in Fgfr2$^{ind-/-}$ mice only in chronic EAE. Autoreactive T cells against myelin proteins play a role in EAE development. The Th1 and Th17 infiltrates release a large amount of pro-inflammatory cytokines in CNS (IFN-γ, IL-17, IL-12, IL-23) which induce demyelination and neuronal death in the inflamed CNS (Jiang et al., 2014). In the later phase of EAE anti-inflammatory Th2 and regulatory T cells develop and control inflammation by damping Th1 cell activity and pro-inflammatory cytokine release (Unutmaz et al., 2010). There are no data on direct association between FGFRs/ FGFR2 and immune infiltration. However, the downstream mediators of FGF receptors such as AKT and ERK are known to interfere immune response in different interfaces which will be discussed in the following passages.

5.5 FGFR2 downstream signaling in MOG_{35-55}-EAE

In this study the underlying mechanisms behind the milder EAE clinical course concomitant with reduced immune infiltration, reduced demyelination, and better axonal preservation in $Fgfr2^{ind-/-}$ mice could be illustrated from investigating downstream FGFR2 signaling of spinal cord. Our data demonstrate that in chronic EAE $Fgfr2^{ind-/-}$ mice shows increased AKT phosphorylation, reduced ERK phosphorylation and enhanced TrkB expression.

5.5.1 p-AKT upregulation in $Fgfr2^{ind-/-}$ mice plays an ameliorating role in pathology of MOG_{35-55}-EAE

We demonstrated that the loss of FGFR2 in oligodendrocyte lineage cells lead to increased AKT phosphorylation in different CNS regions which is concomitant with a milder course of $MOG_{35–55}$-EAE. AKT signaling is a key regulatory pathway, involved in a variety of cellular and biological functions. *In vitro* AKT/mTOR signaling is imminent to achieve proper differentiation of oligodendrocyte progenitor cells into mature oligodendrocytes (Dai et al., 2014). It is also showed that IGF-1 stimulates oligodendrocyte progenitor proliferation by sustained AKT phosphorylation (Cui and Almazan, 2007). In astrocyte-conditioned media AKT phosphorylation provides trophic support for oligodendrocyte progenitors of rat brain against cellular insults such as oxidative stress, starvation, and oxygen-glucose deprivation (Arai and Lo, 2009). In contrary, our analysis of spinal cord sections indicate no significant change in precursor or mature oligodendrocyte populations of $Fgfr2^{ind-/-}$ mice in acute or chronic EAE. While others reported that p-AKT downregulation reduced myelin thickness in mice and AKT over-activation resulted in hypermyelination (Fyffe-Maricich et al., 2013).

Our histological and immunohistochemical data demonstrate lower demyelination and better preserved axons in $Fgfr2^{ind-/-}$ mice in chronic EAE. Multiple lines of evidence support these findings, proposing a positive role for AKT phosphorylation in protecting

axons during neurodegenerative conditions. *In vitro* AKT phosphorylation protected the cultured cortical neurons against hypoxia induced neuronal death (Siren et al., 2001). *In vivo* AKT phosphorylation included neuroprotective (Diem et al., 2001), anti-apoptotic (Kermer et al., 2000), and pro-survival and pro-functional effects in retinal ganglion cells (Sättler et al., 2004). BTBD10, a neuronal cell death suppressor and neuronal growth enhancer, improved ALS condition via positive regulation of AKT phosphorylation (Nawa et al., 2008). EAE Treatment with arylpiperazine (a neuroprotective compound) contribute to the delayed onset, progression, and overall suppression of EAE. These effects are exerted by reducing apoptosis of CNS cells via increased activation of anti-apoptotic mediator of AKT and its downstream effector kinases (Popovic et al., 2015).

Through immunohistochemical analysis we assessed a decreased number of macrophages/activated microglia and B220 (+) B cells in the spinal cord of $Fgfr2^{ind-/-}$ mice in both acute and chronic EAE. Furthermore, in $Fgfr2^{ind-/-}$ mice CD3 (+) T cells infiltration was significantly reduced in the chronic phase of the disease. These data suggest a negative relation between immunomodulatory response and AKT phosphorylation in the course of EAE. The further substantiating data in support of this relation comes from an $AKT3^{-/-}$ study. These mice were more severely affected by EAE immunization and the demyelination was higher in $AKT3^{-/-}$ mice spinal cord lesions in both acute and chronic EAE. The mRNA level of proinflammatory cytokines (IL-2, IL-17, and IFN-γ) were higher in spinal cords of $AKT3^{-/-}$ mice. Immunohistochemical analysis revealed decreased numbers of $Foxp3^{+}$ regulatory T cells in the spinal cord of $AKT3^{-/-}$ mice. *In vitro* suppression assays showed that AKT3-deficient Th cells are less susceptible to regulatory T cell–mediated suppression (Tsiperson et al., 2013). Another study shows that RGMa plays a role in Th17-cell-mediated neuronal death by inducing AKT de-phosphorylation and is involved in both apoptosis and axonal degeneration. (Tanabe and Yamashita, 2014). Moreover, AKT phosphorylation is reported to contribute in BBB integrity. A selective acetylcholinesterase inhibitor, donepezil, revealed ameliorating clinical and pathological parameters in EAE including improved magnetic resonance imaging outcomes and reduced permeability of BBB coupled with increasing AKT phosphorylation (Jiang et al., 2013). Putting together we conclude an ameliorating role

for PI3K/AKT pathway in the pathology of $MOG_{35–55}$-EAE potentially through providing trophic, neuroprotective, and anti-apoptotic support for neurons and enhancing oligodendrocyte functionality but not population which leads to improved myelin composition. Furthermore, AKT phosphorylation may contribute in attenuating the immunomodulatory response and providing support for BBB integrity.

5.5.2 ERK phosphorylation exerts negative immunomodulatory effects in pathology of MOG_{35-55}-EAE

In our study downregulation of ERK2 phosphorylation in spinal cord was associated with the milder clinical course of chronic $MOG_{35–55}$-EAE in $Fgfr2^{ind-/-}$ mice. In Chronic EAE the demyelination was lower in $Fgfr2^{ind-/-}$ mice and axons were better preserved. Different studies indicate that the Ras/Raf/MEK/ERK pathways, as a result of activation by various growth factors, provide imminent functions in the proliferation, migration, or survival of oligodendrocyte progenitor cells (Guardiola-Diaz et al., 2012). However, there are contradictions on the role this pathways play in oligodendrocyte progenitor cells and mature myelinating oligodendrocytes. Oligodendrocyte progenitor cell differentiation was not affected in primary cortical cultures of ERK1-null knockout mice while it was only transiently interrupted in ERK2 conditional single knockout mouse brain cultures (Fyffe-Maricich et al., 2011). *In vitro* studies (utilizing a panel of stage-specific antigenic markers and pharmacological inactivation of ERK1/2) demonstrated that distinct stages in oligodendrocyte developmental pathway are differentially regulated by ERK1/2 phosphorylation. In particular, the progression of the early to late progenitor stage requires ERK1/2 activation (Guardiola-Diaz et al., 2012). In the current study the immunohistological investigations of chronic $MOG_{35–55}$-EAE spinal cord sections showed p-ERK2 downregulation does not impact progenitor or mature oligodendrocyte number in $Fgfr2^{ind-/-}$ mice.

FGFR1/2 contribute to upstream and downstream signalling of ERK1/2 which is crucial for oligodendrocyte functions in maintaining the myelin and axonal integrity (Ishii et al.,

2014). ERK1/2 inhibition in cultured oligodendrocytes result in attenuated extension of oligodendrocyte processes. In mice lacking oligodendroglial FGFR1/2 myelin thickness was reduced which was accompanied by downregulation of ERK1/2 phosphorylation, suggesting a correlation between ERK/MAPK activation and myelin thickness (Furusho et al., 2012). However, in mature oligodendrocytes the expression of ERK1 and ERK2 overlaps, therefore, it is unlikely that single gene deletions will fully interrupt the function of ERK1/ERK2 signalling in myelination (Fyffe-Maricich et al., 2011). ERK1-null knockout in OPCs and oligodendrocytes coupled with floxed-ERK2 conditional knockout showed in the absence of ERK1/2 signalling OPCs were able to complete cell cycle, differentiate, and initiate myelination normally. However, they failed to increase myelin thickness in proportion to axon calibre in the spinal cord. This suggest late-stage regulatory role for ERK1/2 in CNS myelination (Ishii et al., 2012). In our study, the immunohistology of spinal cord sections for MBP showed no regulation in myelin expression in $Fgfr2^{ind-/-}$ mice.

A number of investigations including the current study, attribute immunomodulatory roles to ERK signaling. Here we discuss the correlation between pERK2 downregulation and reduced immune infiltration of T-cells, B-cells, macrophages/ microglia. ERK1 null knockout mice showed enhanced susceptibility to myelin $MOG_{35–55}$-EAE and displayed a bias toward Th1 type immune response which reflected by increased INF-γ production by MOG-specific T cells and lower IL-5 secretion (Agrawal et al., 2006). In accordance to our findings, the combined inhibition of MEK1/2, the kinase upstream of ERK, during or after EAE induction reduced the clinical signs of EAE by suppressing dendritic cell IL-23 and IL-1β production and suppressing autoantigen-specific T cell. ERK activation promote Th17 responses *in vivo* while ERK inhibition suppressed autoantigen-specific Th17 and Th1 responses and attenuated EAE (when administered at the induction of acute EAE or therapeutically in a relapsing-remitting model). ERK inhibition also suppressed IFN- γ as well as IL-17 production (Brereton et al., 2009). ERK activity is essential for the process of positive selection, and it differentially affects CD4 and CD8 T cell maturation (Fischer et al., 2005). ERK1/2 activation to some extent determines the fate of Th1/ Th2 immune cells. Loss of ERK2 severely impedes Th1 differentiation while enhances the development of $Foxp3^{+}$-induced T regulatory cells (Chang et al., 2012).

ERK signalling is reported to play profound role in BBB integrity and therefore, mediating immune infiltration. *In vitro* BBB model assessments show microwave radiation induces BBB damage by activating the VEGF/Flk-1-ERK pathway, enhancing Tyr phosphorylation of occludin (Wang et al., 2014). Moreover, Somatostatin hormone has been demonstrated to reduce local and systemic inflammation reactions as well as maintaining the integrity of the BBB by decreasing the LPS-induced phosphorylation of ERK1/2 (Lei et al., 2014). Dendritic cell recruitment by CNS in $MOG_{35–55}$-EAE was shown to go through CCL2 chemotaxis and paracellular transmigration across the BBB which was facilitated by ERK phosphorylation (Sagar et al., 2012).

5.5.3 TrkB signaling may play a Janus-like role in pathology of MOG_{35-55}-EAE

Our data provide evidence that glial TrkB signaling might play a dual role in pathology of EAE. We investigated the expression of TrkB and its activating ligand BDNF, before and after EAE immunization in $Fgfr2^{ind-/-}$ mice. Experimental axotomy suggests BDNF is promoting neuronal survival, oligodendrocyte proliferation and axonal remyelination (Gravel et al., 1997). Moreover, in *vitro* studies revealed, BDNF and other neurotrophins are also produced by human T cells, B cells, and macrophages (Song et al., 2013). BDNF is found in cells forming perivascular infiltrates and in the lesions invading cells of acute disseminated encephalomyelitis and MS brain autopsy (Stadelmann et al., 2002). BDNF synthesis related to inflammatory responses can exert regenerative and protective effects during CNS tissue damage (De Santi et al., 2009). However, EAE studies show the conditional BDNF gene deletion in T cell lineage, results in reduction of neuroinflammation, reduced T cell infiltration and proliferation, and reduction of *in vitro* cytokine release (Ralf Linker, 2007).

In our study BDNF was not significantly regulated but since most, if not all known functions of BDNF are exerted through TrkB receptor, we focused on TrkB expression. After EAE immunization in a readily TrkB downregulated $Fgfr2^{ind-/-}$ mice (compared to WT controls), the TrkB expression further decreases. However, the reduction proportion in $Fgfr2^{ind-/-}$

mice is much lower than controls. In other words TrkB expression reduced in both $Fgfr2^{ind-/-}$ and controls due to EAE induction but $Fgfr2^{ind-/-}$ mice undergoes less TrkB fluctuations (by having a lower level of TrkB at the time of EAE induction and less decrease of TrkB expression after EAE immunization). Therefore and considering a milder course of EAE in $Fgfr2^{ind-/-}$ mice, it is not possible to attribute a mere negative or positive role for TrkB in pathology of EAE. This could explain the source of discrepancy on the described role of TrkB and BDNF, reported from different research studies.

TrkB is robustly expressed in neurons in immediate vicinity to MS plaques. Observation of single neurons with pronounced TrkB-immunoreactivity near MS lesions, suggested upregulation of TrkB in a proportion of damaged neurons (Stadelmann et al., 2002). The soluble factors released by astrocytes as a result of TrkB signalling induced neuronal degeneration and apoptosis (Colombo et al., 2012). While astrocyte specific TrkB knockout mice showed a milder course of EAE and were better protected from neurodegeneration, BDNF specific depletion in astrocytes showed enhanced disease severity associated with axonal loss, suggesting a BDNF-mediated neuroprotective mechanism (Linker et al., 2010, Colombo et al., 2012). In MS, TrkB influences the susceptibility of activated T cells to apoptosis. These encephalitogenic T cells are generally believed to be the initiator of autoimmune inflammatory attack against the myelin sheaths and neuronal elements in MS (Zang et al., 1999). Putting together, we conclude the discrepancy of TrkB expression pre and post EAE immunization in $Fgfr2^{ind-/-}$ mice, which is coupled with a milder course of EAE, might be the result of a Janus-like role that TrkB signaling plays in the pathology of EAE. In other words TrkB might escalate the immune response initially but promote neuronal protective mechanisms later on during chronic EAE.

5.6 GA treatment further ameliorates MOG_{35-55}-EAE in $Fgfr2^{ind-/-}$ mice

Our data demonstrated that GA administration (prevention regimen) delayed and further reduced severity of $MOG_{35–55}$-EAE clinical score in $Fgfr2^{ind-/-}$ mice while these ameliorating impacts were more trivial in WT controls. Characterizing of neurodegeneration is one of the major objectives in scientific investigations to tackle neurological autoimmune disorders. A salient feature in the course of multiple sclerosis is oligodendrocyte degeneration followed by myelin and axonal damage. Persuading more efficient treatments, combination therapies are emerging as promising approaches in targeting neurodegenerative diseases. FGFR2 is known to play profound role in neurons and oligodendrocyte proliferation, migration and maturation as well as central nervous system myelination. It is demonstrated by our group that FGFR2 could serve as a potent target for addressing the pathology of $MOG_{35–55}$-EAE by interfering immunomodulatory pathways induced due to EAE immunization. On the other hand GA or Copaxone, a mixture of synthetic peptides, is one of the potent approved drugs available for MS therapy. Although, not clearly understood, the neuroprotective effects of GA are exerted through restoring the impaired neurotrophic factor secretion in CNS and neurogenesis in the site of injury. Moreover, it induces the production of secreted IL-1 receptor antagonist, sIL-1Ra, which is a natural inhibitor of IL-1β, the essential cytokine for differentiation of IL-17-producing T helper cells (Carpintero et al., 2010). The immunomodulatory mechanisms of GA are mainly attributed to its capacity in stimulating specific Th2/3 cells that cross BBB, accumulate in CNS and express IL-10 and TGF- β as well as neurotrophic factors such as BDNF (Aharoni et al., 2008). Using kinase knockdown and specific inhibitors, it is demonstrated that GA induces sIL-1Ra (a major compound determining its anti-inflammatory effects) production via the activation of PI3Kδ, AKT, MEK1/2, and ERK1/2, demonstrating that both PI3Kδ/Akt and MEK/ERK pathways rule sIL-1Ra expression in human monocytes (Carpintero et al., 2010). These findings suggest GA and FGFR2 signalling might share some neuroprotective and immunomodulatory pathways (AKT, ERK pathways) however, in the opposite direction and with the reverse outcomes. We conclude the combined therapy approach of inhibiting FGFR2 signalling with GA treatment could further delay the onset/progression and overall suppression of $MOG_{35–55}$-EAE.

6 SUMMARY

Myelin is a bioactive membrane established by oligodendrocytes during postnatal development and is essential for receiving and conducting electrical impulses by axons. Myelin acts as a target during many autoimmune neurological conditions such as MS. FGF signaling is known to be crucial for development, proliferation and maintenance of oligodendrocytes and OPCs, hence, influencing myelination. Yet, the role of FGFR signaling in MS and EAE is poorly understood. Hypothesizing MOG_{35-55}-EAE will cause more severe symptoms in oligodendroglial Fgfr2 depleted mice, we designed a Tamoxifen inducible PLP Cre mediated conditional Fgfr2 knockout in oligodendrocyte passage under C57BL/6 background. No phenotypic changes were observed in $Fgfr2^{ind-/-}$ mice. To our surprise, $Fgfr2^{ind-/-}$ showed a milder disease course of MOG_{35-55}-EAE coupled with reduced immune infiltration (T-cells, B-cells, macrophages/ microglia), reduced demyelination, less inflammation, and better axonal preservation. Ablation of Fgfr2 in oligodendrocytes caused reduced ERK phosphorylation as well as increased TrkB expression and AKT phosphorylation. The number of OLs and OPCs were not altered in $Fgfr2^{ind-/-}$ mice in EAE induced or non-EAE condition when compared to their respective controls. Prevention regimen of GA treatment delayed and further ameliorated the MOG_{35-55}-EAE manifestation in $Fgfr2^{ind-/-}$ mice. Taken together, our findings indicate a deteriorating role for FGFR2 in the pathology of MOG_{35-55}-EAE by boosting immune response through MEK/ERK, PI13/AKT, and TrkB crosstalk and signaling. Therefore, FGFR2 and its downstream signaling mediators could serve as effective potential treatment prospects in tackling immunological related CNS disorders.

ZUSAMMENFASSUNG

Myelin ist eine Biomembran, die von Oligodendrozyten postnatal gebildet wird. Myelin ermöglicht eine schnelle Erregungsleitung elektrischer Impulse. Die Myelinscheiden, die Axone umgeben, sind Angriffspunkt bei autoimmun bedingten neurologischen Erkrankungen des ZNS wie Multiple Sklerose. Über den FGF Signalweg werden Entwicklung und Proliferation von Oligodendrozyten und Oligodendrozyten-Vorläuferzellen (OPCs) gesteuert. Dieser FGFR Signalweg wurde bislang bei MS und dem Tiermodell experimentelle autoimmune Enzephalomyelitis (EAE) kaum charakterisiert. Unsere Hypothese war die, dass bei MOG_{35-55}-EAE in Mäusen, deren oligodendrozytäres FGFR2 entfernt wurde, EAE schwerer verläuft. Hierfür nutzten wir einen durch Tamoxifen induzierbaren PLP Cre vermittelten konditionalen FGFR2 Knockout ($Fgfr2^{ind-/-}$). Es wurden keine phänotypischen Veränderungen bei den $Fgfr2^{ind-/-}$ Mäusen beobachtet. Die $Fgfr2^{ind-/-}$ Mäuse zeigten im Gegensatz zur Hypothese einen milderen EAE Krankheitsverlauf, weniger Immuninfiltration (T-Zellen, B-Zellen, Makrophagen/Mikroglia), eine geringere Demyelinisierung und besser erhaltene Axone. Weiterhin führte die Entfernung von FGFR2 in den Oligodendrozyten zu einer reduzierten Phosphorylierung von ERK und einer gesteigerten Expression von TrkB und Phosphorylierung von AKT. Die Anzahl der Oligodendrozyten und OPCs änderte sich weder bei den $Fgfr2^{ind-/-}$ Mäusen ohne EAE noch im EAE Experiment. Eine frühe Behandlung mit Glatiramerazetat milderte Symptome einer EAE bei den $Fgfr2^{ind-/-}$ Mäusen ab. Zusammengefasst zeigen unsere Ergebnisse, dass FGFR2 in Oligodendrozyten die Pathologie der MOG35-55-EAE durch eine verstärkte Immunantwort durch MEK / ERK, PI13 / AKT und TrkB Interaktionen und Signalwege negativ beeinflusst. Daher könnten FGFR2 und die nachgeschalteten Signalmediatoren mögliche molekulare Behandlungsziele bei immunologisch vermittelten Erkrankungen des ZNS sein.

AGRAWAL, A., DILLON, S., DENNING, T. L. & PULENDRAN, B. 2006. ERK1-/- mice exhibit Th1 cell polarization and increased susceptibility to experimental autoimmune encephalomyelitis. *J Immunol,* 176**,** 5788-96.

AHARONI, R., HERSCHKOVITZ, A., EILAM, R., BLUMBERG-HAZAN, M., SELA, M., BRUCK, W. & ARNON, R. 2008. Demyelination arrest and remyelination induced by glatiramer acetate treatment of experimental autoimmune encephalomyelitis. *Proc Natl Acad Sci U S A,* 105**,** 11358-63.

AIVO, J., HANNINEN, A., ILONEN, J. & SOILU-HANNINEN, M. 2015. Vitamin D3 administration to MS patients leads to increased serum levels of latency activated peptide (LAP) of TGF-beta. *J Neuroimmunol,* 280**,** 12-5.

ARAI, K. & LO, E. H. 2009. Astrocytes protect oligodendrocyte precursor cells via MEK/ERK and PI3K/Akt signaling. *Journal of Neuroscience Research***,** NA-NA.

ARAQUE, A. & NAVARRETE, M. 2010. Glial cells in neuronal network function. *Philos Trans R Soc Lond B Biol Sci,* 365**,** 2375-81.

AUF DEMKELLER, U., KRAMPERT, M., KUMIN, A., BRAUN, S. & WERNER, S. 2004. Keratinocyte growth factor: effects on keratinocytes and mechanisms of action. *Eur J Cell Biol,* 83**,** 607-12.

BANKSTON, A. N., MANDLER, M. D. & FENG, Y. 2013. Oligodendroglia and neurotrophic factors in neurodegeneration. *Neurosci Bull,* 29**,** 216-28.

BANSAL, R., LAKHINA, V., REMEDIOS, R. & TOLE, S. 2003. Expression of FGF receptors 1, 2, 3 in the embryonic and postnatal mouse brain compared with Pdgfralpha, Olig2 and Plp/dm20: implications for oligodendrocyte development. *Dev Neurosci,* 25**,** 83-95.

BEENKEN, A. & MOHAMMADI, M. 2009. The FGF family: biology, pathophysiology and therapy. *Nat Rev Drug Discov,* 8**,** 235-53.

BLAK, A. A., NASERKE, T., SAARIMAKI-VIRE, J., PELTOPURO, P., GIRALDO-VELASQUEZ, M., VOGT WEISENHORN, D. M., PRAKASH, N., SENDTNER, M., PARTANEN, J. & WURST, W. 2007. Fgfr2 and Fgfr3 are not required for patterning and maintenance of the midbrain and anterior hindbrain. *Dev Biol,* 303**,** 231-43.

BOESMANS, W., LASRADO, R., VANDEN BERGHE, P. & PACHNIS, V. 2015. Heterogeneity and phenotypic plasticity of glial cells in the mammalian enteric nervous system. *Glia,* 63**,** 229-41.

BORETIUS, S., ESCHER, A., DALLENGA, T., WRZOS, C., TAMMER, R., BRUCK, W., NESSLER, S., FRAHM, J. & STADELMANN, C. 2012. Assessment of lesion pathology in a new animal model of MS by multiparametric MRI and DTI. *Neuroimage,* 59**,** 2678-88.

BRADL, M. & LASSMANN, H. 2010. Oligodendrocytes: biology and pathology. *Acta Neuropathol,* 119**,** 37-53.

BRERETON, C. F., SUTTON, C. E., LALOR, S. J., LAVELLE, E. C. & MILLS, K. H. 2009. Inhibition of ERK MAPK suppresses IL-23- and IL-1-driven IL-17 production and attenuates autoimmune disease. *J Immunol,* 183**,** 1715-23.

BRUCK, W. 2005. The pathology of multiple sclerosis is the result of focal inflammatory demyelination with axonal damage. *J Neurol,* 252 Suppl 5**,** v3-9.

BRYANT, M. R., MARTA, C. B., KIM, F. S. & BANSAL, R. 2009. Phosphorylation and lipid raft association of fibroblast growth factor receptor-2 in oligodendrocytes. *Glia,* 57**,** 935-46.

BUTT, A. M. & DINSDALE, J. 2005. Fibroblast growth factor 2 induces loss of adult oligodendrocytes and myelin in vivo. *Exp Neurol,* 192**,** 125-33.

CARPINTERO, R., BRANDT, K. J., GRUAZ, L., MOLNARFI, N., LALIVE, P. H. & BURGER, D. 2010. Glatiramer acetate triggers PI3Kdelta/Akt and MEK/ERK pathways to induce IL-1 receptor antagonist in human monocytes. *Proc Natl Acad Sci U S A,* 107**,** 17692-7.

CHANG, C. F., D'SOUZA, W. N., CH'EN, I. L., PAGES, G., POUYSSEGUR, J. & HEDRICK, S. M. 2012. Polar Opposites: Erk Direction of CD4 T Cell Subsets. *The Journal of Immunology,* 189**,** 721-731.

CHENG, W. & CHEN, G. 2014. Chemokines and chemokine receptors in multiple sclerosis. *Mediators Inflamm,* 2014**,** 659206.

CLEMENTE, D., ORTEGA, M. C., ARENZANA, F. J. & DE CASTRO, F. 2011. FGF-2 and Anosmin-1 are selectively expressed in different types of multiple sclerosis lesions. *J Neurosci,* 31**,** 14899-909.

CLEMENTE, D., ORTEGA, M. C., MELERO-JEREZ, C. & DE CASTRO, F. 2013. The effect of glia-glia interactions on oligodendrocyte precursor cell biology during development and in demyelinating diseases. *Front Cell Neurosci,* 7**,** 268.

COLOMBO, E., CORDIGLIERI, C., MELLI, G., NEWCOMBE, J., KRUMBHOLZ, M., PARADA, L. F., MEDICO, E., HOHLFELD, R., MEINL, E. & FARINA, C. 2012. Stimulation of the neurotrophin

receptor TrkB on astrocytes drives nitric oxide production and neurodegeneration. *J Exp Med,* 209**,** 521-35.

COMPSTON, A. 1988. The 150th anniversary of the first depiction of the lesions of multiple sclerosis. *J Neurol Neurosurg Psychiatry,* 51**,** 1249-52.

CRAWFORD, A. H., STOCKLEY, J. H., TRIPATHI, R. B., RICHARDSON, W. D. & FRANKLIN, R. J. 2014. Oligodendrocyte progenitors: adult stem cells of the central nervous system? *Exp Neurol,* 260**,** 50-5.

CUDRICI, C., NICULESCU, T., NICULESCU, F., SHIN, M. L. & RUS, H. 2006. Oligodendrocyte cell death in pathogenesis of multiple sclerosis: Protection of oligodendrocytes from apoptosis by complement. *J Rehabil Res Dev,* 43**,** 123-32.

CUI, Q.-L. & ALMAZAN, G. 2007. IGF-I-induced oligodendrocyte progenitor proliferation requires PI3K/Akt, MEK/ERK, and Src-like tyrosine kinases. *Journal of Neurochemistry,* 0**,** 070210024758017-???

CZAPLINSKA, D., TURCZYK, L., GRUDOWSKA, A., MIESZKOWSKA, M., LIPINSKA, A. D., SKLADANOWSKI, A. C., ZACZEK, A. J., ROMANSKA, H. M. & SADEJ, R. 2014. Phosphorylation of RSK2 at Tyr529 by FGFR2-p38 enhances human mammary epithelial cells migration. *Biochim Biophys Acta,* 1843**,** 2461-70.

DAI, J., BERCURY, K. K. & MACKLIN, W. B. 2014. Interaction of mTOR and Erk1/2 signaling to regulate oligodendrocyte differentiation. *Glia,* 62**,** 2096-2109.

DE SANTI, L., ANNUNZIATA, P., SESSA, E. & BRAMANTI, P. 2009. Brain-derived neurotrophic factor and TrkB receptor in experimental autoimmune encephalomyelitis and multiple sclerosis. *J Neurol Sci,* 287**,** 17-26.

DIEM, R., MEYER, R., WEISHAUPT, J. H. & BAHR, M. 2001. Reduction of potassium currents and phosphatidylinositol 3-kinase-dependent AKT phosphorylation by tumor necrosis factor-(alpha) rescues axotomized retinal ganglion cells from retrograde cell death in vivo. *J Neurosci,* 21**,** 2058-66.

ESWARAKUMAR, V. P., LAX, I. & SCHLESSINGER, J. 2005. Cellular signaling by fibroblast growth factor receptors. *Cytokine Growth Factor Rev,* 16**,** 139-49.

FISCHER, A. M., KATAYAMA, C. D., PAGÈS, G., POUYSSÉGUR, J. & HEDRICK, S. M. 2005. The Role of Erk1 and Erk2 in Multiple Stages of T Cell Development. *Immunity,* 23**,** 431-443.

FLORES, A. I., NARAYANAN, S. P., MORSE, E. N., SHICK, H. E., YIN, X., KIDD, G., AVILA, R. L., KIRSCHNER, D. A. & MACKLIN, W. B. 2008. Constitutively Active Akt Induces Enhanced Myelination in the CNS. *Journal of Neuroscience,* 28**,** 7174-7183.

FORTIN, D., ROM, E., SUN, H., YAYON, A. & BANSAL, R. 2005. Distinct fibroblast growth factor (FGF)/FGF receptor signaling pairs initiate diverse cellular responses in the oligodendrocyte lineage. *J Neurosci,* 25**,** 7470-9.

FRAGOSO, Y. D. 2014. Modifiable environmental factors in multiple sclerosis. *Arq Neuropsiquiatr,* 72**,** 889-94.

FROM, R., EILAM, R., BAR-LEV, D. D., LEVIN-ZAIDMAN, S., TSOORY, M., LOPRESTI, P., SELA, M., ARNON, R. & AHARONI, R. 2014. Oligodendrogenesis and myelinogenesis during postnatal development effect of glatiramer acetate. *Glia,* 62**,** 649-65.

FURUSHO, M., DUPREE, J. L., NAVE, K. A. & BANSAL, R. 2012. Fibroblast growth factor receptor signaling in oligodendrocytes regulates myelin sheath thickness. *J Neurosci,* 32**,** 6631-41.

FURUSHO, M., KAGA, Y., ISHII, A., HEBERT, J. M. & BANSAL, R. 2011. Fibroblast growth factor signaling is required for the generation of oligodendrocyte progenitors from the embryonic forebrain. *J Neurosci,* 31**,** 5055-66.

FURUSHO, M., ROULOIS, A. J., FRANKLIN, R. J. & BANSAL, R. 2015. Fibroblast growth factor signaling in oligodendrocyte-lineage cells facilitates recovery of chronically demyelinated lesions but is redundant in acute lesions. *Glia*.

FYFFE-MARICICH, S. L., KARLO, J. C., LANDRETH, G. E. & MILLER, R. H. 2011. The ERK2 Mitogen-Activated Protein Kinase Regulates the Timing of Oligodendrocyte Differentiation. *Journal of Neuroscience,* 31**,** 843-850.

FYFFE-MARICICH, S. L., SCHOTT, A., KARL, M., KRASNO, J. & MILLER, R. H. 2013. Signaling through ERK1/2 Controls Myelin Thickness during Myelin Repair in the Adult Central Nervous System. *Journal of Neuroscience,* 33**,** 18402-18408.

GARBER, K. 2006. The second wave in kinase cancer drugs. *Nat Biotechnol,* 24**,** 127-30.

GIATTI, S., BORASO, M., ABBIATI, F., BALLARINI, E., CALABRESE, D., SANTOS-GALINDO, M., RIGOLIO, R., PESARESI, M., CARUSO, D., VIVIANI, B., CAVALETTI, G., GARCIA-SEGURA, L. M. & MELCANGI, R. C. 2013. Multimodal analysis in acute and chronic experimental autoimmune encephalomyelitis. *J Neuroimmune Pharmacol,* 8**,** 238-50.

GOLD, R. 2006. Understanding pathogenesis and therapy of multiple sclerosis via animal models: 70 years of merits and culprits in experimental autoimmune encephalomyelitis research. *Brain,* 129**,** 1953-1971.

GOTTLE, P., SABO, J. K., HEINEN, A., VENABLES, G., TORRES, K., TZEKOVA, N., PARRAS, C. M., KREMER, D., HARTUNG, H. P., CATE, H. S. & KURY, P. 2015. Oligodendroglial maturation is dependent on intracellular protein shuttling. *J Neurosci,* 35**,** 906-19.

GOURRAUD, P. A., HARBO, H. F., HAUSER, S. L. & BARANZINI, S. E. 2012. The genetics of multiple sclerosis: an up-to-date review. *Immunol Rev,* 248**,** 87-103.

GRAVEL, C., GOTZ, R., LORRAIN, A. & SENDTNER, M. 1997. Adenoviral gene transfer of ciliary neurotrophic factor and brain-derived neurotrophic factor leads to long-term survival of axotomized motor neurons. *Nat Med,* 3**,** 765-70.

GRITTI, A., PARATI, E. A., COVA, L., FROLICHSTHAL, P., GALLI, R., WANKE, E., FARAVELLI, L., MORASSUTTI, D. J., ROISEN, F., NICKEL, D. D. & VESCOVI, A. L. 1996. Multipotential stem cells from the adult mouse brain proliferate and self-renew in response to basic fibroblast growth factor. *J Neurosci,* 16**,** 1091-100.

GUARDIOLA-DIAZ, H. M., ISHII, A. & BANSAL, R. 2012. Erk1/2 MAPK and mTOR signaling sequentially regulates progression through distinct stages of oligodendrocyte differentiation. *Glia,* 60**,** 476-86.

GUILLEMOT, F. & ZIMMER, C. 2011. From cradle to grave: the multiple roles of fibroblast growth factors in neural development. *Neuron,* 71**,** 574-88.

GUNZLER, D. D., PERZYNSKI, A., MORRIS, N., BERMEL, R., LEWIS, S. & MILLER, D. 2015. Disentangling Multiple Sclerosis and depression: an adjusted depression screening score for patient-centered care. *J Behav Med,* 38**,** 237-50.

GUSTAVSEN, M. W., PAGE, C. M., MOEN, S. M., BJOLGERUD, A., BERG-HANSEN, P., NYGAARD, G. O., SANDVIK, L., LIE, B. A., CELIUS, E. G. & HARBO, H. F. 2014. Environmental exposures and the risk of multiple sclerosis investigated in a Norwegian case-control study. *BMC Neurol,* 14**,** 196.

HADDAD, L. E., KHZAM, L. B., HAJJAR, F., MERHI, Y. & SIROIS, M. G. 2011. Characterization of FGF receptor expression in human neutrophils and their contribution to chemotaxis. *Am J Physiol Cell Physiol,* 301**,** C1036-45.

HARADA, C., GUO, X., NAMEKATA, K., KIMURA, A., NAKAMURA, K., TANAKA, K., PARADA, L. F. & HARADA, T. 2011. Glia- and neuron-specific functions of TrkB signalling during retinal degeneration and regeneration. *Nat Commun,* 2**,** 189.

HARIRCHIAN, M. H., TEKIEH, A. H., MODABBERNIA, A., AGHAMOLLAII, V., TAFAKHORI, A., GHAFFARPOUR, M., SAHRAIAN, M. A., NAJI, M. & YAZDANBAKHSH, M. 2012. Serum and CSF PDGF-AA and FGF-2 in relapsing-remitting multiple sclerosis: a case-control study. *Eur J Neurol,* 19**,** 241-7.

HEMMER, B., ARCHELOS, J. J. & HARTUNG, H. P. 2002. New concepts in the immunopathogenesis of multiple sclerosis. *Nat Rev Neurosci,* 3**,** 291-301.

HOGLUND, R. A. & MAGHAZACHI, A. A. 2014. Multiple sclerosis and the role of immune cells. *World J Exp Med,* 4**,** 27-37.

HOHLFELD, R., KERSCHENSTEINER, M., STADELMANN, C., LASSMANN, H. & WEKERLE, H. 2000. The neuroprotective effect of inflammation: implications for the therapy of multiple sclerosis. *J Neuroimmunol,* 107**,** 161-6.

HOHLFELD, R., KERSCHENSTEINER, M., STADELMANN, C., LASSMANN, H. & WEKERLE, H. 2006. The neuroprotective effect of inflammation: implications for the therapy of multiple sclerosis. *Neurol Sci,* 27 Suppl 1**,** S1-7.

HU, Y., MINTZ, A., SHAH, S. R., QUINONES-HINOJOSA, A. & HSU, W. 2014. The FGFR/MEK/ERK/brachyury pathway is critical for chordoma cell growth and survival. *Carcinogenesis,* 35**,** 1491-1499.

HUANG, Y. L., CHOU, W. C., HSIUNG, C. N., HU, L. Y., CHU, H. W. & SHEN, C. Y. 2015. FGFR2 regulates Mre11 expression and double-strand break repair via the MEK-ERK-POU1F1 pathway in breast tumorigenesis. *Human Molecular Genetics,* 24**,** 3506-3517.

HURWITZ, B. J. 2009. The diagnosis of multiple sclerosis and the clinical subtypes. *Ann Indian Acad Neurol,* 12**,** 226-30.

IMAMURA, T. 2014. Physiological functions and underlying mechanisms of fibroblast growth factor (FGF) family members: recent findings and implications for their pharmacological application. *Biol Pharm Bull,* 37**,** 1081-9.

ISHII, A., FURUSHO, M., DUPREE, J. L. & BANSAL, R. 2014. Role of ERK1/2 MAPK signaling in the maintenance of myelin and axonal integrity in the adult CNS. *J Neurosci,* 34**,** 16031-45.

ISHII, A., FYFFE-MARICICH, S. L., FURUSHO, M., MILLER, R. H. & BANSAL, R. 2012. ERK1/ERK2 MAPK signaling is required to increase myelin thickness independent of oligodendrocyte differentiation and initiation of myelination. *J Neurosci,* 32**,** 8855-64.

ITOH, N. 2007. The Fgf families in humans, mice, and zebrafish: their evolutional processes and roles in development, metabolism, and disease. *Biol Pharm Bull,* 30**,** 1819-25.

JACKMAN, N., ISHII, A. & BANSAL, R. 2009. Oligodendrocyte development and myelin biogenesis: parsing out the roles of glycosphingolipids. *Physiology (Bethesda),* 24**,** 290-7.

JESSEN, K. R. & MIRSKY, R. 1980. Glial cells in the enteric nervous system contain glial fibrillary acidic protein. *Nature,* 286**,** 736-7.

JIANG, T., GAO, G., FAN, G., LI, M. & ZHOU, C. 2015. FGFR1 amplification in lung squamous cell carcinoma: a systematic review with meta-analysis. *Lung Cancer,* 87**,** 1-7.

JIANG, Y., ZOU, Y., CHEN, S., ZHU, C., WU, A., LIU, Y., MA, L., ZHU, D., MA, X., LIU, M., KANG, Z., PI, R., PENG, F., WANG, Q. & CHEN, X. 2013. The anti-inflammatory effect of donepezil on experimental autoimmune encephalomyelitis in C57 BL/6 mice. *Neuropharmacology,* 73**,** 415-424.

JIANG, Z., JIANG, J. X. & ZHANG, G.-X. 2014. Macrophages: A double-edged sword in experimental autoimmune encephalomyelitis. *Immunology Letters,* 160**,** 17-22.

KAGA, Y., SHOEMAKER, W. J., FURUSHO, M., BRYANT, M., ROSENBLUTH, J., PFEIFFER, S. E., OH, L., RASBAND, M., LAPPE-SIEFKE, C., YU, K., ORNITZ, D. M., NAVE, K. A. & BANSAL, R. 2006. Mice with conditional inactivation of fibroblast growth factor receptor-2 signaling in oligodendrocytes have normal myelin but display dramatic hyperactivity when combined with Cnp1 inactivation. *J Neurosci,* 26**,** 12339-50.

KARUSSIS, D. 2014. The diagnosis of multiple sclerosis and the various related demyelinating syndromes: a critical review. *J Autoimmun,* 48-49**,** 134-42.

KATOH, Y. & KATOH, M. 2009. FGFR2-related pathogenesis and FGFR2-targeted therapeutics (Review). *Int J Mol Med,* 23**,** 307-11.

KEMPURAJ, D., KHAN, M. M., THANGAVEL, R., XIONG, Z., YANG, E. & ZAHEER, A. 2013. Glia maturation factor induces interleukin-33 release from astrocytes: implications for neurodegenerative diseases. *J Neuroimmune Pharmacol,* 8**,** 643-50.

KERMER, P., KLOCKER, N., LABES, M. & BAHR, M. 2000. Insulin-like growth factor-I protects axotomized rat retinal ganglion cells from secondary death via PI3-K-dependent Akt phosphorylation and inhibition of caspase-3 In vivo. *J Neurosci,* 20**,** 2-8.

KIESEIER, B. C., HEMMER, B. & HARTUNG, H. P. 2005. Multiple sclerosis--novel insights and new therapeutic strategies. *Curr Opin Neurol,* 18**,** 211-20.

KINGWELL, E., MARRIOTT, J. J., JETTE, N., PRINGSHEIM, T., MAKHANI, N., MORROW, S. A., FISK, J. D., EVANS, C., BELAND, S. G., KULAGA, S., DYKEMAN, J., WOLFSON, C., KOCH, M. W. & MARRIE, R. A. 2013. Incidence and prevalence of multiple sclerosis in Europe: a systematic review. *BMC Neurol,* 13**,** 128.

KUERTEN, S., JAVERI, S., TARY-LEHMANN, M., LEHMANN, P. V. & ANGELOV, D. N. 2008. Fundamental differences in the dynamics of CNS lesion development and composition in MP4- and MOG peptide 35-55-induced experimental autoimmune encephalomyelitis. *Clin Immunol,* 129**,** 256-67.

KUMAR, D. R., ASLINIA, F., YALE, S. H. & MAZZA, J. J. 2010. Jean-Martin Charcot: The Father of Neurology. *Clinical Medicine & Research,* 9**,** 46-49.

LEI, S., CHENG, T., GUO, Y., LI, C., ZHANG, W. & ZHI, F. 2014. Somatostatin ameliorates lipopolysaccharide-induced tight junction damage via the ERK–MAPK pathway in Caco2 cells. *European Journal of Cell Biology,* 93**,** 299-307.

LINKER, R. A. & LEE, D. H. 2009. Models of autoimmune demyelination in the central nervous system: on the way to translational medicine. *Exp Transl Stroke Med,* 1**,** 5.

LINKER, R. A., LEE, D. H., DEMIR, S., WIESE, S., KRUSE, N., SIGLIENTI, I., GERHARDT, E., NEUMANN, H., SENDTNER, M., LUHDER, F. & GOLD, R. 2010. Functional role of brain-derived neurotrophic factor in neuroprotective autoimmunity: therapeutic implications in a model of multiple sclerosis. *Brain,* 133**,** 2248-63.

LIU, X., MASHOUR, G. A., WEBSTER, H. F. & KURTZ, A. 1998. Basic FGF and FGF receptor 1 are expressed in microglia during experimental autoimmune encephalomyelitis: temporally distinct expression of midkine and pleiotrophin. *Glia,* 24**,** 390-7.

LIU, Y., SHEPHERD, E. G. & NELIN, L. D. 2007. MAPK phosphatases--regulating the immune response. *Nat Rev Immunol,* 7**,** 202-12.

LOMBAERT, I. M., ABRAMS, S. R., LI, L., ESWARAKUMAR, V. P., SETHI, A. J., WITT, R. L. & HOFFMAN, M. P. 2013. Combined KIT and FGFR2b signaling regulates epithelial progenitor expansion during organogenesis. *Stem Cell Reports,* 1**,** 604-19.

LONIC, A., POWELL, J. A., KONG, Y., THOMAS, D., HOLIEN, J. K., TRUONG, N., PARKER, M. W. & GUTHRIDGE, M. A. 2013. Phosphorylation of Serine 779 in Fibroblast Growth Factor Receptor 1 and 2 by Protein Kinase C Regulates Ras/Mitogen-activated Protein Kinase Signaling and Neuronal Differentiation. *Journal of Biological Chemistry,* 288**,** 14874-14885.

LOPATEGUI CABEZAS, I., HERRERA BATISTA, A. & PENTON ROL, G. 2014. The role of glial cells in Alzheimer disease: potential therapeutic implications. *Neurologia,* 29**,** 305-9.

LUBLIN, F. D., REINGOLD, S. C., COHEN, J. A., CUTTER, G. R., SORENSEN, P. S., THOMPSON, A. J., WOLINSKY, J. S., BALCER, L. J., BANWELL, B., BARKHOF, F., BEBO, B., JR., CALABRESI, P. A., CLANET, M., COMI, G., FOX, R. J., FREEDMAN, M. S., GOODMAN, A. D., INGLESE, M., KAPPOS, L., KIESEIER, B. C., LINCOLN, J. A., LUBETZKI, C., MILLER, A. E., MONTALBAN, X., O'CONNOR, P. W., PETKAU, J., POZZILLI, C., RUDICK, R. A., SORMANI, M. P., STUVE, O., WAUBANT, E. & POLMAN, C. H. 2014. Defining the clinical course of multiple sclerosis: the 2013 revisions. *Neurology,* 83**,** 278-86.

MALLUCCI, G., PERUZZOTTI-JAMETTI, L., BERNSTOCK, J. D. & PLUCHINO, S. 2015. The role of immune cells, glia and neurons in white and gray matter pathology in multiple sclerosis. *Prog Neurobiol,* 127-128C**,** 1-22.

MARS, L. T., SAIKALI, P., LIBLAU, R. S. & ARBOUR, N. 2011. Contribution of CD8 T lymphocytes to the immuno-pathogenesis of multiple sclerosis and its animal models. *Biochim Biophys Acta,* 1812**,** 151-61.

MATSUDA, Y., UEDA, J. & ISHIWATA, T. 2012. Fibroblast growth factor receptor 2: expression, roles, and potential as a novel molecular target for colorectal cancer. *Patholog Res Int,* 2012**,** 574768.

MCDONALD, W. I., COMPSTON, A., EDAN, G., GOODKIN, D., HARTUNG, H. P., LUBLIN, F. D., MCFARLAND, H. F., PATY, D. W., POLMAN, C. H., REINGOLD, S. C., SANDBERG-WOLLHEIM, M., SIBLEY, W., THOMPSON, A., VAN DEN NOORT, S., WEINSHENKER, B. Y. & WOLINSKY, J. S. 2001. Recommended diagnostic criteria for multiple sclerosis: guidelines from the International Panel on the diagnosis of multiple sclerosis. *Ann Neurol,* 50**,** 121-7.

MESSERSMITH, D. J., MURTIE, J. C., LE, T. Q., FROST, E. E. & ARMSTRONG, R. C. 2000. Fibroblast growth factor 2 (FGF2) and FGF receptor expression in an experimental demyelinating disease with extensive remyelination. *J Neurosci Res,* 62**,** 241-56.

MEYER, A. N., MCANDREW, C. W. & DONOGHUE, D. J. 2008. Nordihydroguaiaretic acid inhibits an activated fibroblast growth factor receptor 3 mutant and blocks downstream signaling in multiple myeloma cells. *Cancer Res,* 68**,** 7362-70.

MIERZWA, A. J., ZHOU, Y. X., HIBBITS, N., VANA, A. C. & ARMSTRONG, R. C. 2013. FGF2 and FGFR1 signaling regulate functional recovery following cuprizone demyelination. *Neurosci Lett,* 548**,** 280-5.

MIRAOUI, H., OUDINA, K., PETITE, H., TANIMOTO, Y., MORIYAMA, K. & MARIE, P. J. 2008. Fibroblast Growth Factor Receptor 2 Promotes Osteogenic Differentiation in Mesenchymal Cells via ERK1/2 and Protein Kinase C Signaling. *Journal of Biological Chemistry,* 284**,** 4897-4904.

MIRON, V. E., KUHLMANN, T. & ANTEL, J. P. 2011. Cells of the oligodendroglial lineage, myelination, and remyelination. *Biochim Biophys Acta,* 1812**,** 184-93.

MITEW, S., HAY, C. M., PECKHAM, H., XIAO, J., KOENNING, M. & EMERY, B. 2014. Mechanisms regulating the development of oligodendrocytes and central nervous system myelin. *Neuroscience,* 276**,** 29-47.

MOORE, C. S., CUI, Q. L., WARSI, N. M., DURAFOURT, B. A., ZORKO, N., OWEN, D. R., ANTEL, J. P. & BAR-OR, A. 2015. Direct and indirect effects of immune and central nervous system-resident cells on human oligodendrocyte progenitor cell differentiation. *J Immunol,* 194**,** 761-72.

MORITA, J., NAKAMURA, M., KOBAYASHI, Y., DENG, C. X., FUNATO, N. & MORIYAMA, K. 2014. Soluble form of FGFR2 with S252W partially prevents craniosynostosis of the apert mouse model. *Dev Dyn,* 243**,** 560-7.

MORRISON, B. M., LEE, Y. & ROTHSTEIN, J. D. 2013. Oligodendroglia: metabolic supporters of axons. *Trends Cell Biol,* 23**,** 644-51.

MULAKAYALA, N., RAO, P., IQBAL, J., BANDICHHOR, R. & ORUGANTI, S. 2013. Synthesis of novel therapeutic agents for the treatment of multiple sclerosis: a brief overview. *Eur J Med Chem,* 60**,** 170-86.

NAGELHUS, E. A., AMIRY-MOGHADDAM, M., BERGERSEN, L. H., BJAALIE, J. G., ERIKSSON, J., GUNDERSEN, V., LEERGAARD, T. B., MORTH, J. P., STORM-MATHISEN, J., TORP, R., WALHOVD, K. B. & TONJUM, T. 2013. The glia doctrine: addressing the role of glial cells in healthy brain ageing. *Mech Ageing Dev,* 134**,** 449-59.

NARAYANAN, S. P., FLORES, A. I., WANG, F. & MACKLIN, W. B. 2009. Akt Signals through the Mammalian Target of Rapamycin Pathway to Regulate CNS Myelination. *Journal of Neuroscience,* 29**,** 6860-6870.

NAWA, M., KANEKURA, K., HASHIMOTO, Y., AISO, S. & MATSUOKA, M. 2008. A novel Akt/PKB-interacting protein promotes cell adhesion and inhibits familial amyotrophic lateral sclerosis-linked mutant SOD1-induced neuronal death via inhibition of PP2A-mediated dephosphorylation of Akt/PKB. *Cell Signal,* 20**,** 493-505.

NEBEN, C. L., IDONI, B., SALVA, J. E., TUZON, C. T., RICE, J. C., KRAKOW, D. & MERRILL, A. E. 2014. Bent bone dysplasia syndrome reveals nucleolar activity for FGFR2 in ribosomal DNA transcription. *Hum Mol Genet,* 23**,** 5659-71.

NEWLAND, P. K., FLICK, L. H., THOMAS, F. P. & SHANNON, W. D. 2014. Identifying symptom co-occurrence in persons with multiple sclerosis. *Clin Nurs Res,* 23**,** 529-43.

ORR-URTREGER, A., BEDFORD, M. T., BURAKOVA, T., ARMAN, E., ZIMMER, Y., YAYON, A., GIVOL, D. & LONAI, P. 1993. Developmental localization of the splicing alternatives of fibroblast growth factor receptor-2 (FGFR2). *Dev Biol,* 158**,** 475-86.

ORTIZ, G. G., PACHECO-MOISES, F. P., MACIAS-ISLAS, M. A., FLORES-ALVARADO, L. J., MIRELES-RAMIREZ, M. A., GONZALEZ-RENOVATO, E. D., HERNANDEZ-NAVARRO, V. E., SANCHEZ-LOPEZ, A. L. & ALATORRE-JIMENEZ, M. A. 2014. Role of the blood-brain barrier in multiple sclerosis. *Arch Med Res,* 45**,** 687-97.

PACHNER, A. R. 2011. Experimental models of multiple sclerosis. *Curr Opin Neurol,* 24**,** 291-9.

PAGNINI, F., BOSMA, C. M., PHILLIPS, D. & LANGER, E. 2014. Symptom changes in multiple sclerosis following psychological interventions: a systematic review. *BMC Neurol,* 14**,** 222.

PATEL, J. & BALABANOV, R. 2012. Molecular mechanisms of oligodendrocyte injury in multiple sclerosis and experimental autoimmune encephalomyelitis. *Int J Mol Sci,* 13**,** 10647-59.

PATY, D. W. & LI, D. K. 1993. Interferon beta-1b is effective in relapsing-remitting multiple sclerosis. II. MRI analysis results of a multicenter, randomized, double-blind, placebo-

controlled trial. UBC MS/MRI Study Group and the IFNB Multiple Sclerosis Study Group. *Neurology,* 43**,** 662-7.

PAWATE, S. & BAGNATO, F. 2015. Newer agents in the treatment of multiple sclerosis. *Neurologist,* 19**,** 104-17.

PAZ SOLDAN, M. M. & PIRKO, I. 2012. Biogenesis and significance of central nervous system myelin. *Semin Neurol,* 32**,** 9-14.

POLMAN, C. H., REINGOLD, S. C., BANWELL, B., CLANET, M., COHEN, J. A., FILIPPI, M., FUJIHARA, K., HAVRDOVA, E., HUTCHINSON, M., KAPPOS, L., LUBLIN, F. D., MONTALBAN, X., O'CONNOR, P., SANDBERG-WOLLHEIM, M., THOMPSON, A. J., WAUBANT, E., WEINSHENKER, B. & WOLINSKY, J. S. 2011. Diagnostic criteria for multiple sclerosis: 2010 revisions to the McDonald criteria. *Ann Neurol,* 69**,** 292-302.

POPOVIC, M., STANOJEVIC, Z., TOSIC, J., ISAKOVIC, A., PAUNOVIC, V., PETRICEVIC, S., MARTINOVIC, T., CIRIC, D., KRAVIC-STEVOVIC, T., SOSKIC, V., KOSTIC-RAJACIC, S., SHAKIB, K., BUMBASIREVIC, V. & TRAJKOVIC, V. 2015. Neuroprotective arylpiperazine dopaminergic/serotonergic ligands suppress experimental autoimmune encephalomyelitis in rats. *Journal of Neurochemistry,* 135**,** 125-138.

POSER, C. M., PATY, D. W., SCHEINBERG, L., MCDONALD, W. I., DAVIS, F. A., EBERS, G. C., JOHNSON, K. P., SIBLEY, W. A., SILBERBERG, D. H. & TOURTELLOTTE, W. W. 1983. New diagnostic criteria for multiple sclerosis: guidelines for research protocols. *Ann Neurol,* 13**,** 227-31.

PROCACCINI, C., DE ROSA, V., PUCINO, V., FORMISANO, L. & MATARESE, G. 2015. Animal models of Multiple Sclerosis. *Eur J Pharmacol,* 759**,** 182-91.

RACKE, M. K. 2001. Experimental autoimmune encephalomyelitis (EAE). *Curr Protoc Neurosci,* Chapter 9**,** Unit9 7.

RAJENDRAN, R. 2014. Evaluation of the Fibroblast growth factor receptor 1 (FGFR1) in Experimental Autoimmune Encephalomyelitis (EAE). *Justus-Liebig-Universität Gießen*.

RALF LINKER, D.-H. L., INES SIGLIENTI, RALF GOLD 2007. Is there a role for neurotrophins in the pathology of multiple sclerosis. *JOURNAL OF NEUROLOGY***,** 33-40.

RANGACHARI, M. & KUCHROO, V. K. 2013. Using EAE to better understand principles of immune function and autoimmune pathology. *J Autoimmun,* 45**,** 31-9.

ROHMANN, E., BRUNNER, H. G., KAYSERILI, H., UYGUNER, O., NURNBERG, G., LEW, E. D., DOBBIE, A., ESWARAKUMAR, V. P., UZUMCU, A., ULUBIL-EMEROGLU, M., LEROY, J. G., LI, Y., BECKER, C., LEHNERDT, K., CREMERS, C. W., YUKSEL-APAK, M., NURNBERG, P., KUBISCH, C., SCHLESSINGER, J., VAN BOKHOVEN, H. & WOLLNIK, B. 2006. Mutations in different components of FGF signaling in LADD syndrome. *Nat Genet,* 38**,** 414-7.

ROTTLAENDER, A., VILLWOCK, H., ADDICKS, K. & KUERTEN, S. 2011. Neuroprotective role of fibroblast growth factor-2 in experimental autoimmune encephalomyelitis. *Immunology,* 133**,** 370-8.

RUFFINI, F., FURLAN, R., POLIANI, P. L., BRAMBILLA, E., MARCONI, P. C., BERGAMI, A., DESINA, G., GLORIOSO, J. C., COMI, G. & MARTINO, G. 2001. Fibroblast growth factor-II gene therapy reverts the clinical course and the pathological signs of chronic experimental autoimmune encephalomyelitis in C57BL/6 mice. *Gene Ther,* 8**,** 1207-13.

SAGAR, D., LAMONTAGNE, A., FOSS, C. A., KHAN, Z. K., POMPER, M. G. & JAIN, P. 2012. Dendritic cell CNS recruitment correlates with disease severity in EAE via CCL2 chemotaxis at the blood–brain barrier through paracellular transmigration and ERK activation. *Journal of Neuroinflammation,* 9**,** 245.

SAKAMOTO, T., OZAKI, K.-I., FUJIO, K., KAJIKAWA, S.-H., UESATO, S.-I., WATANABE, K., TANIMURA, S., KOJI, T. & KOHNO, M. 2013. Blockade of the ERK pathway enhances the therapeutic efficacy of the histone deacetylase inhibitor MS-275 in human tumor xenograft models. *Biochemical and Biophysical Research Communications,* 433**,** 456-462.

SATO, T., WILSON, T. S., HUGHES, L. F., KONRAD, H. R., NAKAYAMA, M. & HELFERT, R. H. 2001. Age-related changes in levels of tyrosine kinase B receptor and fibroblast growth factor receptor 2 in the rat inferior colliculus: implications for neural senescence. *Neuroscience,* 103**,** 695-702.

SÄTTLER, M. B., MERKLER, D., MAIER, K., STADELMANN, C., EHRENREICH, H., BÄHR, M. & DIEM, R. 2004. Neuroprotective effects and intracellular signaling pathways of erythropoietin in a rat model of multiple sclerosis. *Cell Death and Differentiation,* 11**,** S181-S192.

SCHENCK, M., CARPINTEIRO, A., GRASSME, H., LANG, F. & GULBINS, E. 2007. Ceramide: physiological and pathophysiological aspects. *Arch Biochem Biophys,* 462**,** 171-5.

SCHULLER, A. C., AHMED, Z. & LADBURY, J. E. 2008. Extracellular point mutations in FGFR2 result in elevated ERK1/2 activation and perturbation of neuronal differentiation. *Biochem J,* 410**,** 205-11.

SHAHRBANIAN, S., DUQUETTE, P., KUSPINAR, A. & MAYO, N. E. 2015. Contribution of symptom clusters to multiple sclerosis consequences. *Qual Life Res,* 24**,** 617-29.

SIREN, A. L., FRATELLI, M., BRINES, M., GOEMANS, C., CASAGRANDE, S., LEWCZUK, P., KEENAN, S., GLEITER, C., PASQUALI, C., CAPOBIANCO, A., MENNINI, T., HEUMANN, R., CERAMI, A., EHRENREICH, H. & GHEZZI, P. 2001. Erythropoietin prevents neuronal apoptosis after cerebral ischemia and metabolic stress. *Proc Natl Acad Sci U S A,* 98**,** 4044-9.

SKUNDRIC, D. S. 2005. Experimental models of relapsing-remitting multiple sclerosis: current concepts and perspective. *Curr Neurovasc Res,* 2**,** 349-62.

SONG, F., BANDARA, M., DEOL, H., LOEB, J. A., BENJAMINS, J. & LISAK, R. P. 2013. Complexity of trophic factor signaling in experimental autoimmune encephalomyelitis: differential expression of neurotrophic and gliotrophic factors. *J Neuroimmunol,* 262**,** 11-8.

SOTO, I., ROSENTHAL, J. J., BLAGBURN, J. M. & BLANCO, R. E. 2006. Fibroblast growth factor 2 applied to the optic nerve after axotomy up-regulates BDNF and TrkB in ganglion cells by activating the ERK and PKA signaling pathways. *J Neurochem,* 96**,** 82-96.

STADELMANN, C., KERSCHENSTEINER, M., MISGELD, T., BRUCK, W., HOHLFELD, R. & LASSMANN, H. 2002. BDNF and gp145trkB in multiple sclerosis brain lesions: neuroprotective interactions between immune and neuronal cells? *Brain,* 125**,** 75-85.

STADELMANN, C., WEGNER, C. & BRUCK, W. 2011. Inflammation, demyelination, and degeneration - recent insights from MS pathology. *Biochim Biophys Acta,* 1812**,** 275-82.

STEINHAUSER, C. & SEIFERT, G. 2012. Astrocyte dysfunction in epilepsy. *In:* NOEBELS, J. L., AVOLI, M., ROGAWSKI, M. A., OLSEN, R. W. & DELGADO-ESCUETA, A. V. (eds.) *Jasper's Basic Mechanisms of the Epilepsies.* 4th ed. Bethesda (MD).

SWEETLAND, J., HOWSE, E. & PLAYFORD, E. D. 2012. A systematic review of research undertaken in vocational rehabilitation for people with multiple sclerosis. *Disabil Rehabil,* 34**,** 2031-8.

TANABE, S. & YAMASHITA, T. 2014. Repulsive Guidance Molecule-a Is Involved in Th17-Cell-Induced Neurodegeneration in Autoimmune Encephalomyelitis. *Cell Reports,* 9**,** 1459-1470.

TCHAICHA, J. H., AKBAY, E. A., ALTABEF, A., MIKSE, O. R., KIKUCHI, E., RHEE, K., LIAO, R. G., BRONSON, R. T., SHOLL, L. M., MEYERSON, M., HAMMERMAN, P. S. & WONG, K. K. 2014. Kinase domain activation of FGFR2 yields high-grade lung adenocarcinoma sensitive to a Pan-FGFR inhibitor in a mouse model of NSCLC. *Cancer Res,* 74**,** 4676-84.

TEVEN, C. M., FARINA, E. M., RIVAS, J. & REID, R. R. 2014. Fibroblast growth factor (FGF) signaling in development and skeletal diseases. *Genes Dis,* 1**,** 199-213.

TSIPERSON, V., GRUBER, R. C., GOLDBERG, M. F., JORDAN, A., WEINGER, J. G., MACIAN, F. & SHAFIT-ZAGARDO, B. 2013. Suppression of Inflammatory Responses during Myelin Oligodendrocyte Glycoprotein-Induced Experimental Autoimmune Encephalomyelitis Is Regulated by AKT3 Signaling. *The Journal of Immunology,* 190**,** 1528-1539.

TURNER, N. & GROSE, R. 2010. Fibroblast growth factor signalling: from development to cancer. *Nat Rev Cancer,* 10**,** 116-29.

UNUTMAZ, D., LAVASANI, S., DZHAMBAZOV, B., NOURI, M., FÅK, F., BUSKE, S., MOLIN, G., THORLACIUS, H., ALENFALL, J., JEPPSSON, B. & WESTRÖM, B. 2010. A Novel Probiotic Mixture Exerts a Therapeutic Effect on Experimental Autoimmune Encephalomyelitis Mediated by IL-10 Producing Regulatory T Cells. *PLoS ONE,* 5**,** e9009.

VENKEN, K., HELLINGS, N., HENSEN, K., RUMMENS, J. L. & STINISSEN, P. 2010. Memory CD4+CD127high T cells from patients with multiple sclerosis produce IL-17 in response to myelin antigens. *J Neuroimmunol,* 226**,** 185-91.

VON BUDINGEN, H. C., PALANICHAMY, A., LEHMANN-HORN, K., MICHEL, B. A. & ZAMVIL, S. S. 2015. Update on the autoimmune pathology of multiple sclerosis: B-cells as disease-drivers and therapeutic targets. *Eur Neurol,* 73**,** 238-46.

VOß, E. V., ŠKULJEC, J., GUDI, V., SKRIPULETZ, T., PUL, R., TREBST, C. & STANGEL, M. 2012. Characterisation of microglia during de- and remyelination: Can they create a repair promoting environment? *Neurobiology of Disease,* 45**,** 519-528.

WANG, L.-F., LI, X., GAO, Y.-B., WANG, S.-M., ZHAO, L., DONG, J., YAO, B.-W., XU, X.-P., CHANG, G.-M., ZHOU, H.-M., HU, X.-J. & PENG, R.-Y. 2014. Activation of VEGF/Flk-1-ERK Pathway Induced Blood–Brain Barrier Injury After Microwave Exposure. *Molecular Neurobiology,* 52**,** 478-491.

WEBB, D. R. 2014. Animal models of human disease: inflammation. *Biochem Pharmacol,* 87**,** 121-30.

WOODBURY, M. E. & IKEZU, T. 2013. Fibroblast Growth Factor-2 Signaling in Neurogenesis and Neurodegeneration. *J Neuroimmune Pharmacol*.

YAO, Y., LI, W., WU, J., GERMANN, U. A., SU, M. S. S., KUIDA, K. & BOUCHER, D. M. 2003. Extracellular signal-regulated kinase 2 is necessary for mesoderm differentiation. *Proceedings of the National Academy of Sciences,* 100**,** 12759-12764.

ZANG, Y. C., KOZOVSKA, M. M., HONG, J., LI, S., MANN, S., KILLIAN, J. M., RIVERA, V. M. & ZHANG, J. Z. 1999. Impaired apoptotic deletion of myelin basic protein-reactive T cells in patients with multiple sclerosis. *Eur J Immunol,* 29**,** 1692-700.

ZHANG, X., IBRAHIMI, O. A., OLSEN, S. K., UMEMORI, H., MOHAMMADI, M. & ORNITZ, D. M. 2006. Receptor specificity of the fibroblast growth factor family. The complete mammalian FGF family. *J Biol Chem,* 281**,** 15694-700.

ZHOU, Y., OUDIN, M. J., GAJENDRA, S., SONEGO, M., FALENTA, K., WILLIAMS, G., LALLI, G. & DOHERTY, P. 2015. Regional effects of endocannabinoid, BDNF and FGF receptor signalling on neuroblast motility and guidance along the rostral migratory stream. *Mol Cell Neurosci,* 64**,** 32-43.

ACKNOWLEDGEMENTS

First and foremost I would like to express my sincere gratitude to my supervisor, **PD Dr. Martin Berghoff**, for the continuous support and guidance he has provided me throughout these years. He has directed me along my thesis with his patience, motivation, and immense knowledge whilst allowing me the room to work in my own way. I attribute the level of my doctoral degree to his encouragement and effort and without him this thesis, too, would not have been completed or written. Simply said, one could not wish for a better or friendlier supervisor.

I extend my sincerest gratitude to, **Prof. Dr. Wolfgang Clauss,** in accepting to advise me as second supervisor. His generosity in providing insights, constructive feedbacks and comments, and his encouragement were indispensable forward moving elements into completion of my thesis.

I would like to thank **Dr. Mario Giraldo Velazguz,** for designing this very interesting research project which I offered to participate as a Ph.D. candidate and happened to spend some wonderful years in perusing its objectives. He helped me to establish myself in the laboratory and provided the appropriate assistance both scientifically and technically whenever there was a need.

My gratitude also goes to our collaborate **Prof. Dr. Christina Stadelmann**, Institute for Neuropatholgy, Göttingen, Germany, for letting me enter her laboratory, supporting with the material and knowledge for conducting histopathological investigations, providing valuable suggestions and insights and last but not the least, her generosity in treating me as one of her own students.

I would like to appreciate the “Giessen Graduate school of Life Sciences” (**GGL**), for giving me the opportunity to acquire scientific knowledge by offering the seminars and workshops and providing the grant for lab rotation in Université de Montréal, Montreal, Canada.

I had the good fortune to know my best friend and fellow graduate Ranjithkumar Rajendran (now Dr. Rajendran). We had a wonderful mutual presence and support for

one another, the kind of assistance which was in both professional and personal level. Without him this journey would have been much harder and less joyful. I thank my other fellow graduates Backialakshmi and Liza for research discussions and our colleagues Helga, Cornelia, Edith and Marita for the wonderful time in our lab. I also thank Dr. Daniel Zahner, the head of animal facility for his help and assistance.

I am grateful to **TEVA Pharmaceutical Industries Ltd, Ulm, Germany** for the support they have provided to my research project.

I would like to thank the members of PhD committee for their support and advice and suggestions.

I also thank **my friends (too many to list here but you know who you are!!!)**, for providing support and friendship that I needed.

I especially thank my family for their unconditional love and care without whom I would not have made it this far.

PUBLICATIONS

1. **Salar Kamali**, Mario Giraldo, Martin Berghoff (2011) FGF/FGFR downstream signaling cascade after ablation of fibroblast growth factor receptor-2 in C57BL/6 mice. Poster. 5th GGL international conference, Giessen, Germany.

2. **Salar Kamali**, Mario Giraldo, Martin Berghoff (2012) Fibroblast growth factor receptor-2 ameliorates the course of EAE through ERK pathway. Poster. 6th GGL international conference, Giessen, Germany.

3. **Salar Kamali**, Mario Giraldo, Martin Berghoff (2013) Oligodendrocyte FGFR2 Conditional Knockout Mice Exhibit a Milder MOG_{35-55}-Induced EAE Disease Course. 65th American Academy of Neurology Annual Congress, Feb 12, 2013, San Diego, USA Multiple Sclerosis: Treatment Mechanism of Action, P05. 166.

4. **Salar Kamali,** Mario Giraldo, Christine Stadelmann, Martin Berghoff (2016) Oligodendroglial FGFR2 Modulates MOG_{35-55}-Induced EAE through MAPK/ERK pathway. Under Submission.